INTERIM REPORT

5-30-79

Accession No. _____

Contract Program or Project Title:

Subject of this Document: Quick Look Report on LOFT Nuclear Experiment L2-3

Type of Document: Quick Look Report

Author(s): D. L. Reeder

Date of Document: May 1979

Responsible NRC Individual and NRC Office or Division: D. McPherson

This document was prepared primarily for preliminary or internal use. It has not received full review and approval. Since there may be substantive changes, this document should not be considered final.

Kay Rose

H. P. Pearson, Supervisor
Information Processing
EG&G Idaho, Inc.

Prepared for
U.S. Nuclear Regulatory Commission
Washington, D.C. 20555

NRC Fin #A6048

INTERIM REPORT

NRC Research and Technical Assistance Report

QLR-L2-3

PROJECT NO. P 394

for U.S. Nuclear Regulatory Commission

QUICK-LOOK REPORT ON LOFT NUCLEAR EXPERIMENT L2-3

DOUGLAS L. REEDER

May 1979

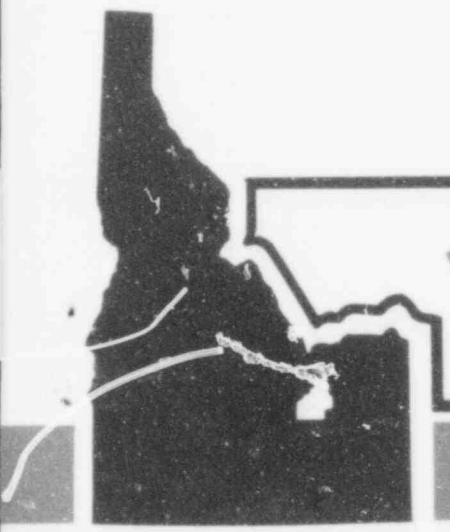

EG&G Idaho, Inc.

IDAHO NATIONAL ENGINEERING LABORATORY

DEPARTMENT OF ENERGY

IDAHO OPERATIONS OFFICE UNDER CONTRACT EY-76-C-07-1570

NOTICE

This report was prepared as an account of work sponsored by the United States Government. Neither the United States nor the Department of Energy, nor any of their employees, nor any of their contractors, subcontractors, or their employees, makes any warranty, express or implied, or assumes any legal liability or responsibility for the accuracy, completeness or usefulness of any information, apparatus, product or process disclosed, or represents that its use would not infringe privately owned rights.

QUICK LOOK REPORT ON LOFT NUCLEAR EXPERIMENT L2-3

Approved:

L. P. Leach, Manager
LOFT Experimental Program Division

N. C. Kaufman, Director
LOFT

The information contained in this summary report is preliminary and incomplete. Selected pertinent data are presented in order to draw preliminary conclusions and to expedite the reporting or research results.

QLR-L2-3

QUICK LOOK REPORT ON LOFT NUCLEAR EXPERIMENT L2-3

Douglas L. Reeder

EG&G Idaho, Inc.
Idaho Falls, Idaho 83401

Published May 1979

PREPARED FOR THE
U.S. NUCLEAR REGULATORY COMMISSION
AND THE U.S. DEPARTMENT OF ENERGY
IDAHO OPERATIONS OFFICE
UNDER CONTRACT NO. DE-AC07-76ID01570
NRC FIN NO. A6048

SUMMARY

The preliminary evaluation has been completed of the results of the LOFT nuclear Loss-of-Coolant Experiment (LOCE) L2-3, which was successfully conducted on May 12, 1979. LOCE L2-3, the second experiment in the LOFT Power Ascension Series L2, simulated a complete double-ended offset shear break of a large pressurized water reactor inlet pipe. The initial conditions for LOCE L2-3 were selected to simulate the primary coolant and core conditions typical of a commercial reactor operating at normal power. Selected data, presented in this report, confirm that the objectives of LOCE L2-3 were successfully achieved.

At the time of break initiation, the nuclear core was operating at a steady state maximum linear heat generation rate of 39.4 kW/m. Other significant initial conditions for LOCE L2-3 were: system pressure, 15.06 $\pm$ 0.2 MPa; hot leg temperature, 592.85 $\pm$ 3.0 K; and intact loop flow rate, 199.8 $\pm$ 6.3 kg/s. Scaled quantities of high pressure, low pressure, and accumulator emergency core coolant were injected during the LOCE. The primary coolant pumps were operated at constant speed throughout the experiment.

The experiment started with a rapid (~50 ms) drop to hot fluid saturation pressure after simultaneous opening of the quick-opening valves in 20.6 ms. Departure from nucleate boiling occurred at about 0.96 s after rupture on the hot pins of the core, which reached a peak cladding temperature (PCT) of 914 K at 4.95 s after rupture. The emergency core coolant flow from the high-pressure system started at 14 s, the accumulator system flow started at 16 s, and the low-pressure system flow started at 29 s after rupture. The core was reflooded at 55 s after rupture. The final quench occurred from the bottom up and the top down, with the hot rods in the central core region being rewet by 54 s.

The core thermal response was dominated by the system hydraulics causing a core wide rewet during the early blowdown phase of LOCE L2-3 in the same manner as in LOCE L2-2. The emergency core cooling system performance was not significantly degraded by the initial power level of LOCE L2-3 in that the core was quenched at a rate of approximately 0.1 m/s, which is just slightly less than the 0.12 m/s in LOCE L2-2. No loss of cladding integrity or other fuel rod degradation is believed to have occurred during LOCE L2-3.

The instrumentation and data acquisition system performed well. Of the 888 instruments (includes discrete event measurements) recorded, 861 (97%) are estimated to have operated successfully.

The LOCE L2-3 pretest calculation, using the RELAP4/MOD6 computer code, of thermal-hydraulic response in the primary coolant system appears to compare reasonably well with LOCE L2-3 data. The fuel cladding temperature response predicted using the RELAP4/MOD6 computer code did not agree with LOCE L2-3 data except in regions near the periphery of the core; the calculated maximum cladding temperatures exceeded those measured by approximately 100 K. The PCT calculated using the TRAC-P1A computer code was higher than that measured in LOCE L2-3 by approximately 50 K. Both codes predicted the final quench to occur at approximately the same time as was measured at 55 s. Additional codes and calculations [specifically, RETRAN and the developmental TRAC-P1A+Iloeje, and WREM and Combustion Engineering (CE) calculations] were applied to LOCE L2-3. All of the predictions of PCT during the blowdown phase of the transient with these calculations exceeded the measured value except TRAC-PIA+Iloeje, which was very close in predicting the PCT (lower than measured by about 5 K). RETRAN, CE calculations, and WREM predicted PCTs were higher than measured by about 120 K, 95 K, and 575 K, respectively.

LOFT LOCE L2-3, the second experiment in LOFT Power Ascension Series L2, provided experimental data on thermal-hydraulic behavior, nuclear core response, and the behavior of emergency core cooling

systems during a loss-of-coolant accident in a pressurized water nuclear reactor. The intensive analysis of the results of LOCE L2-3 currently underway will result in additional understanding of loss-of-coolant accidents and together with results from other Nuclear Regulatory Commission experimental programs will contribute to the data base required for development and assessment of analytical models for licensing commercial pressurized water reactors.

CONTENTS

FIGURES

QUICK LOOK REPORT ON LOFT NUCLEAR EXPERIMENT L2-3

I. INTRODUCTION

The Loss-of-Fluid Test (LOFT) facility[1] is a 50 MW(t) volumetrically scaled pressurized water reactor (PWR) system designed to study the response of the engineered safety features (ESF) of commercial PWR systems during the postulated loss-of-coolant accident (LOCA). With recognition of the differences in commercial PWR designs and inherent distortions in reduced scale systems, the design objective for the LOFT facility was to produce the significant thermal-hydraulic phenomena that would occur in commercial PWR systems in the same sequence and with approximately the same time frames and magnitudes. The objectives of the LOFT experimental program are:

(1) To provide data required to evaluate the adequacy and improve the analytical methods currently used to predict the LOCA response of large PWRs. The performance of the ESFs, with particular emphasis on emergency core cooling systems (ECCS), and the quantitative margins of safety inherent in the performance of the ESF are of primary interest.

(2) To identify and investigate any unexpected event(s) or threshold(s) in the response of either the plant or the ESF and develop analytical techniques that adequately describe and account for such unexpected behavior.

The information acquired from loss-of-coolant experiments (LOCE) is thus used for evaluation and development of LOCA analytical methods and assessment of the quantitative margins of safety of ESFs in response to a LOCA.

LOCE L2-3, the second experiment in the LOFT Power Ascension Series L2 (first series of nuclear LOCEs) scheduled for performance in the LOFT facility, was successfully completed May 12, 1979.

Experiment Series L2 was designed to provide large scale integrated plant data on thermal-hydraulic and fuel behavior. The general requirements for the LOFT Experiment Series L2 are specified in Reference 2.

The specific objectives for LOCE L2-3, as stated in Reference 3, are as follows:

(1) Determine core wide and spatial variations of fuel rod cladding thermal response

(2) Identify thermal-hydraulic phenomena and determine effects of thermal-hydraulic phenomena on fuel rod cladding thermal response

(3) Determine ECCS performance and core reflood characteristics

(4) Determine the integrity of the fuel rod cladding

(5) Determine principal variables of temperature, pressure, density, mass flow, and mass inventory as functions of time associated with the core, PCS coolant, and ECC, sufficient for comparison with and assessment of code predictions.

This report presents a preliminary examination of the plant performance (Section II) and a summary of the results from LOFT LOCE L2-3 (Section III). Section IV presents conclusions reached from this preliminary examination of results. Data plots are presented in Section V to allow preliminary evaluation of LOCE L2-3 relative to the experiment objectives. The data plots presented include comparisons of LOCE L2-3 data with (a) Semiscale Test S-06-3[4], which is the counterpart to LOCE L2-3; (b) LOCE L2-3 pretest calculations[5,6] using the RELAP4/MOD6[7] computer code; and (c) LOCE L2-3 pretest calculation made by Los Alamos Scientific Laboratory[8] using the

TRAC-P1A[9] computer code. Other calculational methods, identified as RETRAN[10], Combustion Engineering (CE)[11], WREM[12], and the developmental TRAC-P1A+Iloeje[13], were applied to LOCE L2-3. The predictions of peak cladding temperature during the blowdown phase of the transient from all of these methods and from RELAP4/MOD6 and TRAC-P1A are compared with the measured data.

LOCE L2-3 simulated a 200% (100% break area in each leg of the LOFT broken loop) double-ended offset shear in the cold leg of a four-loop large PWR. The LOFT system geometry is shown in Figure 1, and a representation of the core configuration illustrating the instrumentation and position designations is shown in Figures 2 and 3, respectively. Additional details of the core and fuel modules are given in Reference 1.

LOCE L2-3 was designated as United States Standard Problem 10 by the NRC. In light of this designation, the results from this experiment will provide data for important computer code assessment. The peak cladding temperature calculations by several standard problem participants are compared with the measured data as described above.

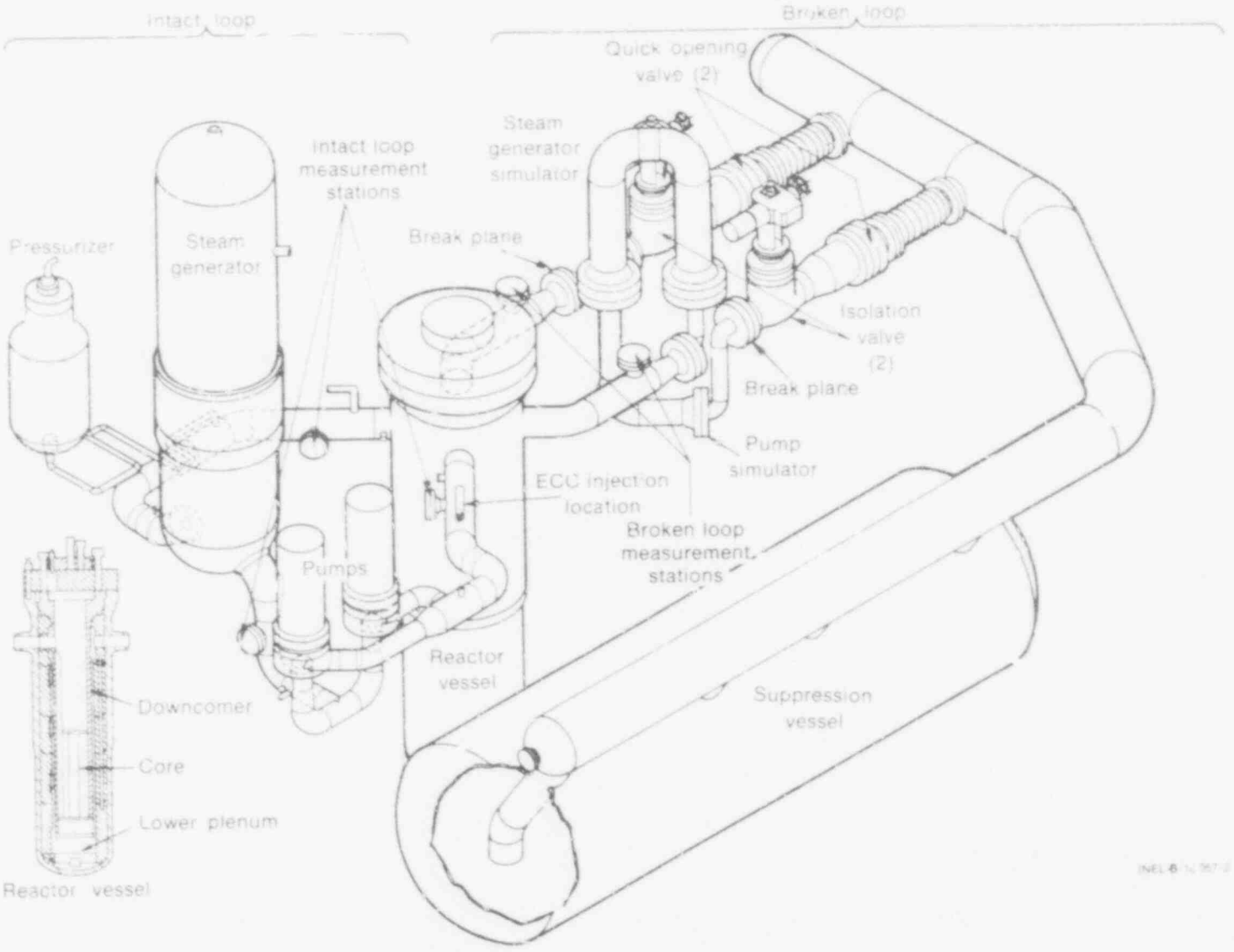

Fig. 1 Axonometric projection of LOFT system.

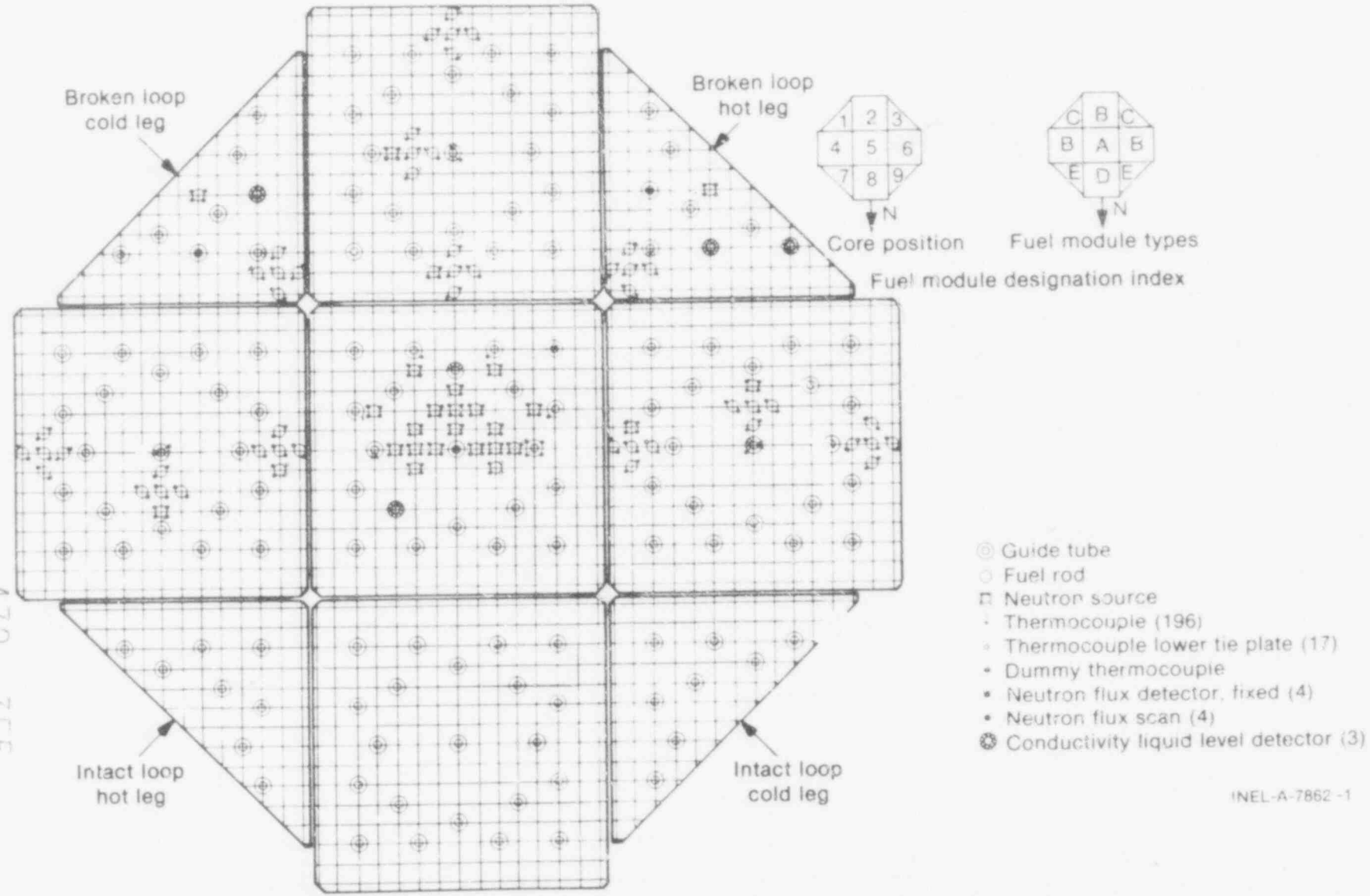

Fig. 2 LOFT core configuration and instrumentation.

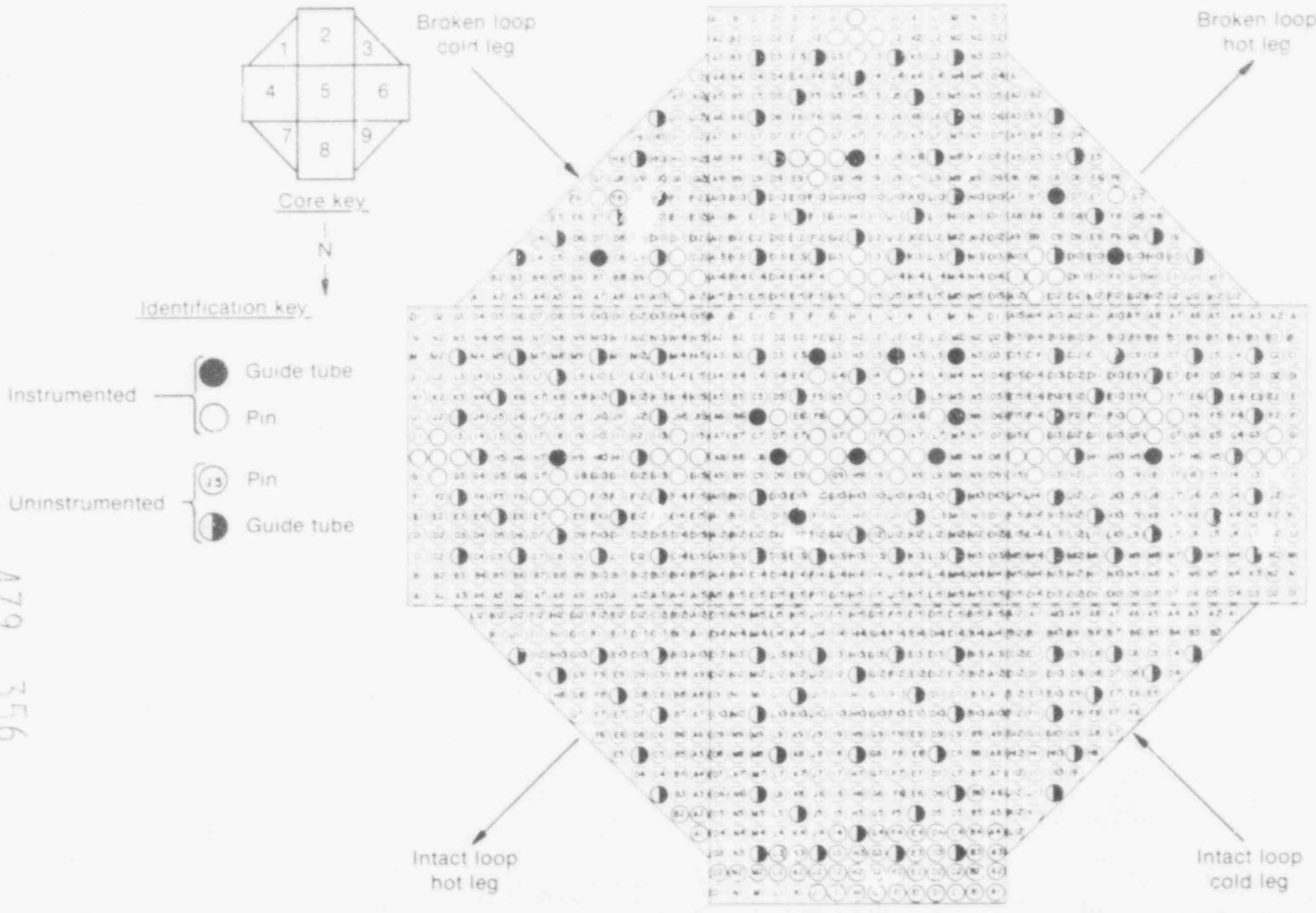

Fig. 3 LOFT core map showing position designations.

II. PLANT EVALUATION

An evaluation of plant performance is presented. The discussion summarizes the initial experimental conditions, the identifiable significant events, and the instrumentation performance for LOCE L2-3.

1. INITIAL EXPERIMENTAL CONDITIONS

A summary of the specified and measured system conditions immediately prior to LOCE L2-3 blowdown initiation is given in Table I. The measured average initial temperature of the primary coolant was 576.8 K; initial temperatures ranged from 560.7 to 592.9 K. The measured average initial cladding temperature was 598.4 K; the range of cladding temperatures was 567.4 to 618.4 K. The initial mass flow rate in the primary coolant loop was 199.8 kg/s, and pressurizer pressure was 15.1 MPa. The initial power level of 36.7 MW yielded a maximum linear heat generation rate (MLHGR) of 39.4 kW/m.

TABLE I

INITIAL CONDITIONS FOR NUCLEAR LOCE L2-3

Parameter	EOS Specified Value[3]	Measured Value
Primary Coolant System		
Mass flow rate (kg/s)[a]	--	199.8 ± 6.3
Pressure (MPa)	14.95 ± 0.34	15.06 ± 0.03
Temperature, T^h (K)	591.67 $^{+\ 2.2}_{-\ 7.2}$	592.9 ± 3
Boron concentration (ppm)	As required	679 ± 4
Cold leg temperature (K)	--	560.7 ± 3
Reactor Vessel		
Power level (MW)	--	36.7 ± 1
Maximum linear heat generation rate (kW/m)	39.4	39.4 ± 1
Control rod position (meters above full-in position)	1.372 ± 0.013	1.37 ± 0.01

TABLE I (continued)

Parameter	EOS Specified Value[3]	Measured Value
Pressurizer		
Steam volume (m^3)	--	0 2873 ± 0.008
Water volume (m^3)	--	0.7028 ± 0.008
Water temperature (K)	As required to establish pressure	615.3 ± 3
Pressure (MPa)	14.95 ± 0.34	15.06 ± 0.03
Level (m)	1.13 ± 0.178	1.19 ± 0.01
Broken Loop		
Hot leg fluid temperature (K)	587.6 $^{+\ 0}_{-\ 44.4}$	
Near vessel	--	565.49 ± 3
Near break	--	556.48 ± 3
Cold leg fluid temperature (K)	563.8 $^{+\ 0}_{-\ 14}$	
Near vessel	--	554.32 ± 3
Near break	--	550.37 ± 3
Steam Generator Secondary Side[b]		
Water level (m)	3.16	3.11 ± 0.025
Water temperature (K)	--	482 ± 3
Pressure (MPa)	--	6.17 ± 0.08
Mass flow rate (kg/s)	--	19.5 ± 0.4
ECC Accumulator A		
Gas volume (m^3)	--	0.9592 ± 0.03
Water volume injected (including line volume) (m^3)	--	1.714 ± 0.03
Pressure (MPa)	4.22 ± 0.17	4.18 ± 0.05
Temperature (K)	305.4 ± 8.3	307.2 ± 3
Boron concentration (ppm)	3100	3281 ± 17
Liquid level (m)	2.045 ± 0.03	2.037 ± 0.02
Suppression Tank		
Liquid level (m)	1.27 ± 0.0254	1.25 ± 0.02
Gas volume (m^3)	--	54.2 ± 0.59

TABLE I (continued)

Parameter	EOP Specified Value[3]	Measured Value
Suppression Tank (continued)		
Liquid volume (m^3)	--	28.68 ± 0.59
Downcomer submergence (m)[c]	--	0.3861 ± 0.02
Water temperature (K)	356 ± 3.6	350.1 ± 3
Pressure (gas space) (MPa)	0.086 ± 0.007	0.10 ± 0.01

a. Calculated.

b. Not controlled.

c. Based on average submergence of four downcomers.

d. Out of specification but did not affect results.

2. CHRONOLOGY OF EVENTS

Identifiable significant events that occurred during LOCE L2-3 are listed in Table II along with values from nonnuclear LOCE L1-5[14] and nuclear LOCE L2-2[15] for comparison. For LOCE L2-3, the emergency core coolant (ECC) injection from the high-pressure injection system (HPIS) and low-pressure injection system (LPIS) was initiated automatically upon receipt of a primary system hot leg low pressure indication coincident with a low pressurizer level trip. Accumulator ECC injection was initiated automatically when the primary system pressure reached 4.18 MPa. As shown in Table II, the HPIS, accumulator, and LPIS started injection 14, 17, and 29 s after experiment initiation, respectively.

The plant protection system (PPS) initiated the reactor scram during LOCE L2-3 and would have taken control of the LPIS and accumulator injection had not occurred within a specified time after rupture. This condition did not occur during LOCE L2-3 and the ECCS performed as planned.

479 359

TABLE II

CHRONOLOGY OF EVENTS FOR NUCLEAR LOCE L2-3 WITH LOCEs L2-2 AND L1-5 COMPARATIVE VALUES

Event	Time After LOCE Initiation (s)		
	LOCE L2-3	LOCE L2-2	LOCE L1-5
LOCE initiated	0	0	0
Subcooled blowdown ended[a]	0.05	0.07	0.1
Reactor scram signal received at control room	0.103	0.085	0.087
First indication of DNB[b]	0.96	1.0	25.6
Control rods completely inserted	1.683	1.725	
Subcooled break flow ended[c]	3.0	3.8	0.1
Maximum cladding temperature attained	4.95	5.8	0
Earliest core-wide rewet following DNB	8	8	48
HPIS injection initiated	14	12	13
Pressurizer emptied	14	15	14
Accumulator injection initiated	16	18	19
LPIS injection initiated	29	29	34
Lower plenum filled with liquid	35	35	37
Saturated blowdown ended	40	44	47
Accumulator liquid flow ended	45	49	54
Core volume reflooded	55	55	59

a. End of subcooled blowdown is defined as the occurrence of the first phase transition in the system excepting the pipe break location.

b. DNB - departure from nucleate boiling.

c. End of subcooled break flow is defined as the first time both break nozzles complete discharge of subcooled fluid.

479 360

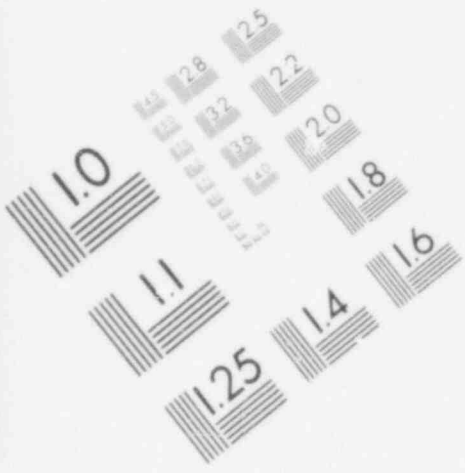

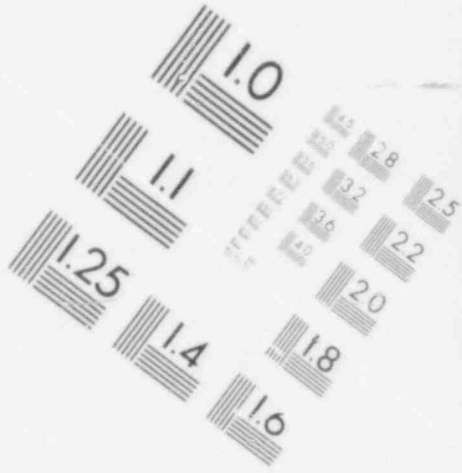

IMAGE EVALUATION TEST TARGET (MT-3)

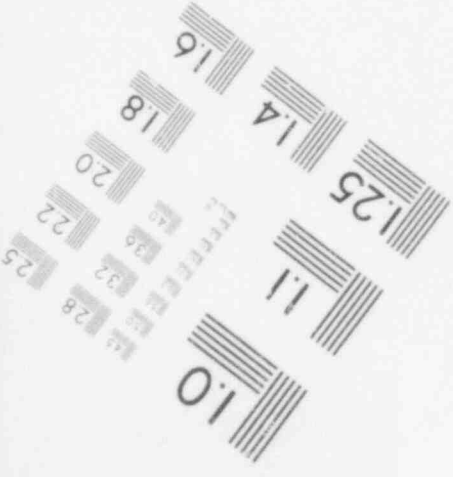

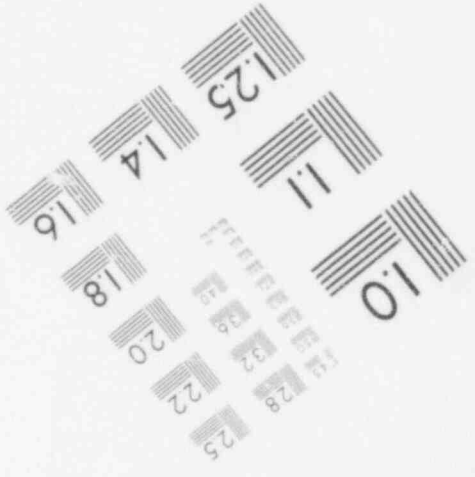

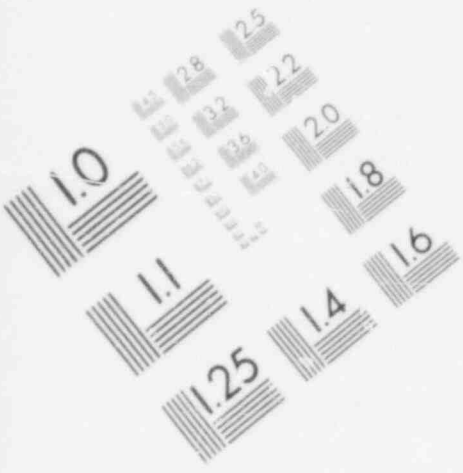

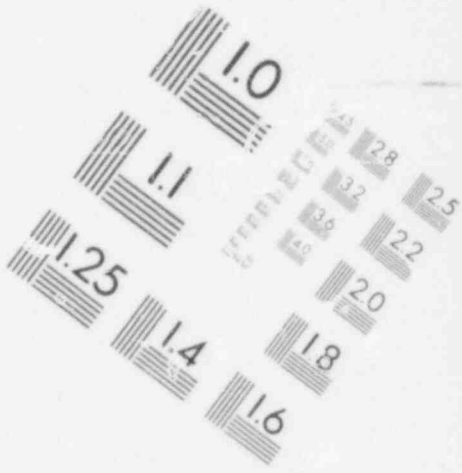

IMAGE EVALUATION TEST TARGET (MT-3)

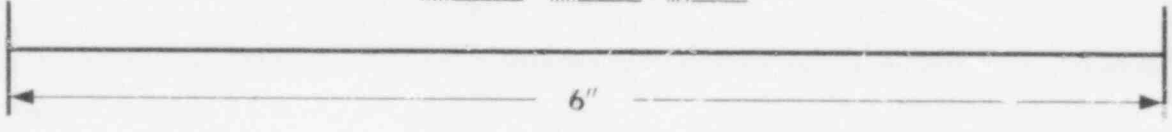

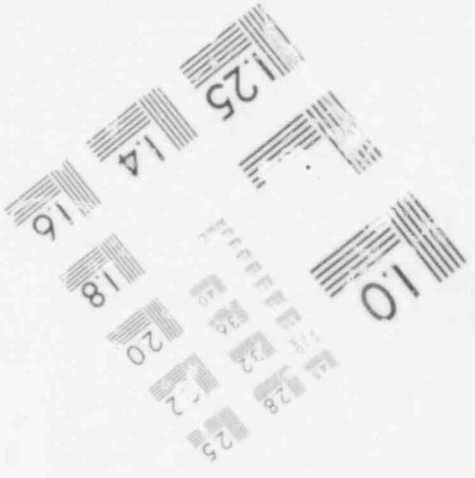

3. INSTRUMENTATION PERFORMANCE

The performance of the instruments and the data acquisition system during LOCE L2-3 was excellent. Of 888 instruments recorded for LOCE L2-3, it is estimated that 861 (97%) performed satisfactorily. The instrument failures did not significantly affect achievement of the objectives of LOCE L2-3. The loss of the Beam A in several of the gamma densitometers did not cause loss of density information at those measurement locations, since calculational techniques have been developed to provide good compensation for the loss of a single beam. The loss of the turbine meters in the upper plenum and downcomer (five locations) was not significant, since the drag discs at four of those measurement locations were operational. Some thermocouples and absolute pressure transducers failed. However, sufficient redundancy in these measurements existed to provide information on transient phenomena such that the failed instruments did not affect achievement of experiment objectives.

III. EXPERIMENTAL RESULTS FROM LOCE L2-3

The experimental results from LOCE L2-3 are summarized in the following sections: The section number corresponds to the objective being addressed in that section.

1. CORE THERMAL RESPONSE

The fuel rod cladding thermocouples performed well and provided core-wide data on fuel rod cladding thermal response satisfying this objective. The core-wide and spatial variations of fuel rod cladding thermal response are shown in Figures 4 through 7 and in Table III. The measured peak cladding temperature was 914 K, which occurred in the center module 0.38 m from the core bottom of fuel Rod E8.

The measured peak cladding temperature (PCT) of 914 K was measured at 5 s into the blowdown, prior to an early core-wide return to nucleate boiling (RNB) occurring by 8 s. This early RNB was the dominant influence on core thermal response as was the case in LOCE L2-2. The RNB time was essentially the same in both experiments. The temperatures measured in the core were higher and the duration of the intervals of film boiling was longer than in LOCE L2-2. All cladding temperature measurements showed that the core was completely quenched at about 54 s.

The hot rods in the core first experienced departure from nucleate boiling (DNB) at 0.96 s, after which the cladding temperature rose rapidly. This rise began to moderate at about 3 s, and the rods experienced a core-wide RNB from the bottom to the top of the core by 8 s. The cooler rods in the core did not experience the early DNB. Following the first RNB, at about 10 s, the hot rods experienced dryout and remained in a dryout condition until the ECC quenched the core. During this time, the cooler rods in the peripheral fuel modules and the upper and lower portions of the center fuel module underwent several dryout/RNB cycles. The temperature excursions during these cycles were generally smaller than those experienced

TABLE III

SUMMARY OF CORE TEMPERATURE RESPONSE CHARACTERISTICS

Instrument	$T_{initial}$(K)	T_{peak}(K)	t_{DNB}(s)[a]	t_{peak}(s)	t_{quench}(s)[b]
TE-1A11-030	608.28	733.41	2.99	6.19	41.33
TE-1B10-037	603.93	640.95	N/A[c]	6.37	40.09
TE-1B11-028	605.32	726.09	N/A	6.19	42.19
TE-1B11-032	606.31	712.87	2.99	6.25	42.25
TE-1B12-026	604.75	750.79	2.99	6.19	42.13
TE-1C11-021	594.85	700.13	2.99	0	37.47
TE-1F7-015	585.28	613.89	N/A	6.09	37.49
TE-1F7-021	585.11	632.60	N/A	6.19	39.83
TE-1F7-026	588.65	626.33	N/A	6.25	39.99
TE-1F7-030	596.66	639.52	N/A	6.23	42.17
TE-2E8-011	586.81	591.11	N/A	0.29	37.45
TE-2E8-030	603.63	609.19	N/A	6.53	42.27
TE-2E8-045	607.89	609.67	N/A	0	42.39
TE-2F7-015	603.32	604.49	N/A	0	40.05
TE-2F7-037	588.57	591.37	N/A	0.21	36.07
TE-2F8-028	601.08	603.20	N/A	0	40.03
TE-2F8-032	604.57	606.17	N/A	0	44.97
TE-2F9-026	599.95	604.03	N/A	16.50	42.09
TE-2F9-041	604.05	608.33	N/A	15.51	46.19
TE-2G02-030	590.81	593.17	N/A	0	39.97
TE-2G08-021	596.98	610.99	N/A	16.23	39.85
TE-2G08-039	604.33	605.74	N/A	0	42.23
TE-2G14-011	595.55	790.73	1.17	4.87	39.77
TE-2G14-030	612.00	799.84	1.19	5.57	52.35
TE-2G14-045	615.56	663.95	1.35	6.55	44.01
TE-2H01-037	585.03	589.67	N/A	0.21	39.99
TE-2H02-028	585.07	591.32	N/A	0.13	39.93
TE-2H02-032	587.06	590.98	N/A	0.13	40.05
TE-2H03-026	592.02	595.47	N/A	0	39.93
TE-2H08-039	583.44	591.85	N/A	0.11	44.53
TE-2H13-021	601.55	752.33	2.17	5.55	39.89
TE-2H13-049	612.55	647.32	N/A	6.55	43.39
TE-2H14-028	606.62	782.95	1.59	5.29	50.47
TE-2H14-032	611.23	805.28	1.55	6.33	46.01
TE-2H15-026	608.22	853.01	2.37	5.15	50.51

480 003

TABLE III (continued)

Instrument	$T_{initial}$(K)	T_{peak}(K)	t_{DNB}(s)[a]	t_{peak}(s)	t_{quench}(s)[b]
TE-2H15-041	613.29	745.93	1.63	6.31	47.53
TE-2I02-021	589.78	604.61	N/A	6.11	37.55
TE-2I02-039	584.52	589.94	N/A	0.19	40.19
TE-2I14-021	600.32	841.53	1.31	4.47	42.05
TE-2I14-039	611.95	760.61	2.25	3.39	46.71
TE-3A11-030	604.26	745.53	2.99	6.23	45.85
TE-3B10-037	603.35	649.92	N/A	37.55	42.17
TE-3B11-028	605.46	695.32	N/A	6.23	50.43
TE-3B11-032	610.63	716.60	N/A	6.31	48.27
TE-3B12-026	608.16	757.81	2.99	6.21	50.33
TE-3C11-021	591.95	674.55	N/A	5.71	37.49
TE-3C11-039	608.09	656.64	N/A	6.47	46.39
TE-3F7-015	581.32	611.90	N/A	6.11	39.37
TE-3F7-021	586.46	635.21	N/A	6.21	39.83
TE-3F7-026	587.97	637.34	N/A	6.21	42.07
TE-[illegible]-030	593.66	645.47	N/A	6.21	42.33
TE-4E8-011	586.88	591.13	N/A	0.27	37.41
TE-4E8-030	604.34	612.40	N/A	6.25	40.09
TE-4E8-045	613.70	615.60	N/A	0	42.27
TE-4F7-015	582.77	594.26	N/A	6.13	37.45
TE-4F7-037	596.16	597.67	N/A	0	40.1[illegible]
TE-4F8-028	603.05	605.91	N/A	0	40.0[illegible]
TE-4F8-032	602.70	604.52	N/A	0	40.14
TE-4F9-026	599.42	601.04	N/A	0	44.44
TE-4F9-041	607.88	609.42	N/A	0	42.24
TE-4G02-030	593.13	622.96	N/A	6.16	40.14
TE-4G08-021	594.82	596.89	N/A	0	37.60
TE-4G08-039	608.11	609.64	N/A	0	42.24
TE-4G14-030	611.20	847.15	1.32	5.22	37.72
TE-4G14-045	614.58	691.52	1.34	6.40	42.30
TE-4H01-037	586.61	590.32	N/A	0.34	40.12
TE-4H02-028	587.61	615.40	N/A	6.16	40.00
TE-4H02-032	589.87	608.46	N/A	6.50	40.24
TE-4H03-026	589.24	612.92	N/A	6.40	39.99
TE-4H08-039	545.94	548.93	N/A	1.12	44.58
TE-4H13-037	615.28	657.43	2.48	3.06	40.12
TE-4H14-028	610.20	860.27	1.56	6.20	40.12
TE-4H14-032	606.89	840.64	1.38	5.36	42.14
TE-4H15-026	617.87	875.27	1.40	5.76	39.96

480 004

TABLE III (continued)

Instrument	$T_{initial}$(K)	T_{peak}(K)	t_{DNB}(s)[a]	t_{peak}(s)	t_{quench}(s)[b]
TE-4H15-041	616.74	782.49	2.10	6.36	40.22
TE-4I02-021	582.95	604.31	N/A	5.92	37.58
TE-4I02-039	593.39	594.15	N/A	0	42.28
TE-4I14-021	613.68	832.68	1.38	4.76	37.54
TE-4I14-039	616.75	790.10	1.52	6.32	40.08
TE-5C6-024	574.34	581.97	N/A	0.66	37.96
TE-5D6-030	608.71	879.05	1.54	6.30	50.86
TE-5D6-032	613.60	876.29	1.34	6.20	52.80
TE-5D6-037	612.00	839.89	1.34	4.94	46.78
TE-5D6-039	616.01	859.52	1.40	6.34	50.50
TE-5E8-015	596.41	914.07	0.94	4.96	42.92
TE-5E8-034.5	605.81	807.02	1.36	5.76	40.70
TE-5E8-049	614.87	787.74	1.30	6.42	43.50
TE-5F3-024	573.91	658.[illegible]	N/A	40.28	47.74
TE-5F4-015	596.08	873.[illegible]	1.18	5.78	42.06
TE-5F4-021	609.94	878.66	[illegible].20	5.72	46.38
TE-5F4-026	610.23	856.97	1.32	5.56	50.52
TE-5F4-030	612.19	908.05	1.30	5.80	54.32
TE-5F7-005	581.35	796.05	1.06	4.04	35.80
TE-5F7-039	608.85	38.43	1.30	5.56	47.40
TE-5F7-054	614.66	762.42	1.60	6.44	42.30
TE-5F8-024	610.06	886.85	1.04	4.36	52.34
TE-5F8-028	608.38	890.38	1.12	5.32	53.70
TE-5F8-032	611.42	860.49	1.04	5.76	52.74
TE-5F8-037	615.96	852.02	1.12	5.56	46.30
TE-5F9-011	593.06	838.41	0.98	5.78	39.80
TE-5F9-030	607.42	867.69	1.24	5.56	48.18
TE-5F9-045	616.98	807.82	1.44	6.38	38.18
TE-5F9-062	614.79	710.69	1.84	6.52	40.30
TE-5G6-011	591.83	835.44	1.0	5.70	39.76
TE-5G6-030	608.78	859.84	1.20	5.52	54.96
TE-5G6-045	613.10	918.50	1.52	6.42	44.50
TE-5G6-062	612.03	708.82	1.82	6.50	42.52
TE-5G8-008	592.72	816.49	1.08	4.14	37.44
TE-5G8-026	606.81	887.15	1.24	5.52	51.68
TE-5G8-041	615.13	805.78	1.32	5.52	47.58
TE-5G8-058	614.52	717.80	1.78	6.48	42.38
TE-5H5-002	569.77	706.55	1.32	3.24	60.52
TE-5H5-015	594.44	884.74	1.12	5.00	46.06
TE-5H5-034.5	610.59	848.97	1.20	6.30	44.08

TABLE III (continued)

Instrument	$T_{initial}$(K)	T_{peak}(K)	t_{DNB}(s)[a]	t_{peak}(s)	t_{quench}(s)[b]
TE-5H5-049	614.10	774.34	1.32	6.42	43.18
TE-5H6-024	603.46	879.83	1.12	4.80	51.04
TE-5H6-028	607.07	884.49	1.14	5.40	53.94
TE-5H6-032	610.65	879.27	1.20	5.90	53.70
TE-5H6-037	611.75	846.59	0.96	5.70	46.78
TE-5H7-008	597.19	817.71	1.28	4.40	37.44
TE-5H7-026	606.83	894.00	1.14	5.70	51.88
TE-5H7-041	612.03	826.24	1.14	6.34	43.34
TE-5H7-058	612.50	729.45	1.78	6.48	42.38
TE-5I6-005	577.43	806.20	1.12	3.94	35.58
TE-5I6-021	609.75	898.31	1.22	5.38	42.12
TE-5I6-039	613.18	848.08	1.06	5.66	48.72
TE-5I6-054	613.41	746.22	1.62	6.44	40.34
TE-5I8-008	595.76	823.78	1.18	4.84	37.42
TE-5I8-026	611.84	895.97	1.26	5.72	51.14
TE-5I8-041	615.13	821.43	1.26	6.36	50.90
TE-5I8-058	615.18	732.64	1.74	6.50	42.50
TE-5J3-024	572.66	654.38	N/A	40.14	47.78
TE-5J4-015	595.99	887.93	1.24	5.52	42.04
TE-5J4-021	608.40	898.70	1.52	5.36	42.12
TE-5J4-026	611.75	879.54	1.26	5.30	51.16
TE-5J4-030	612.00	907.96	1.12	5.54	54.80
TE-5J7-011	590.97	834.26	1.04	5.64	41.92
TE-5J7-030	609.90	861.70	1.06	6.18	54.50
TE-5J7-045	618.29	804.53	1.34	6.42	40.76
TE-5J7-062	613.49	710.62	1.82	6.48	42.42
TE-5J8-024	612.18	885.90	1.04	4.88	52.20
TE-5J8-028	611.73	905.31	0.96	5.42	54.50
TE-5J8-032	618.15	888.50	1.08	5.54	53.44
TE-5J8-037	610.13	852.40	1.12	5.74	46.74
TE-5J9-005	587.56	760.20	1.06	3.18	35.62
TE-5J9-021	598.52	904.08	1.16	5.38	45.46
TE-5J9-039	614.30	835.07	1.30	5.72	44.20
TE-5J9-054	615.40	744.05	1.56	6.42	42.32
TE-5K8-002	568.57	718.70	1.20	3.26	60.84
TE-5K8-015	603.87	890.87	1.60	5.00	39.90
TE-5K8-034.5	612.22	816.82	1.40	5.70	42.22
TE-5K8-049	612.61	780.44	1.30	5.96	43.08
TE-5L6-030	611.35	892.25	1.26	5.36	52.34
TE-5L6-032	615.10	867.94	1.10	5.16	52.28
TE-5L6-037	614.11	829.56	1.04	5.70	42.28

480 006

TABLE III (continued)

Instrument	$T_{initial}$(K)	T_{peak}(K)	t_{DNB}(s)[a]	t_{peak}(s)	t_{quench}(s)[b]
TE-5L6-039	614.21	806.53	1.34	6.20	50.[illegible]
TE-5L8-011	567.39	578.53	N/A	2.34	35.02
TE-5L8-024	575.49	580.94	N/A	1.28	36.70
TE-5L8-039	588.76	589.66	N/A	0.42	38.16
TE-5L8-045	592.23	593.18	N/A	0	40.50
TE-5M6-024	573.64	657.47	N/A	40.23	47.42
TE-6E8-011	591.88	595.71	N/A	0	37.44
TE-6E8-030	605.27	606.75	N/A	0	42.30
TE-6E8-045	609.18	610.07	N/A	0	42.44
TE-6F7-015	585.52	592.34	N/A	6.06	37.44
TE-6F7-037	602.65	603.81	N/A	0	39.92
TE-6F8-028	599.05	598.05	N/A	0	
TE-6F8-032	602.29	603.89	N/A	0	42.40
TE-6F9-026	593.86	600.32	N/A	13.74	42.06
TE-6F9-041	603.09	604.98	N/A	0	40.24
TE-6G02-030	587.02	596.66	N/A	6.50	37.60
TE-6G08-021	595.65	598.67	N/A	0	39.27
TE-6G08-039	601.92	604.60	N/A	0	40.17
TE-6G14-011	602.41	802.56	1.41	5.11	39.23
TE-6G14-030	616.10	836.08	1.79	4.75	46.55
TE-6G14-045	615.41	728.75	1.45	4.71	44.15
TE-6H01-037	583.43	589.53	N/A	0.34	37.77
TE-6H02-028	588.83	591.99	N/A	0.11	39.91
TE-6H02-032	585.82	589.98	N/A	0.21	42.15
TE-6H03-026	595.33	596.85	N/A	0	39.85
TE-6H08-039	580.94	583.76	N/A	0.91	44.53
TE-6H13-015	595.55	754.48	2.53	4.55	37.49
TE-6H13-037	609.88	696.07	1.91	3.37	40.11
TE-6H14-028	607.64	810.04	1.52	4.62	42.18
TE-6H14-032	614.74	848.82	1.40	4.56	43.14
TE-6H15-026	610.25	867.49	1.42	5.88	42.10
TE-6H15-041	616.15	747.47	1.50	4.66	38.04
TE-6I02-021	582.76	588.88	N/A	0.23	37.48
TE-6I02-039	589.86	591.58	N/A	0	40.12
TE-6I14-021	604.55	867.15	1.28	5.38	42.12
TE-6I14-039	613.96	726.33	1.36	4.22	42.26

a. Time to first DNB.

b. Time to final quench.

c. N/A - not applicable (did not go into DNB).

by the hotter rods. The cooler rods were quenched by the ECC slightly sooner than the central portion of the core.

The thermal response varied with location in the core both axially and radially. The largest temperature excursions and longest durations of film boiling occurred in the central and slightly lower portion of the center fuel module. The response was progressively less severe toward the edges and upper and lower regions of the core. The thermal repsonse was generally axisymmetric near the center of the core becoming less axisymmetric near the periphery. Fuel rods in Modules 2 and 6 had thermal responses similar to those in Module 4 during the first 10 s and generally experienced longer dryout/RNB cycles during the remainder of the transient. Fuel rods in Module 3 generally experienced larger temperature excursions and longer periods of dryout than did rods at axisymmetric positions in Module 1. The final quench occurred from the bottom up and the top down. The quench was basically uniform radially with the rods in the center fuel module quenching slightly slower than in the peripheral fuel modules. All fuel rods were quenched by 54 s. Core reflood was complete at 55 s.

Figures 8 through 10 shown three-dimensional axial temperature histories from three locations in the center bundle. Figures 11 through 15 show three-dimensional axial temperature histories for axisymmetric positions in the three instrumented control modules and radial temperature histories at two axial locations. Figures 16 through 21 show measured cladding temperature along the axial length of the fuel rods clustered about fuel Rod 5F8 (center module).

Testing performed in the Power Burst Facility[16], at Columbia University[17], and in the LOFT Test Support Facility[18] indicate measured DNB times may be in error $\pm$0.5 s due to the thermocouple attached to the fuel rod. Measured peak cladding temperatures may be in error by $\pm$20 K, and quench times may be in error by $\pm$5 s.

480 008

2. THERMAL-HYDRAULIC PHENOMENA

The LOFT experimental instrumentation worked well measuring fluid pressures, temperatures, densities, mass flow rates, and fuel rod cladding temperatures. The measurements allowed a comprehensive determination of the thermal-hydraulic phenomena occurring during the LOCE L2-3 and subsequent effects on fuel rod thermal response.

The system hydraulics during blowdown dominated the transient thermal response as in LOFT LOCE L2-2. The hydraulic effects moderated the cladding temperature rise and rewet the core by 8 s after rupture. The migration of hot core fluid to the cold leg break and the interaction of the intact and broken loop cold leg mass flows were the strongest influences on the thermal-hydraulic response. The ECC quenched all the core fuel rods by 54 s. The core was reflooded completely by 55 s.

Subcooled blowdown ended at about 50 ms and was followed by core initial DNB at about 0.96 s. ore flow stagnated and reversed by 0.12 s with hotter fluid migrating to the broken loop cold leg by about 2.5 s, as seen in Figure 22. Low magnitude positive core flow was reestablished by about 2 s which caused the moderation of cladding temperature rise. The migration of the hotter core fluid to the broken loop cold leg initiated saturated choking at 3.0 s. This choking caused a reduction in flow to below the intact loop cold leg flow rate, as shown in Figure 23, which in turn caused an insurge of coolant to the downcomer. This coolant insurge was the driving force for the early rewet of the core. At about 6.4 s the coolant in the pump suction leg became saturated and reduced the pump suction head causing a reduction in intact loop cold leg flow. This reduction in flow and increased quality was propagated to the core, reduced cooling, and caused the fuel rod cladding temperatures to begin to rise. After initiation of accumulator flow, the localized low pressure in the intact loop cold leg and downcomer caused a minor core flow reversal, which induced a top-down rewet in the core. This rewet only progressed down to approximately the 0.85 m elevation and did not

rewet the entire axial length. The other rewets and dryouts prior to the final quench appear to be caused by local thermal-hydraulic phenomena. The ECC began to penetrate the downcomer at 18 s and filled the lower plenum by about 35 s. The core began to reflood at 0.1 m/s and reflooded completely by 55 s. Thermal-hydraulic data plots are shown in Figures 24 through 34.

3. EMERGENCY CORE COOLING SYSTEM PERFORMANCE

The ECCS performed as expected. The accumulator, LPIS, HPIS, and total ECCS flow rates are shown in Figures 35 through 38. ECCS initiation times are presented in Table II along with other pertinent LOCE events. Preliminary analysis of the data has shown that the ECCS performed in a manner similar to that in LOFT LOCE L2-2, which was performed at a lower power. Indications are that the ECCS performance indices of hot wall delay, ECC bypass, lower plenum refill rate, and core reflood rate were not adversely affected by the presence of stored energy in the core resulting from steady state power generation with a MLHGR of 39.4 kW/m. The magnitudes of the performance indices determined in the LOFT nonnuclear LOCEs and nuclear LOCE L2-2 do not vary significantly as a function of initial core power level in LOFT LOCEs up to this power level.

The ECC quenched the core by 54 s, with reflood starting at 35 s and a reflood rate of 0.1 m/s. The LOCE L2-3 reflood rate was similar to that seen in LOCEs L2-2 and L1-5 and was nearly uniform radially as in these two previous LOCEs. The liquid level plots presented in Figures 39 through 42 indicate the reflood rate for LOCE L2-3.

4. FUEL ROD CLADDING INTEGRITY

No cladding perforation occurred in LOCE L2-3. Chemistry samples taken from the suppression system after the experiment indicated no fission products were released into the blowdown effluent. The lack of fission products in the suppression system is a strong indication that no cladding perforation occurred during the experiment.

Other indices of fuel rod deformation and degradation also indicate the fuel rods were not damaged during LOCE L2-3. The cladding did not enter the buckling, ballooning, or collapse regimes of deformation[19], as shown in Figure 43. The PCT measured during the experiment was below that necessary for significant metal-water reaction to occur. Posttest examination of the fuel will confirm the cladding condition.

5. CODE ASSESSMENT PARAMETERS

The data taken during LOCE L2-3 were sufficient to allow assessment of important computer code calculational capabilities. The experiment was successful in providing data necessary for adequate code assessment.

Examples of LOCE L2-3 data applicable for code assessment are shown in Figures 44 through 50. The data are overlaid with pretest calculations made with the RELAP4/MOD6 and TRAC-P1A computer codes and Semiscale Mod-1 data. The comparison of measured PCT with predicted temperatures is shown in Figure 51.

IV. CONCLUSIONS

The conduct of LOFT LOCE L2-3 and the experimental data acquired concerning integral systems phenomena associated with a loss of coolant are considered to have met the objectives as defined by the experiment operating specification[3] and discussed as in Section III. Conclusions based on the preliminary analyses and experiment assessment are:

(1) The transient response during LOCE L2-3 was dominated by a core-wide rewet during the blowdown phase of the experiment, as was the case in LOFT LOCE L2-2.

(2) No fuel rod damage was indicated to have occurred in LOCE L2-3.

(3) The ECCS functioned as expected and cooled the core to 420 K by 54 s. The ECCS performance was not significantly affected by the initial power level of 39.4 kW/m.

(4) The measured and predicted hydraulic responses agreed quite well. The measured hydraulic behavior of LOCE L2-3 was similar to that seen in LOCE L2-2 and in LOFT counterpart Test S-06-3 performed in the Semiscale Mod-1 facility.

(5) The measured and calculated cladding temperatures did not agree. The PCT measured during blowdown was less than that calculated by all methods except the developmental TRAC-P1A+Iloeje. This method predicted PCT during blowdown within the uncertainty of the measured data. Also, the TRAC-P1A+Iloeje was the only method to predict the early rewet and RNB.

V. DATA PRESENTATION

This section presents selected, preliminary data from LOCE L2-3. LOCE L2-3 data are overlayed with data from LOFT counterpart Test S-06-3[4] performed in Semiscale and LOCE L2-3 pretest calculations using the RELAP4/MOD6[6], FRAP-T4[20], and TRAC-P1A[8] computer codes. A listing of the data plots is presented in Table IV. Table V gives the nomenclature system used in instrumentation identification. A complete list of the LOFT instrumentation and data acquisition requirements for LOCE L2-3 is given in Reference 3.

The maximum uncertainties in the reported data are as follows:

(1) Temperature - $\pm$ 3 K

(2) Pressure - $\pm$ 0.03 MPa

(3) Density - $\pm$ 0.03 Mg/m^3

(4) Mass flow rate - $\pm$ 25 kg/s (est.)

(5) Momentum flux - $\pm$ 12.0 $Mg/m\text{-}s^2$.

The liquid level plots, Figures 39 through 42, are made by analyzing the voltage output of conductivity liquid level probes using the following criteria:

(1) A response time of 550 ms during dryout or wetting was assumed.

(2) The void fraction is assumed to vary linearly with the voltage. The maximum voltage measured during the LOCE from each probe is an indication of 100% void.

480 013

TABLE IV

LIST OF DATA PLOTS

Figure	Title	Measurement Identification	Page
4	Temperature of cladding in fuel Module 5	TE-5K6-030 TE-5D6-032 TE-5D6-037 TE-5D6-039	31
5	Temperature of cladding in fuel Module 3	TE-3C11-021 TE-3B12-026 TE-3B11-032 TE-3B10-037	31
6	Temperature of cladding in fuel Module 2	TE-2I02-021 TE-2H02-028 TE-2H02-032 TE-2H01-037	32
7	Temperature of cladding in fuel Module 1	TE-1C11-021 TE-1B12-026 TE-1B11-032 TE-1B10-037	32
8	Three-dimensional axial profile of cladding temperature in fuel Module 5	TE-5K8-2 TE-5J9-5 TE-5I8-8 TE-5J7-11 TE-5K8-15 TE-5J9-21 TE-5J8-24 TE-5I8-26 TE-5J8-28 TE-5J7-30 TE-5J8-32 TE-5K8-34.5 TE-5J8-37 TE-5J9-39 TE-5I8-41 TE-5J7-45 TE-5K8-49 TE-5J9-54 TE-5I8-58 TE-5J7-62	33

480 014

TABLE IV (continued)

Figure	Title	Measurement Identification	Page
9	Three-dimensional axial profile of cladding temperature in fuel Module 5	TE-5F7-5 TE-5F7-21 TE-5F7-39 TE-5F7-54 TE-5F4-26 TE-5F4-30 TE-5D6-32 TE-5D6-37	34
10	Three-dimensional axial profile of cladding temperature in fuel Module 5	TE-5H5-2 TE-5G6-11 TE-5F4-15 TE-5F4-21 TE-5F4-26 TE-5F4-30 TE-5H5-34.5 TE-5G6-45 TE-5H7-58	35
11	Three-dimensional axial profile of cladding temperature in fuel Module 2	TE-2I2-21 TE-2H3-26 TE-2H2-28 TE-2G2-30 TE-2H2-32 TE-2H1-37 TE-2I2-39	36
12	Three-dimensional axial profile of cladding temperature in fuel Module 4	TE-4G14-11 TE-4H13-15 TE-4I14-21 TE-4H15-26 TE-4H14-28 TE-4G14-30 TE-4H14-32 TE-4H13-37 TE-4I14-39 TE-4H15-41 TE-4G14-45	37
13	Three-dimensional axial profile of cladding temperature in fuel Module 6	TE-6I2-21 TE-6H3-26 TE-6H2-28 TE-6G2-30 TE-6H2-32 TE-6H1-37 TE-6I2-39	38

480 015

TABLE IV (continued)

480 016

480 016

TABLE IV (continued)

480 017

TABLE IV (continued)

480 018

TABLE V

NOMENCLATURE FOR LOFT INSTRUMENTATION

Designations for the different types of transducers:[a]

TE	-	Temperature element	FE	-	Coolant flow transducer
PE	-	Pressure transducer	DE	-	Densitometer
PdE	-	Differential pressure transducer	DiE	-	Displacement transducer
			ME	-	Momentum flux transducer
LE	-	Coolant level transducer	FT	-	Flow rate transducer

Designations for the different systems, except the nuclear core:

PC	-	Primary coolant intact loop	UP	-	Upper plenum
			LP	-	Lower plenum
BL	-	Broken loop	ST	-	Downcomer stalk
RV	-	Reactor vessel	P120	-	ECCS
SV	-	Suppression tank	P128	-	Primary coolant addition and control

Designations for nuclear core instrumentation:

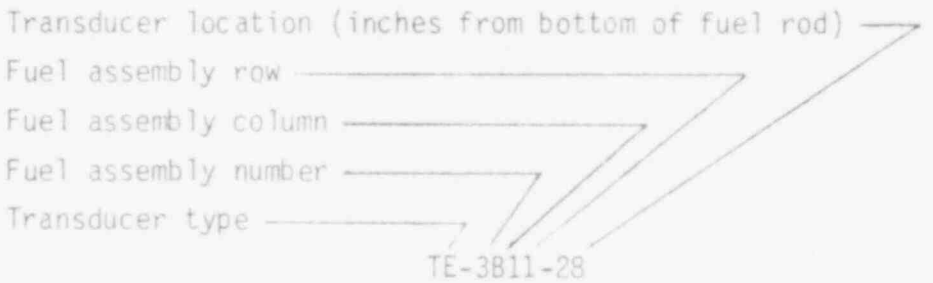

a. Includes only instruments discussed in this report.

(3) When there is a change in prase from water to steam, an "X" is indicated for void fractions less than 20%, with the space left blank for void fractions greater than 80%. A "0" is indicated for void fraction between 20 and 80% void.

480 019

Engineering judgment was required at times on each conductivity probe in order to best satisfy the above criteria.

Caution should be exercised in applying the in-core liquid level data to the core as a whole because the in-core liquid level stings are located at "cold spots" (that is, along guide tubes rather than fuel rods) in the core. Prior to the first rewet, these liquid level plots indicate more fluid than is present at the surrounding hotter fuel rods due to the effects of a strong radial temperature profile.

The data designated RELAP A in the figures are from a RELAP4/MOD6 pretest calculation[5]. Subsequent to that calculation, the experiment initial conditions were changed and some modeling changes were instituted[6]. The data designated RELAP B reflect these changes.

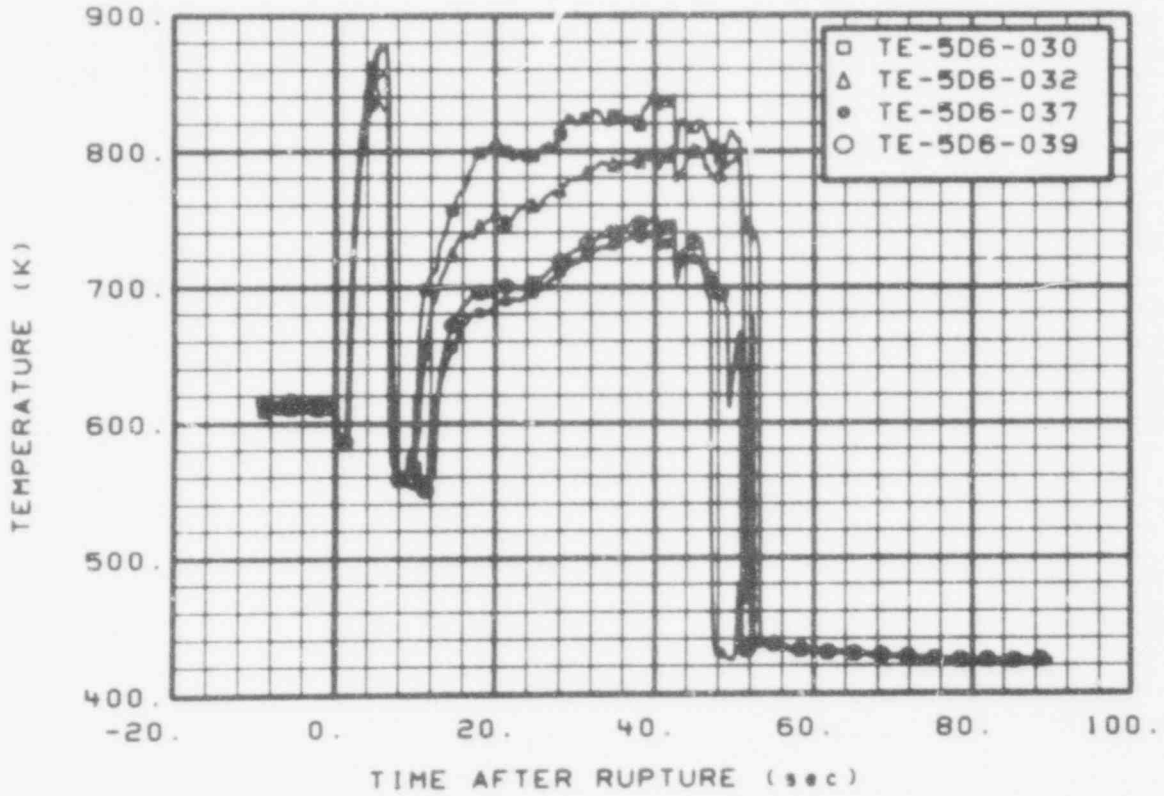

Fig. 4 Temperature of cladding in fuel Module 5.

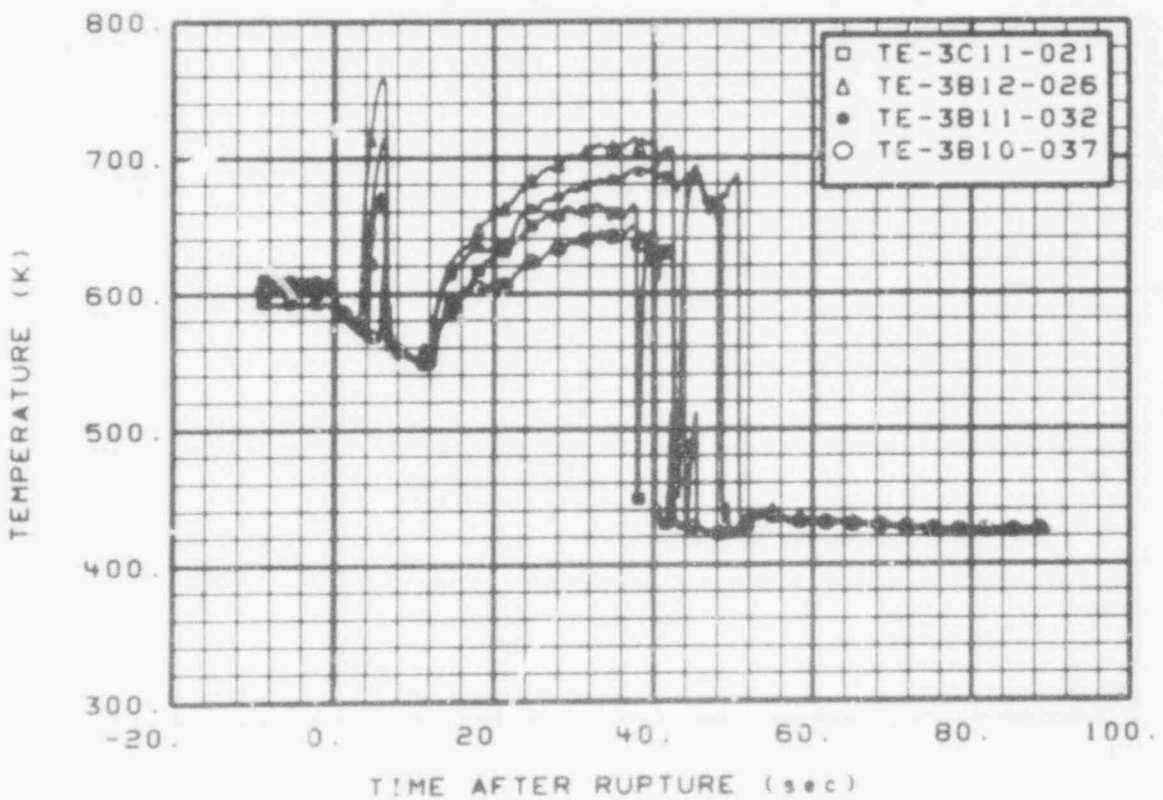

Fig. 5 Temperature of cladding in fuel Module 3.

480 021

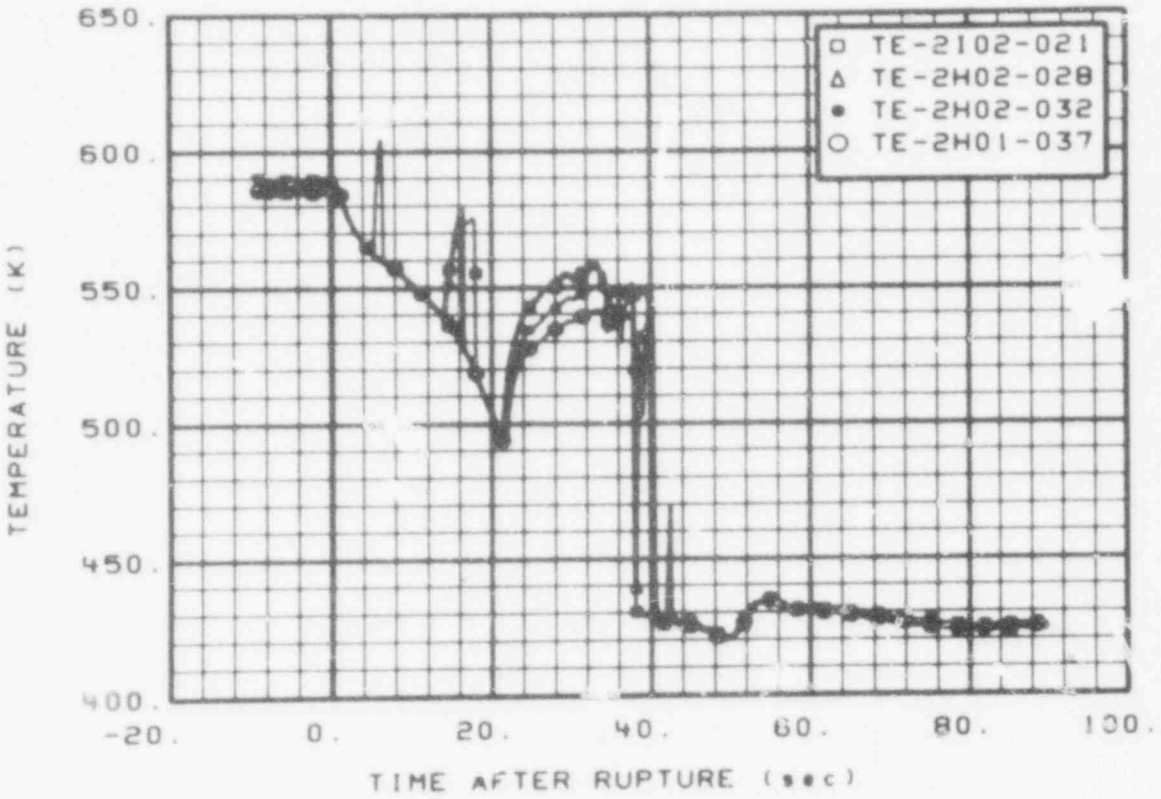

Fig. 6 Temperature of cladding in fuel Module 2.

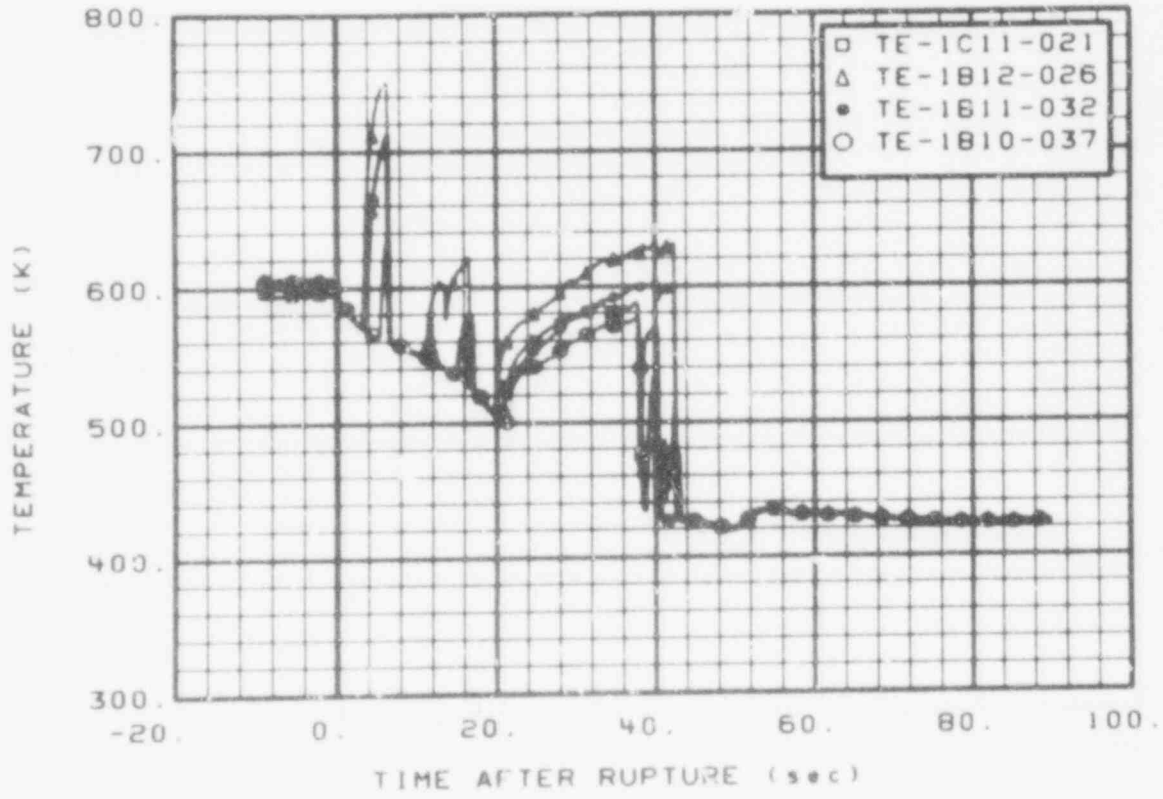

480 022

Fig. 7 Temperature of cladding in fuel Module 1.

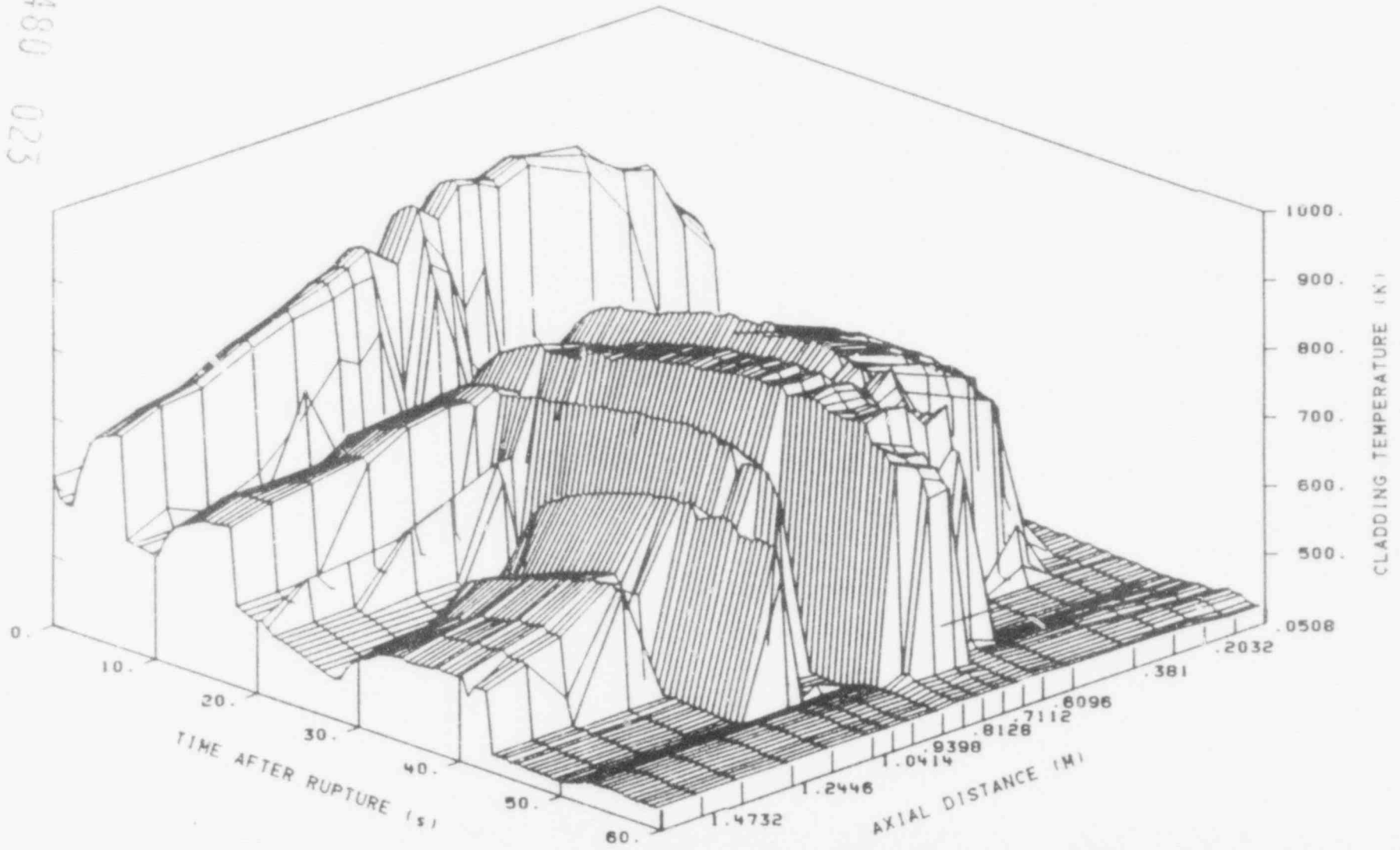

Fig. 8 Three-dimensional axial profile of cladding temperature in fuel Module 5.

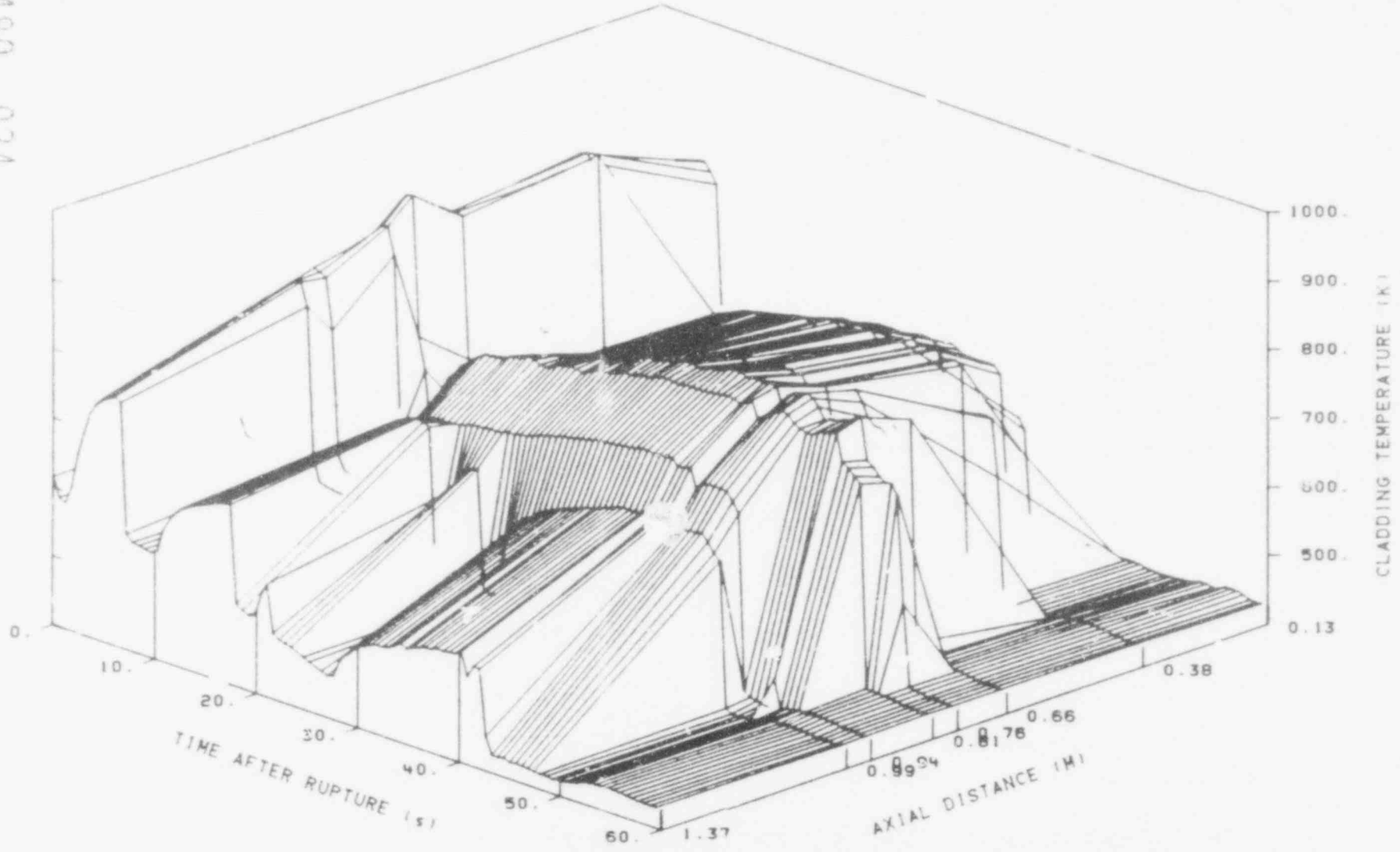

Fig. 9 Three-dimensional axial profile of cladding temperature in fuel Module 5.

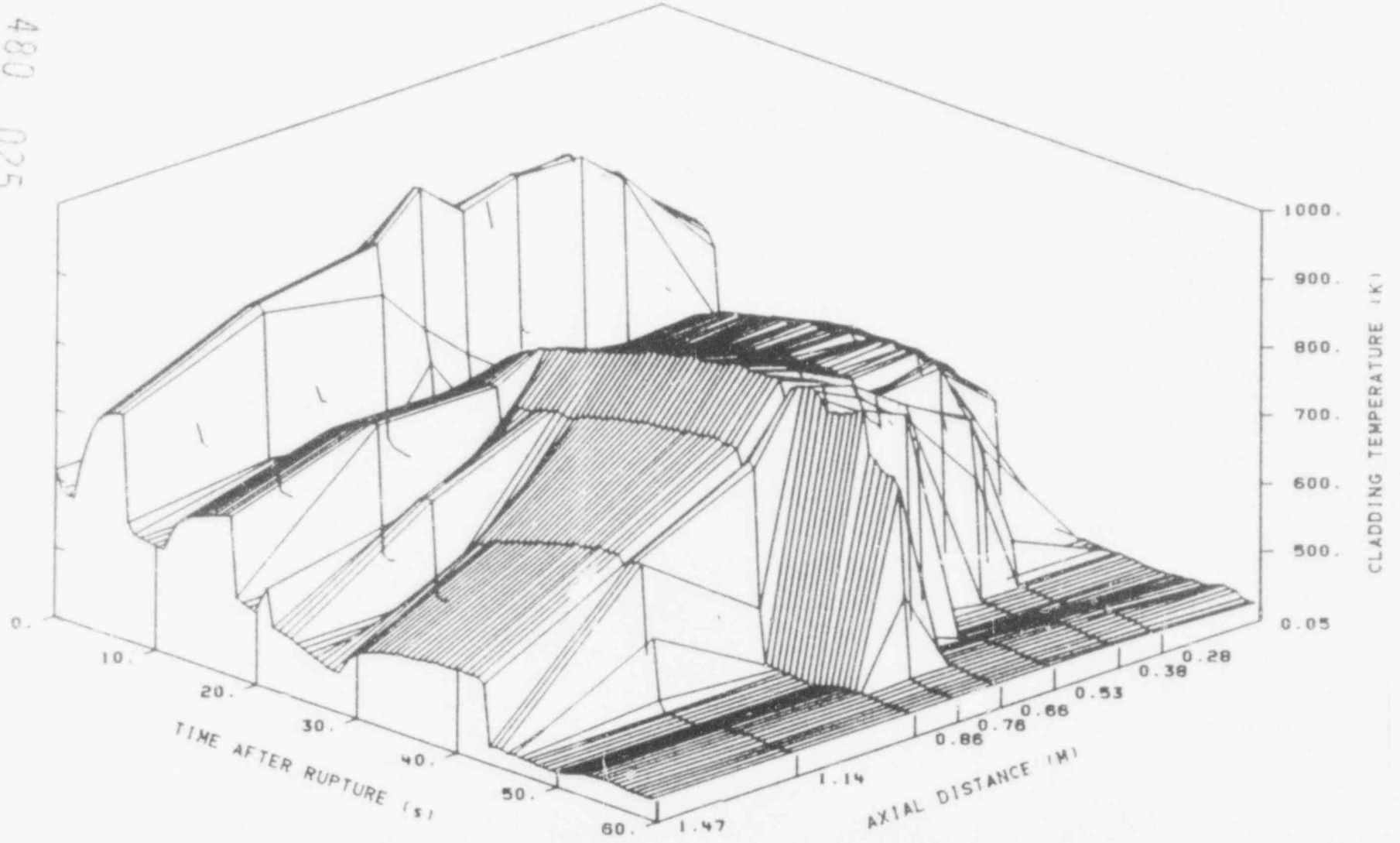

Fig. 10 Three-dimensional axial profile of cladding temperature in fuel Module 5.

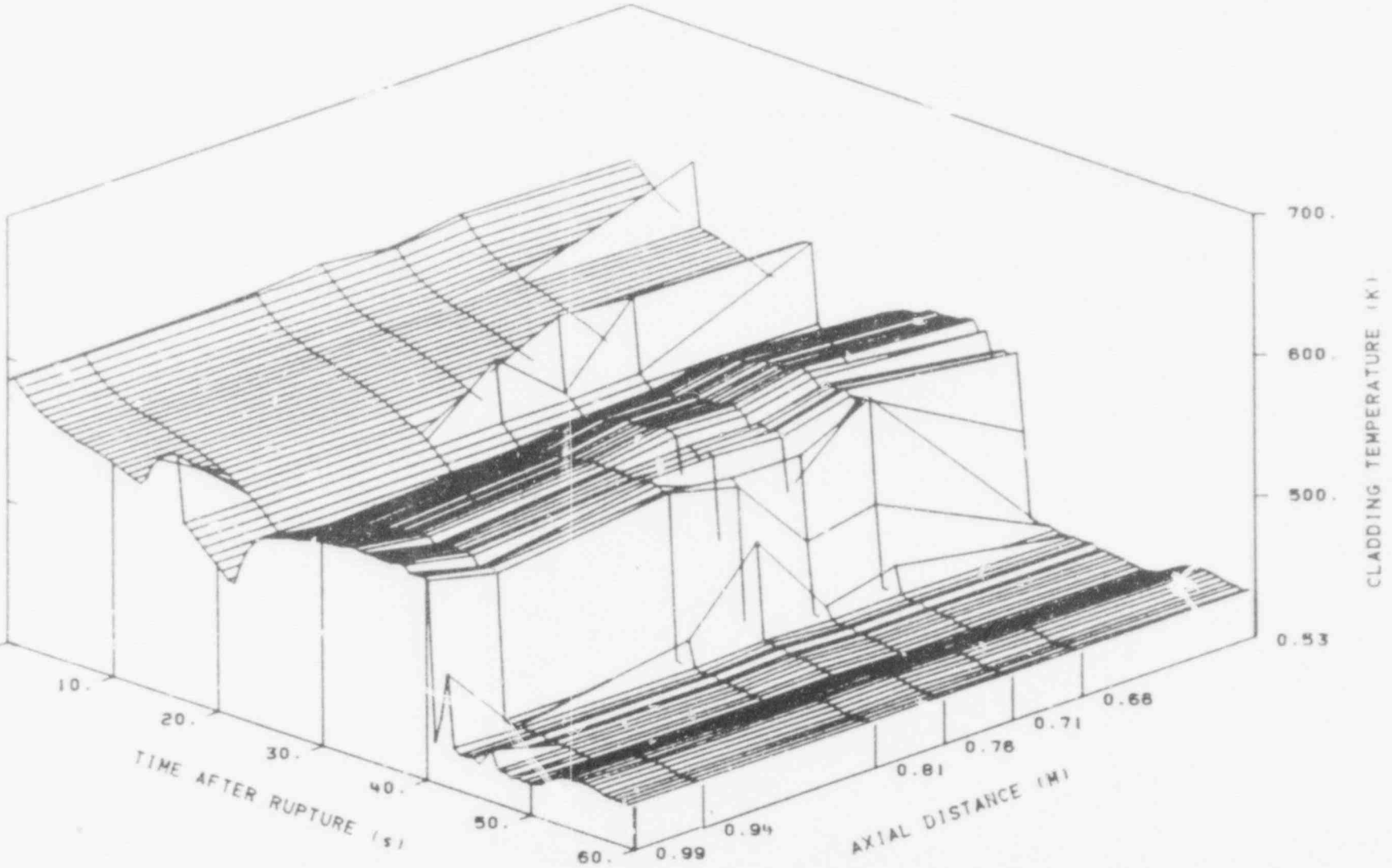

Fig. 11 Three-dimensional axial profile of cladding temperature in fuel Module 2.

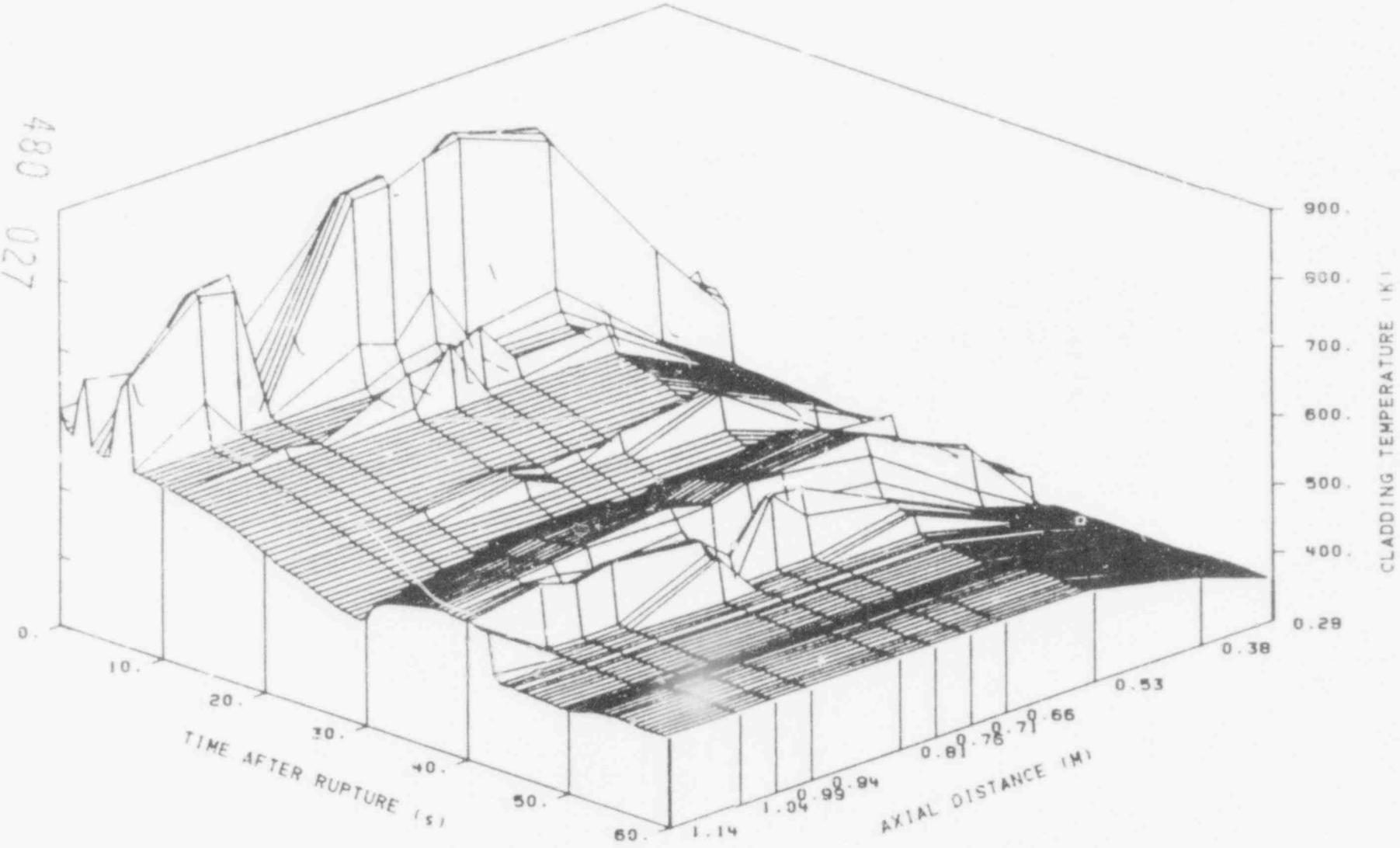

Fig. 12 Three-dimensional axial profile of cladding temperature in fuel Module 4.

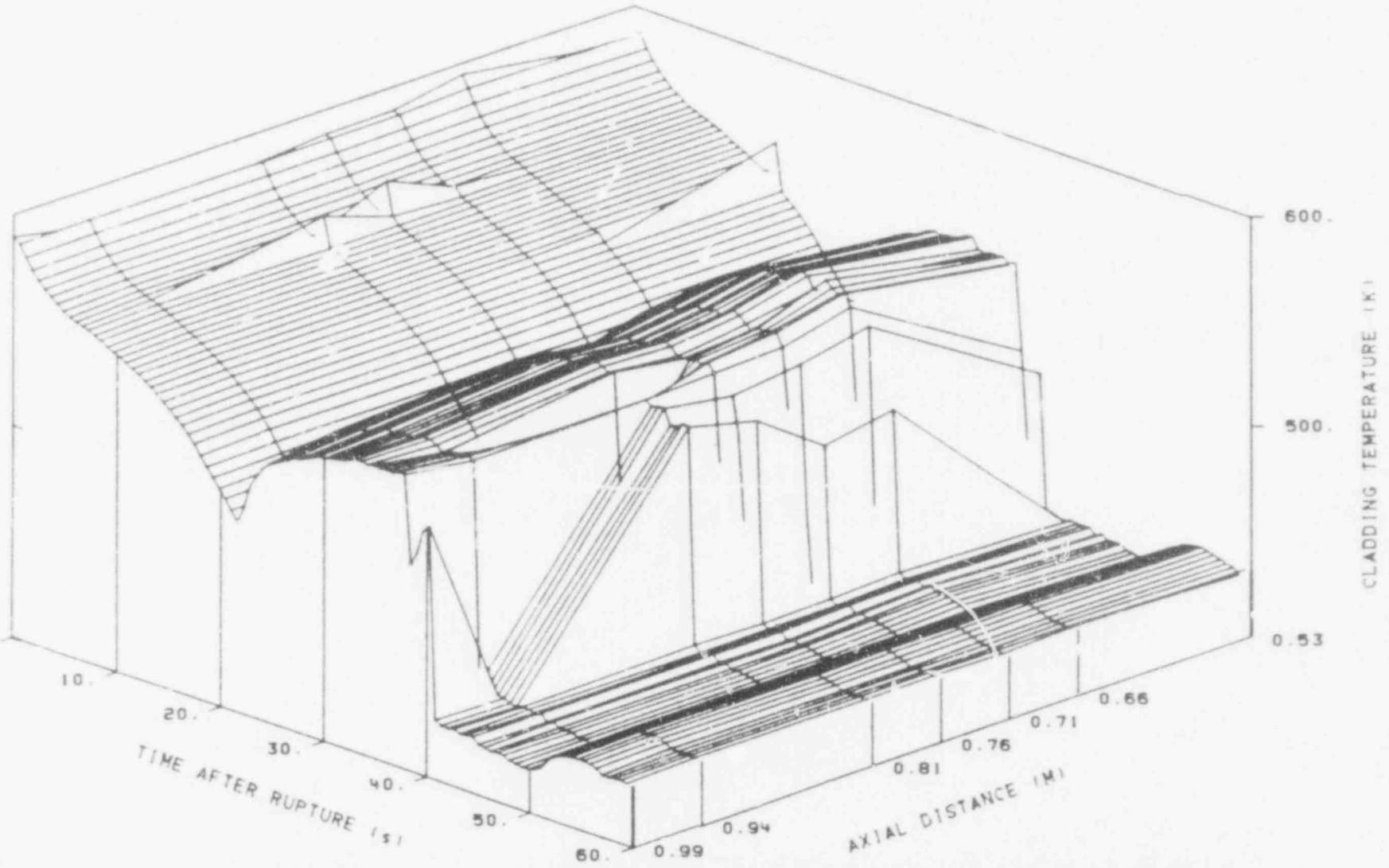

Fig. 13 Three-dimensional axial profile of cladding temperature in fuel Module 6.

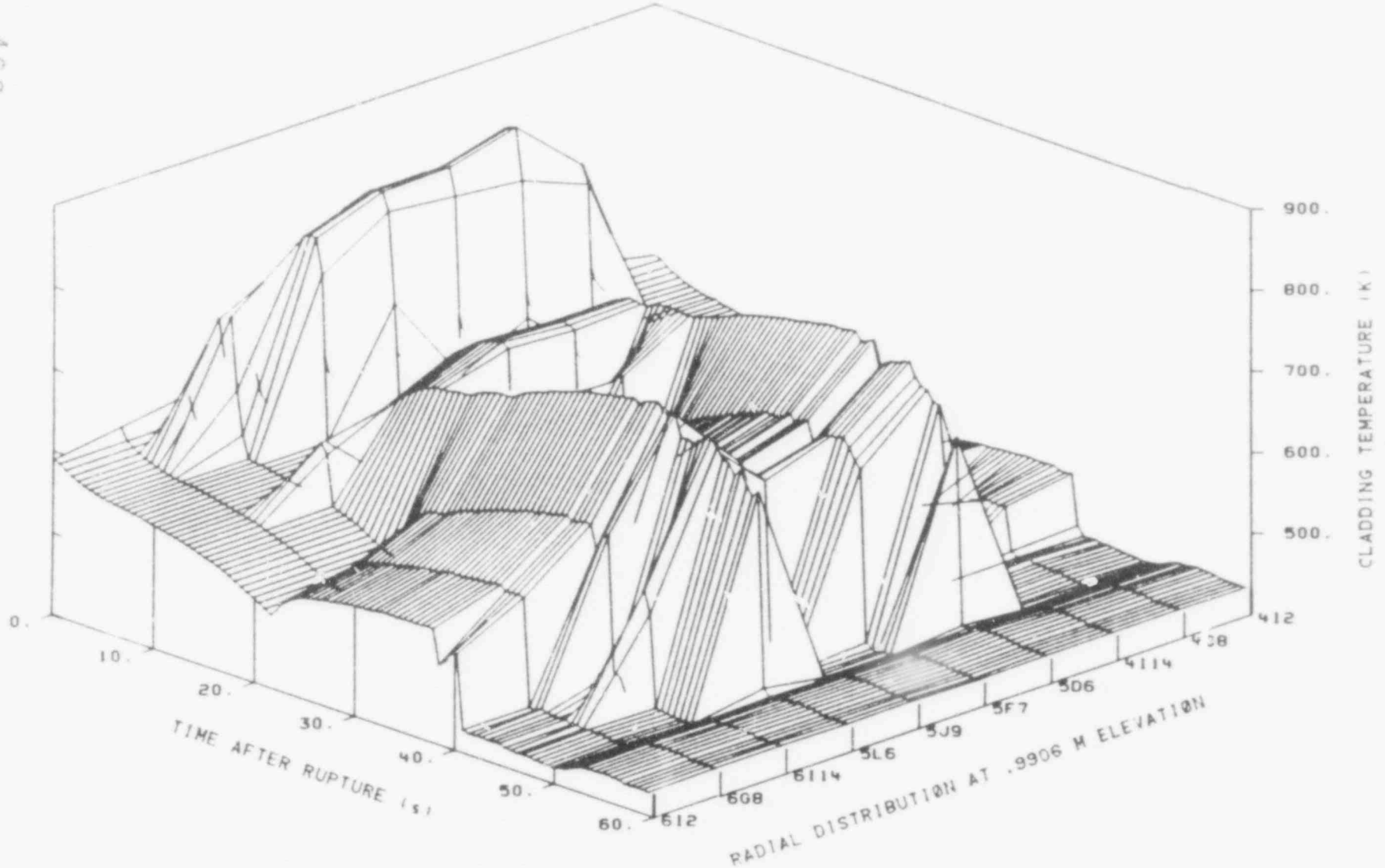

Fig. 14 Three-dimensional radial profile of cladding temperature at 0.99-m core elevation.

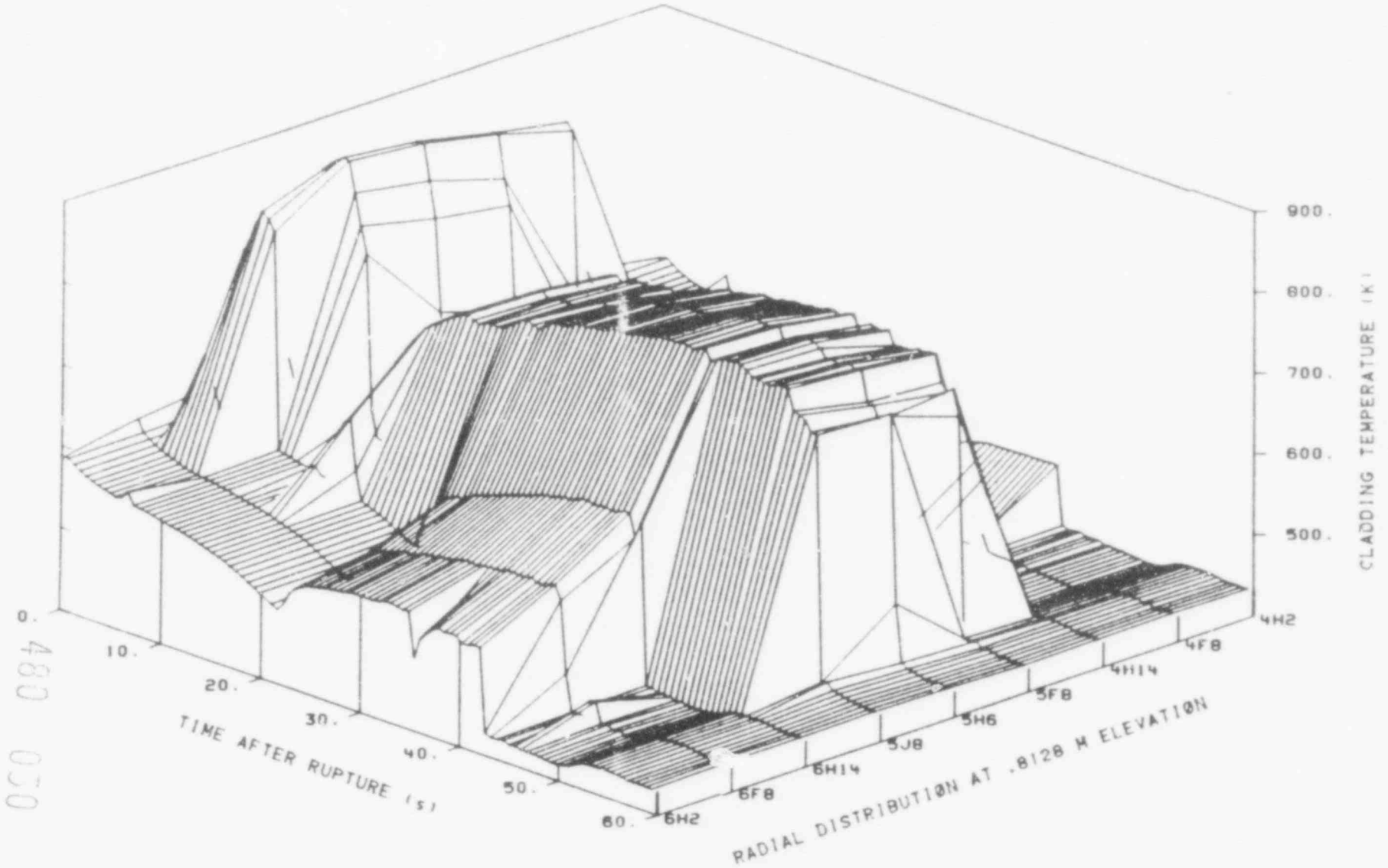

Fig. 15 Three-dimensional radial profile of cladding temperature at 0.81-m core elevation.

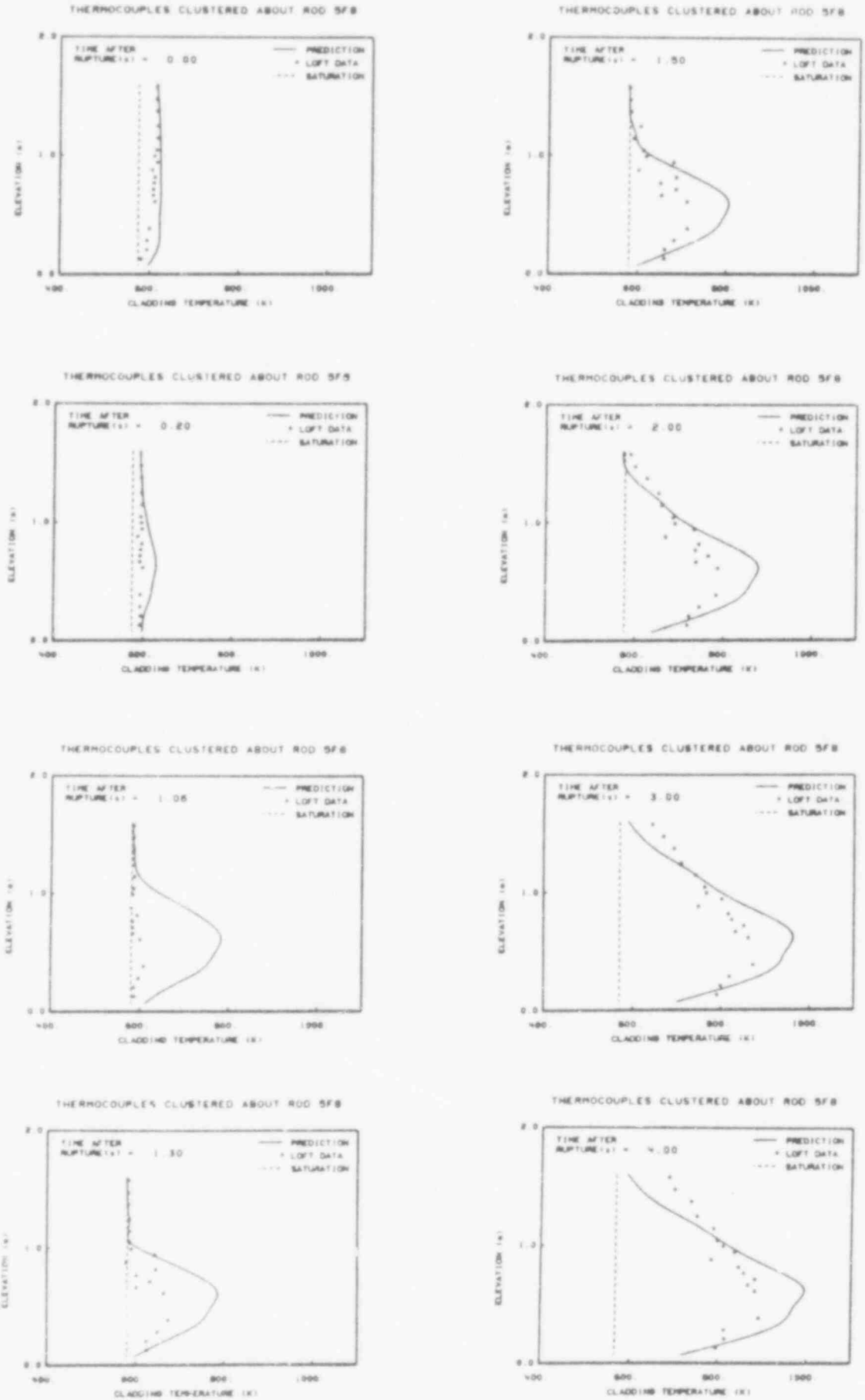

Fig. 16 Initial DNB and rise to peak cladding temperature during 0 to 5 s after rupture (LOCE L2-3 data and FRAP-T4 calculations).

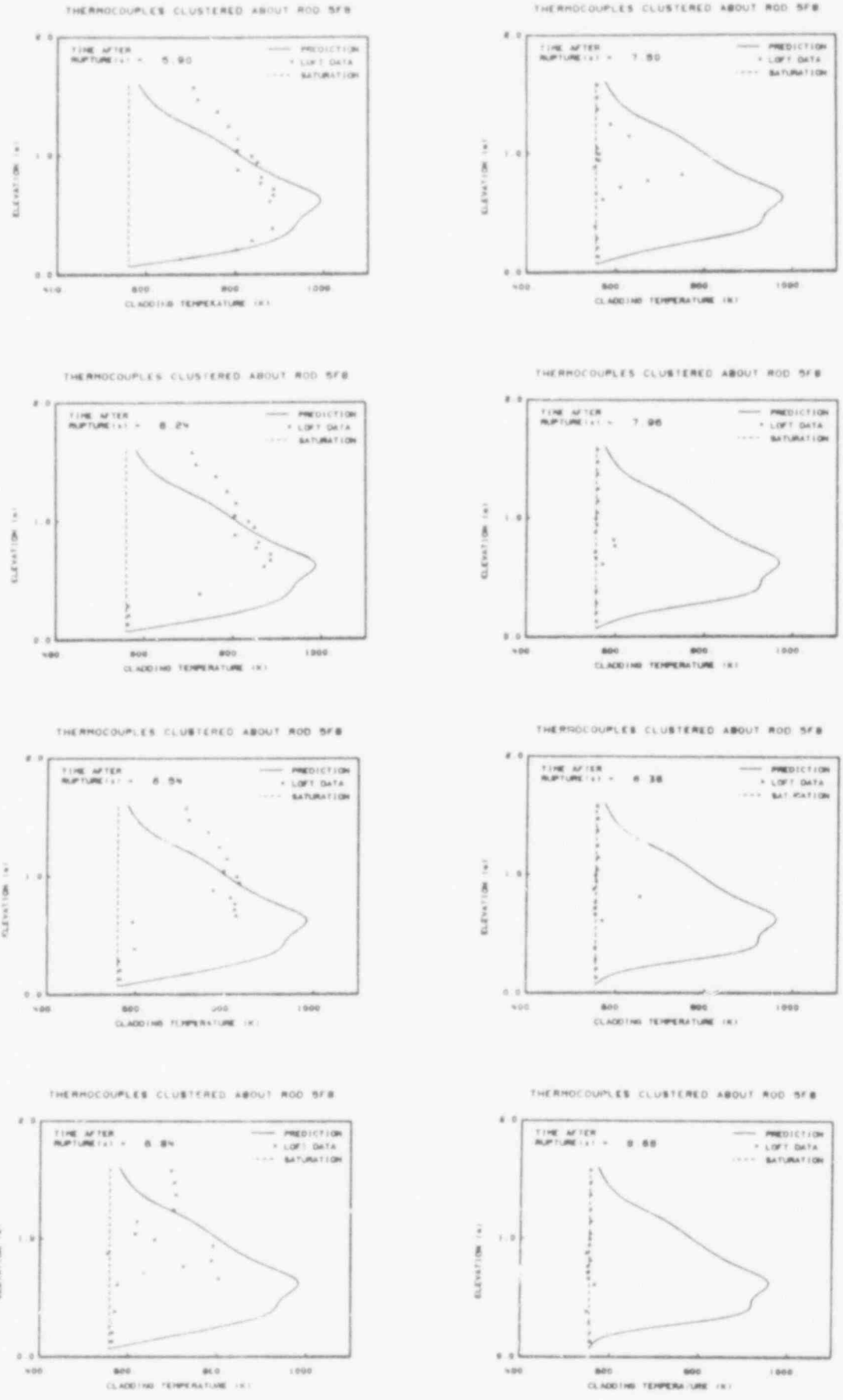

Fig. 17 Initial rewet (from bottom) during 6 to 9 s after rupture (LOCE L2-3 data and FRAP-T4 calculations).

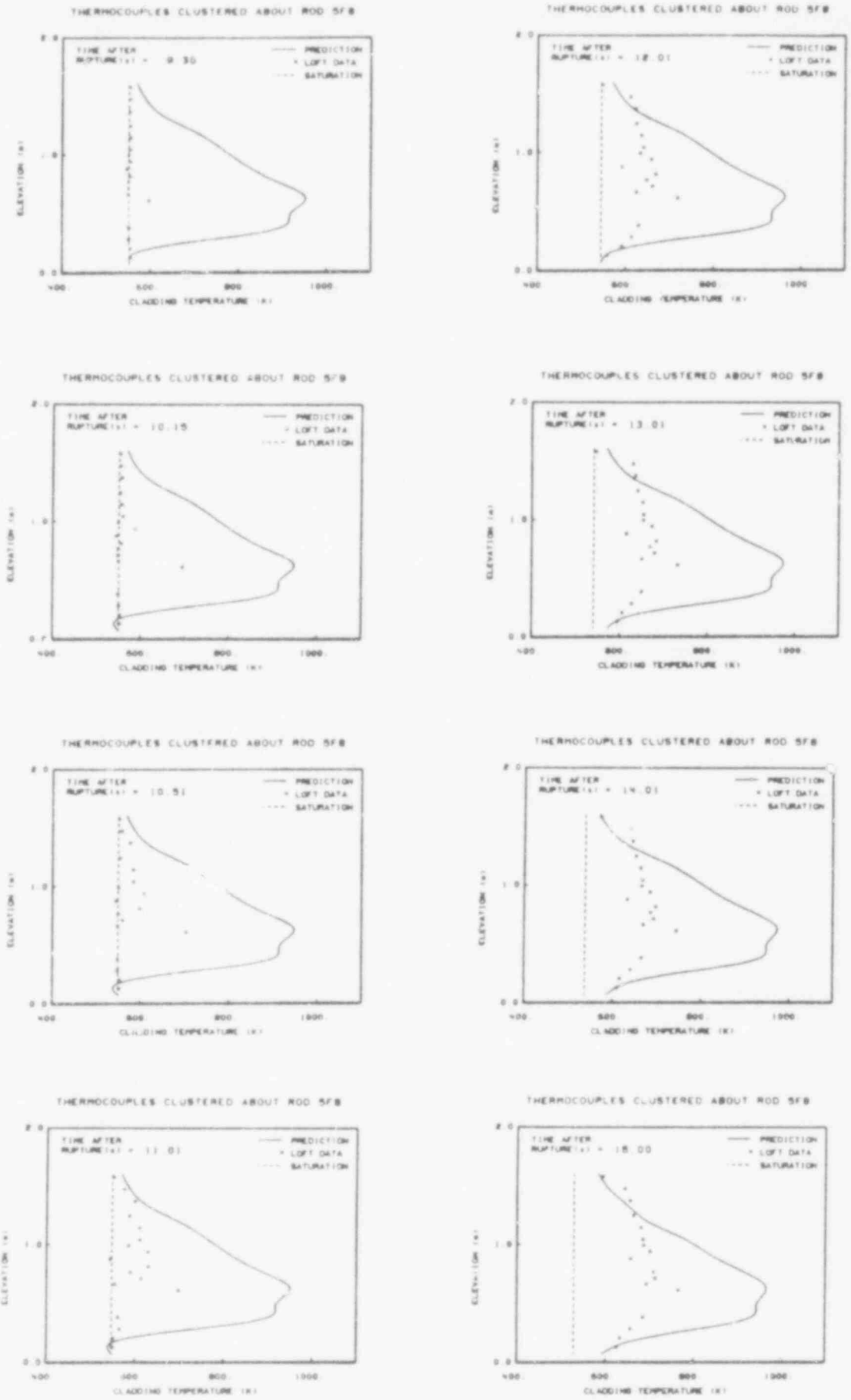

Fig. 18 Secondary DNB during 9 to 16 s after rupture (LOCE L2-3 data and FRAP-T4 calculations).

480 033

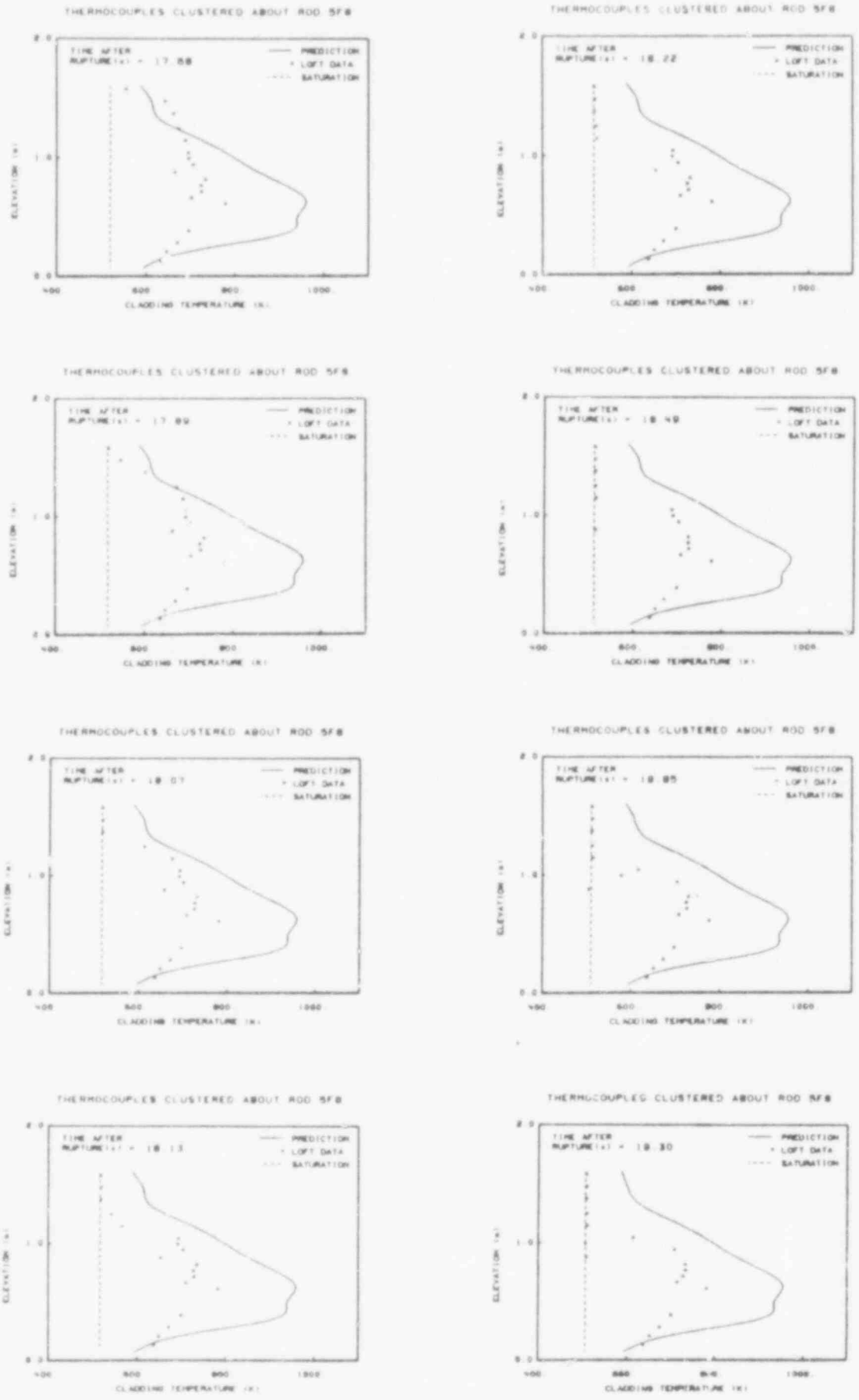

Fig. 19 Top-down rewet following secondary DNB during 17 to 19.3 s after rupture (LOCE 12-3 data and FRAP-T4 calculations).

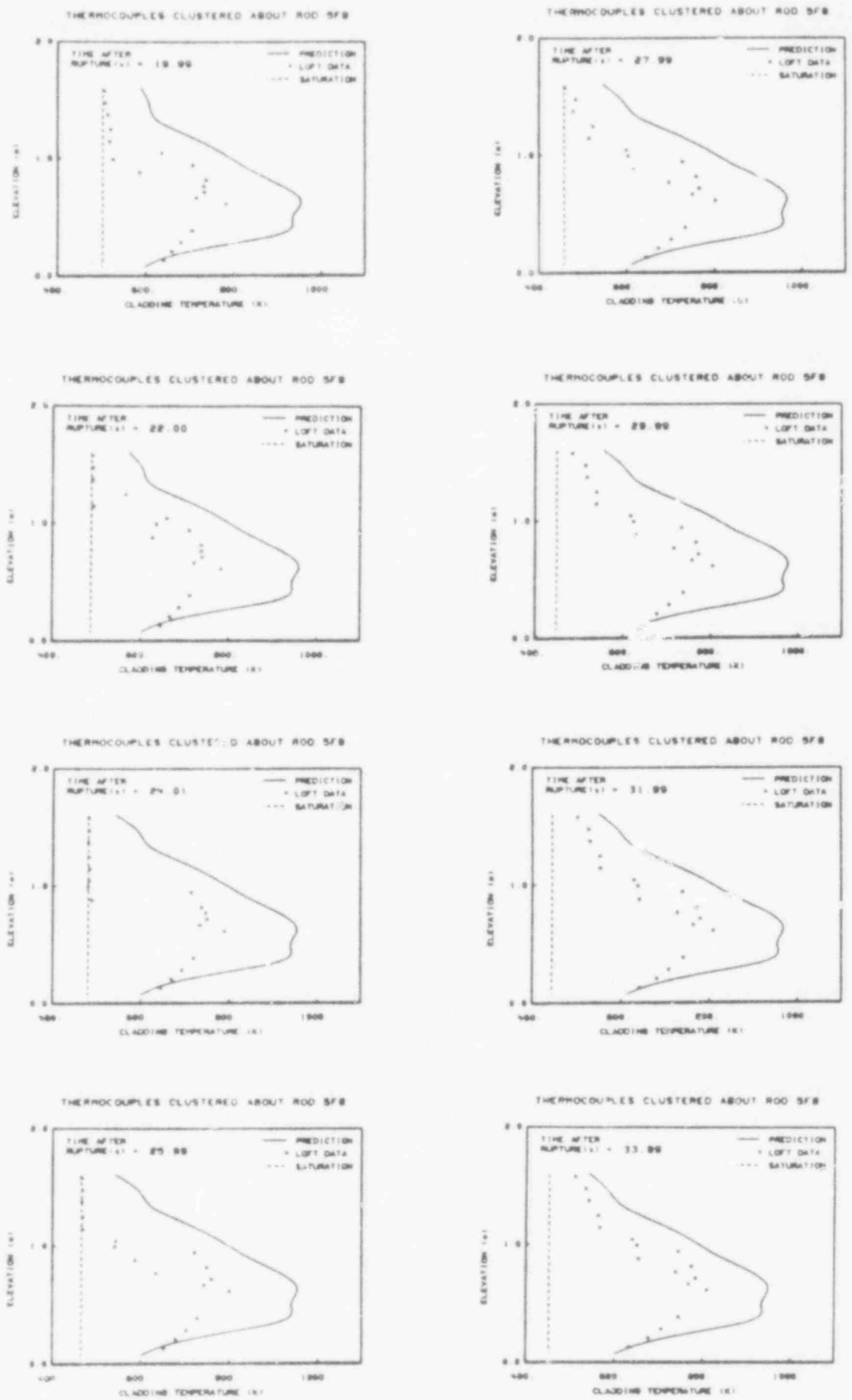

Fig. 20 Dryout during 19 to 34 s after rupture (LOCE L2-3 data and FRAP-T4 calculations).

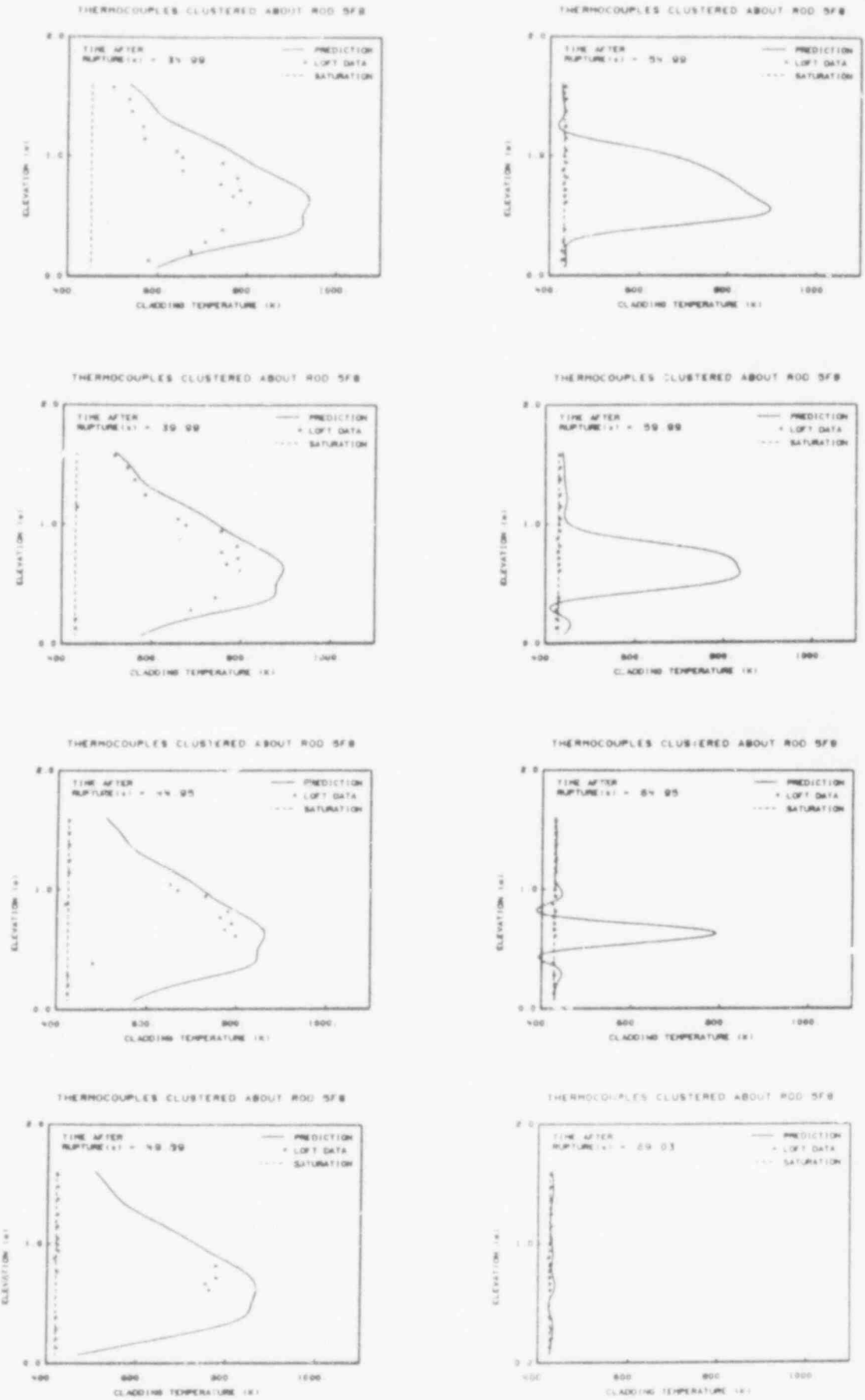

Fig. 21 Reflooding during 34 to 69 s after rupture (LOCE L2-3 data and FRAP-T4 calculations).

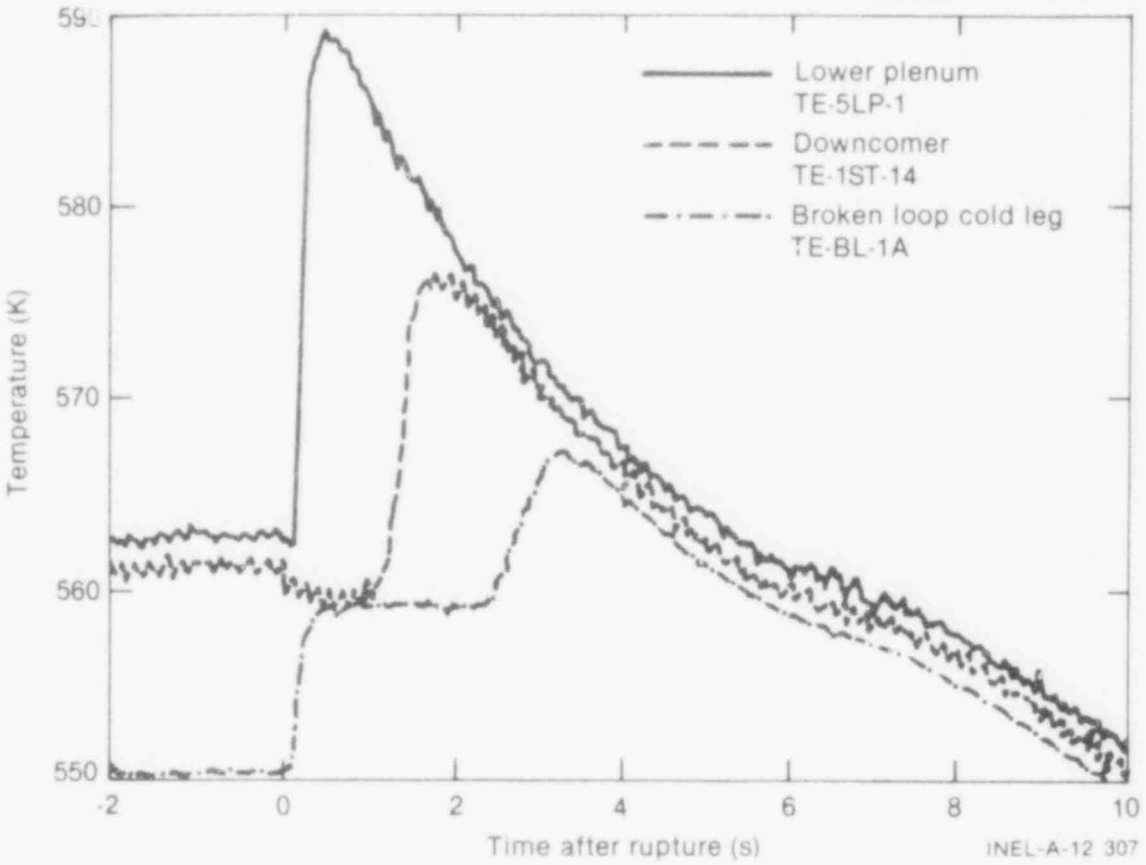

Fig. 22 Migration of hot coolant to the broken loop cold leg.

480 037

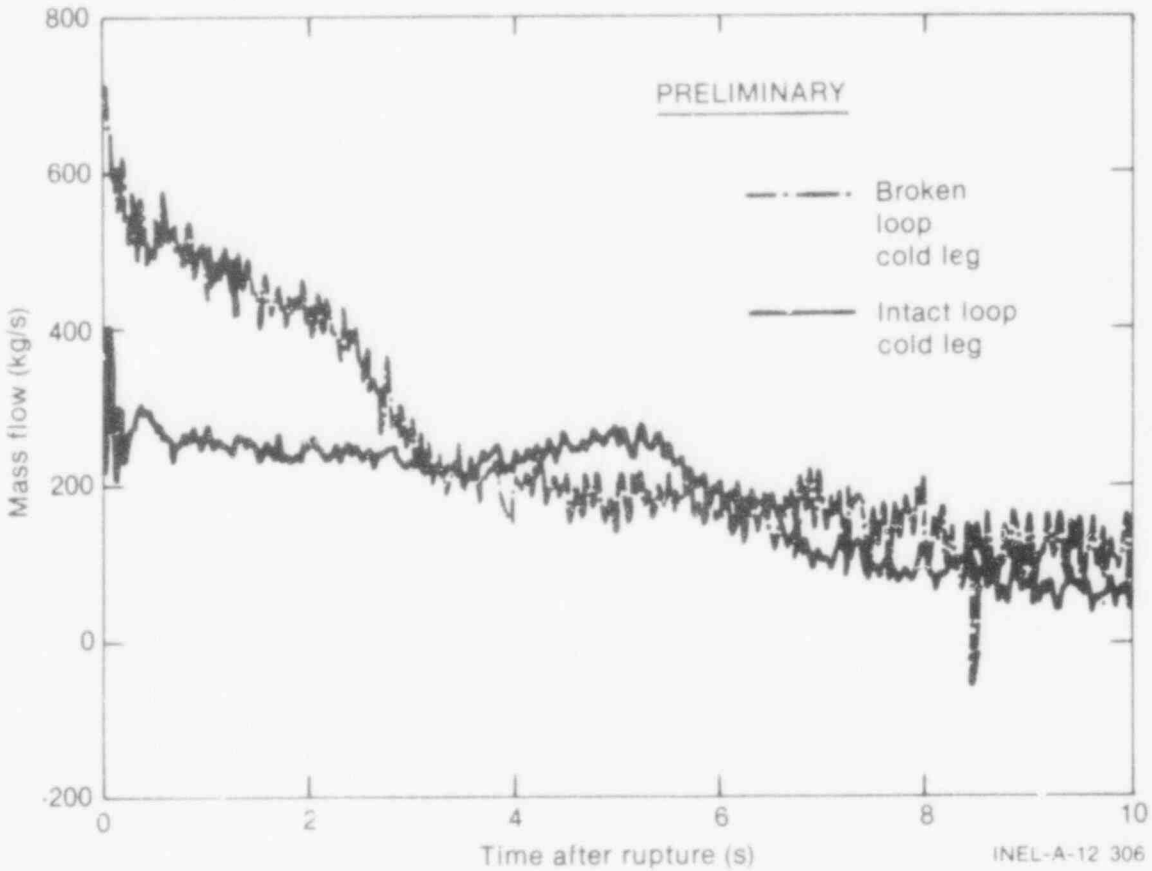

Fig. 23 Broken loop and intact loop cold leg mass flows.

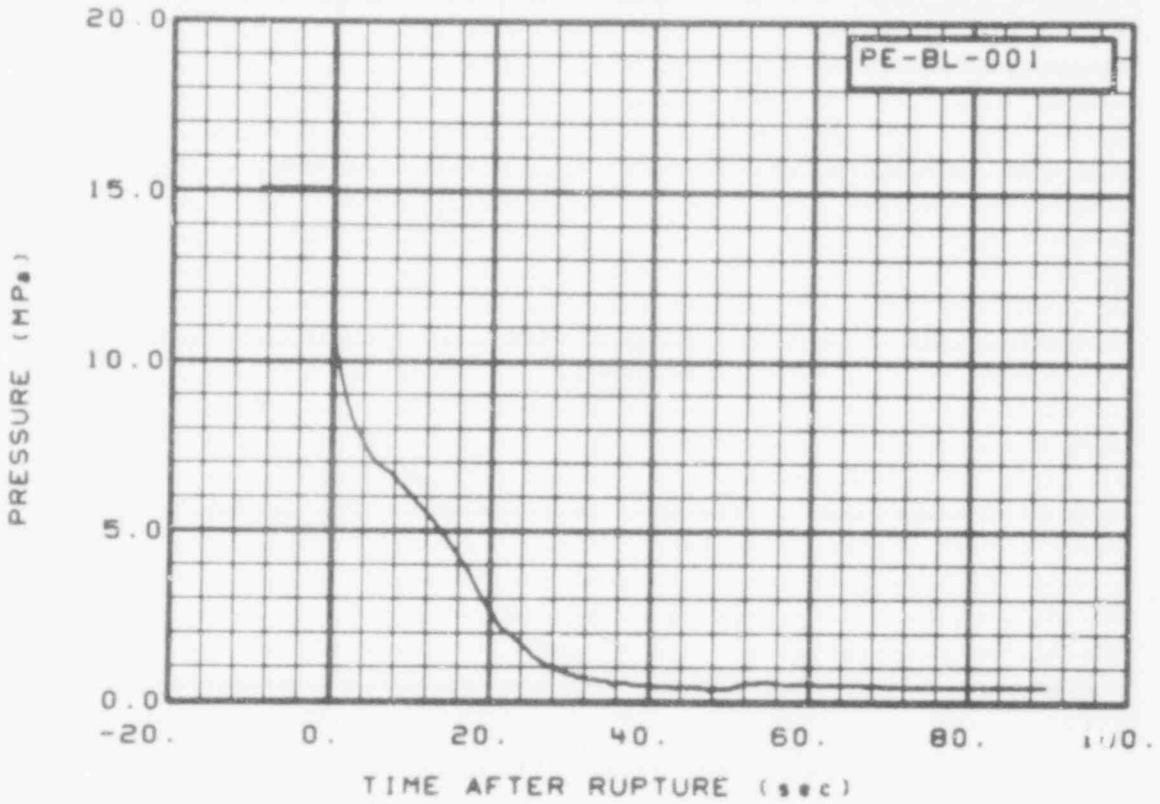

Fig. 24 Pressure in the broken loop cold leg.

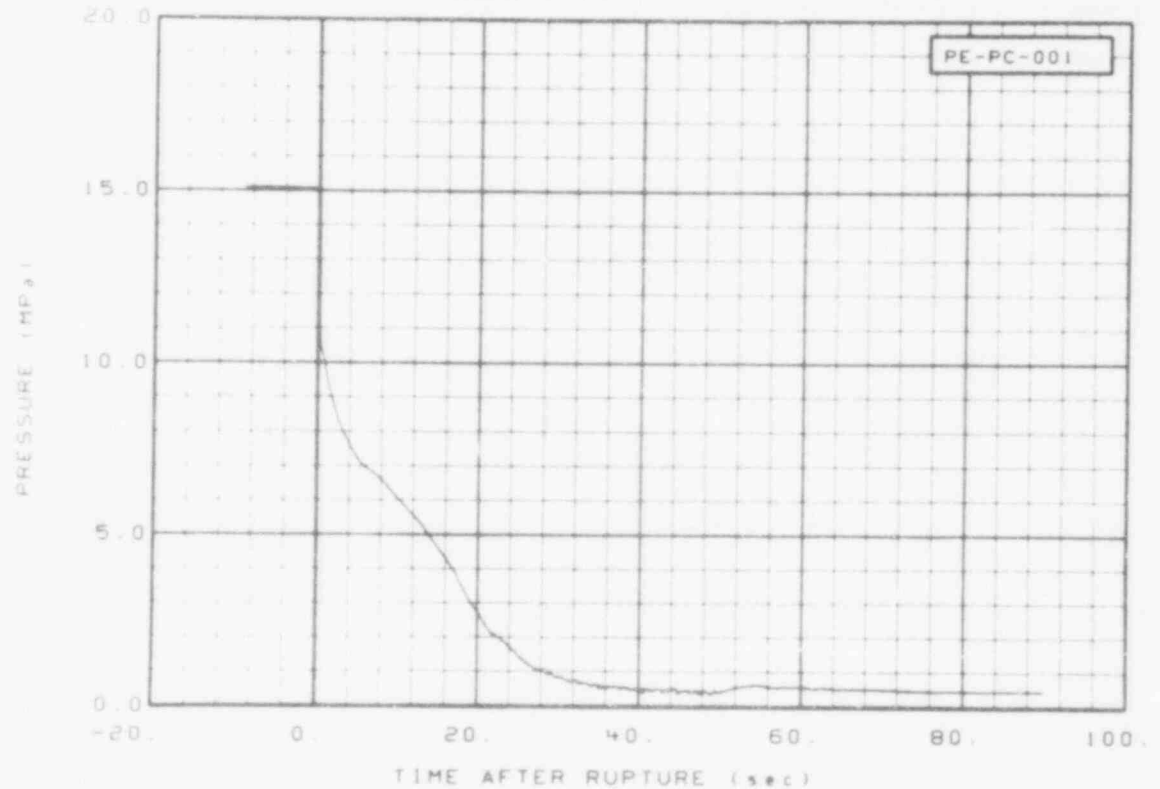

Fig. 25 Pressure in the intact loop cold leg.

480 039

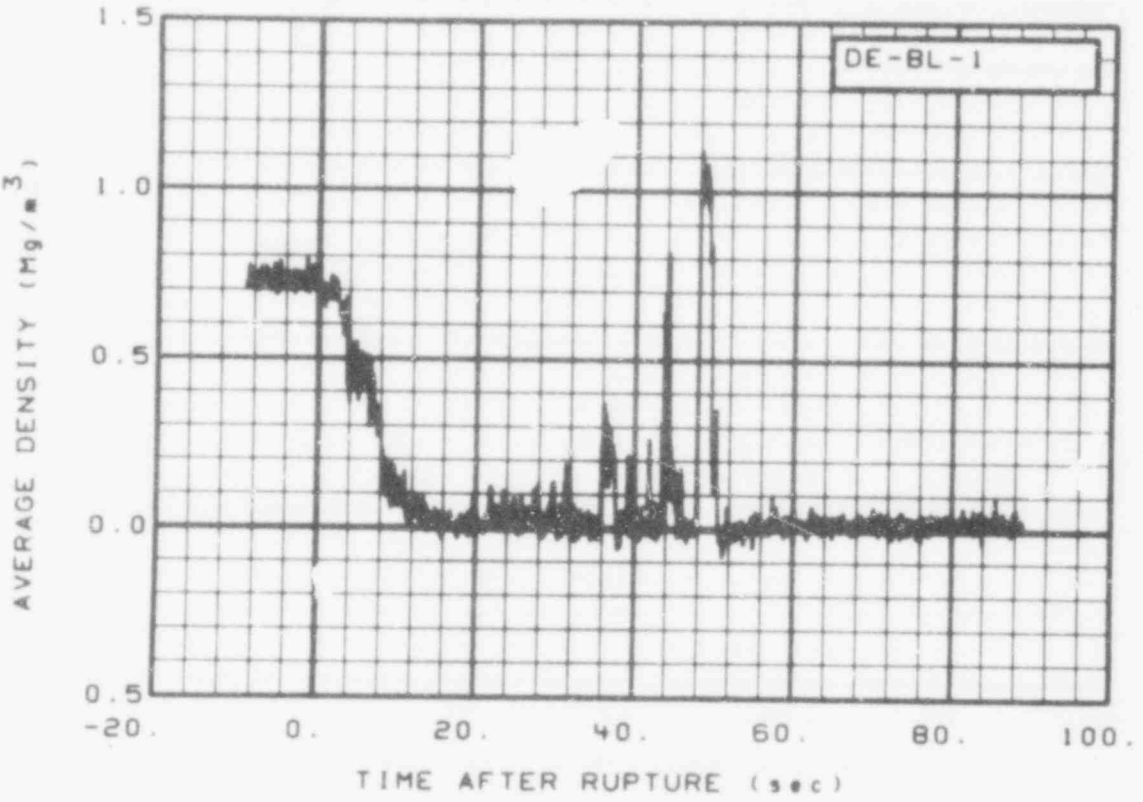

Fig. 26 Average density in the broken loop cold leg.

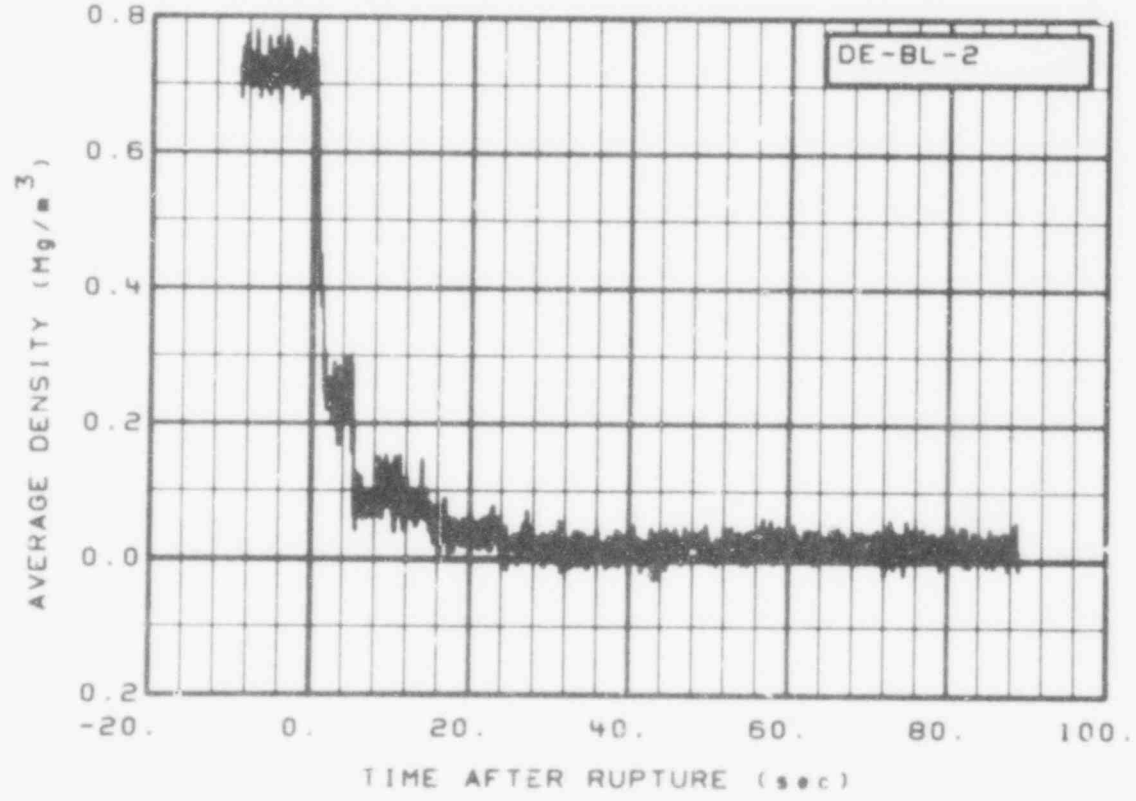

Fig. 27 Average density in the broken loop hot leg.

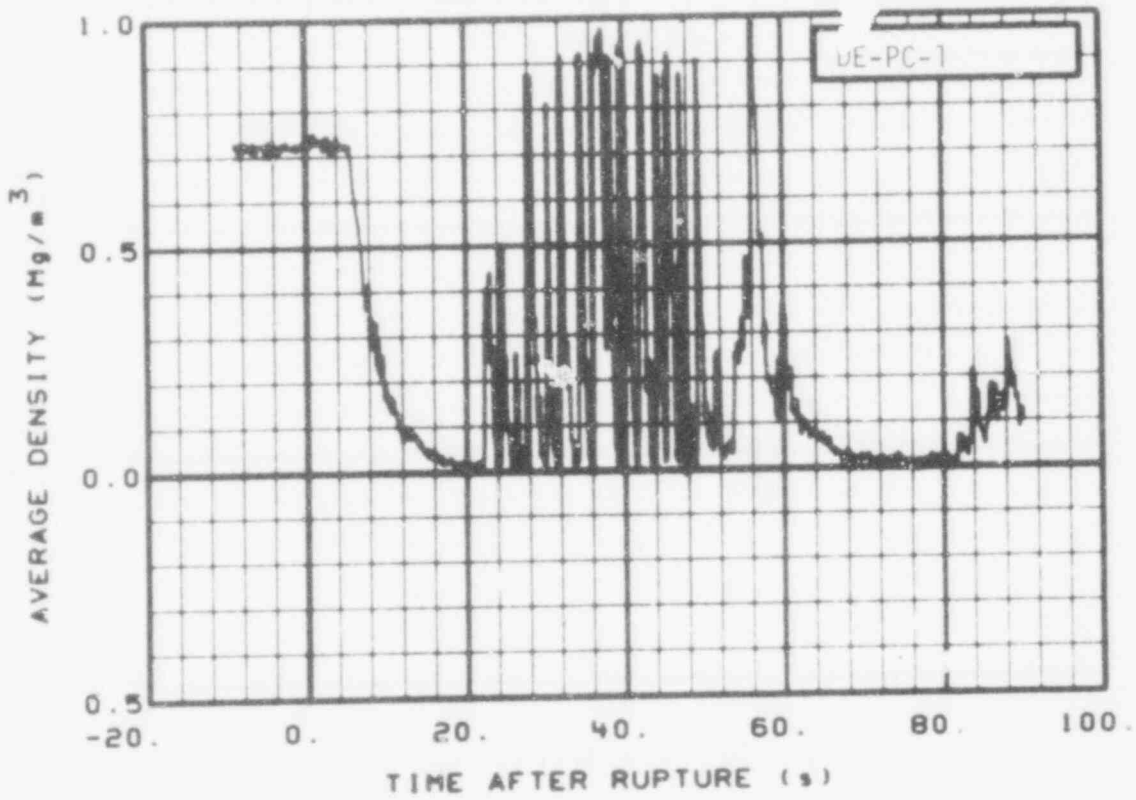

Fig. 28 Average density in the intact loop cold leg.

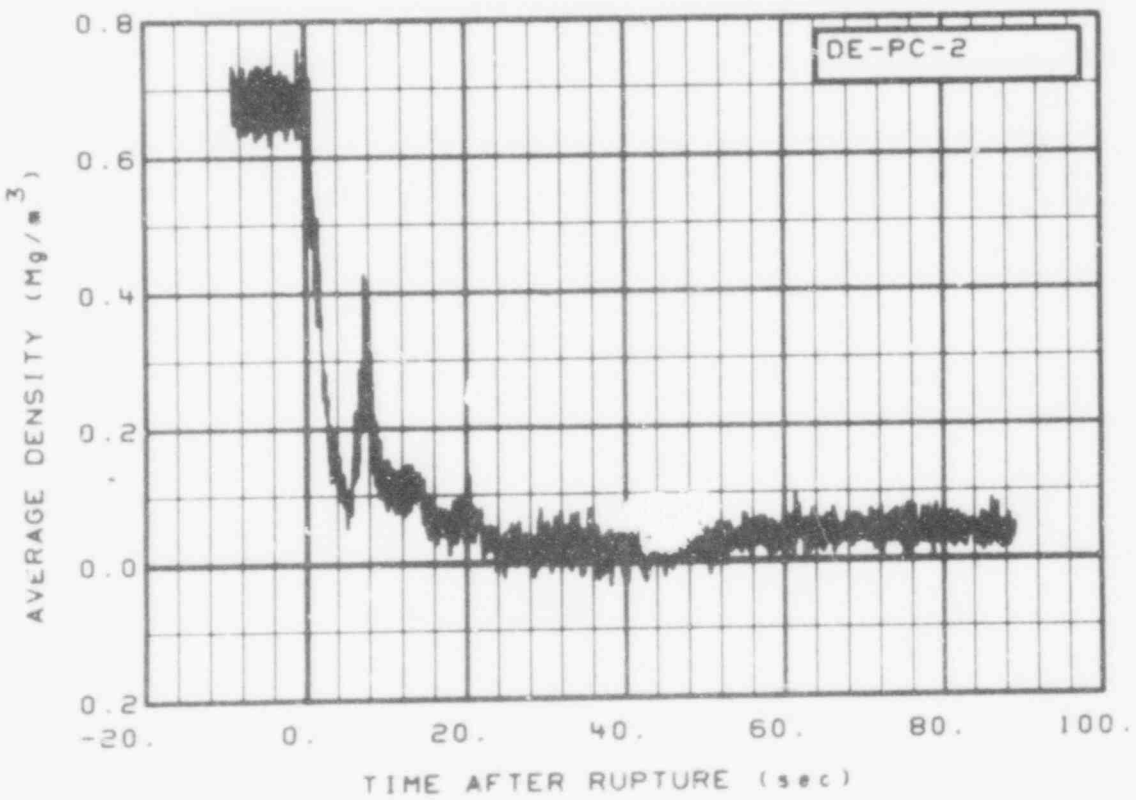

Fig. 29 Average density in the intact loop hot leg.

480 041

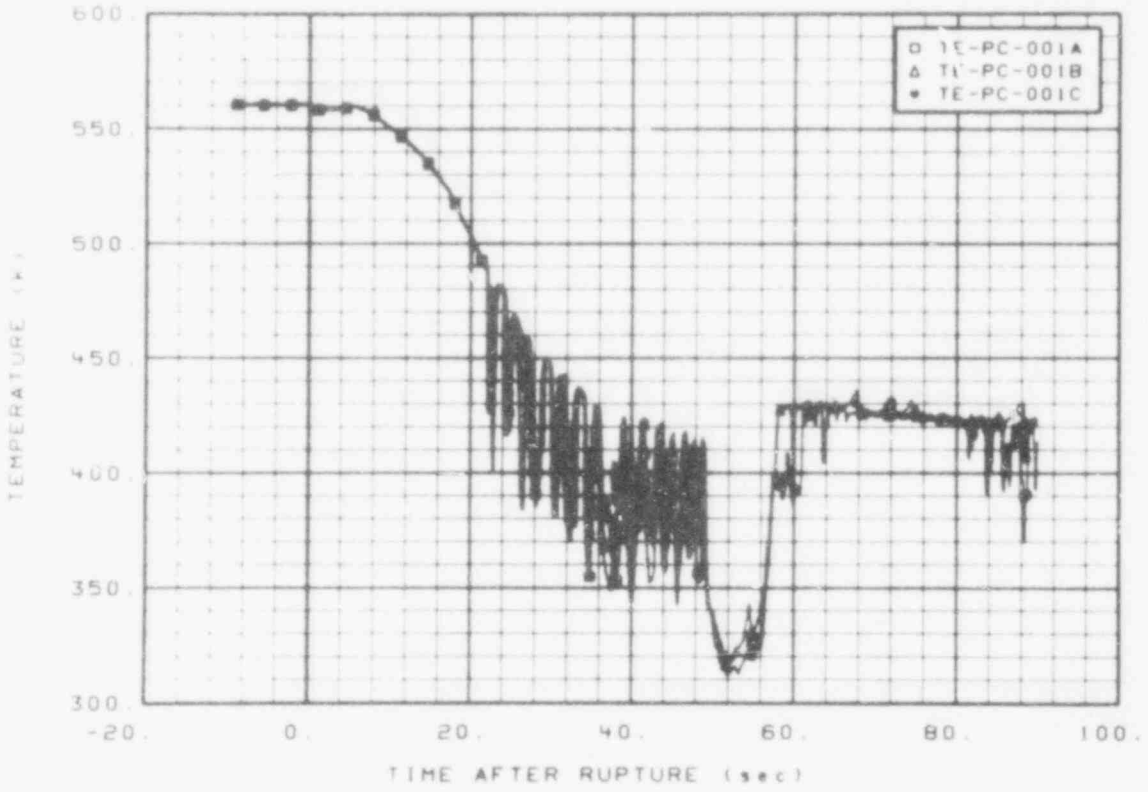

Fig. 30 Temperature in the intact loop cold leg.

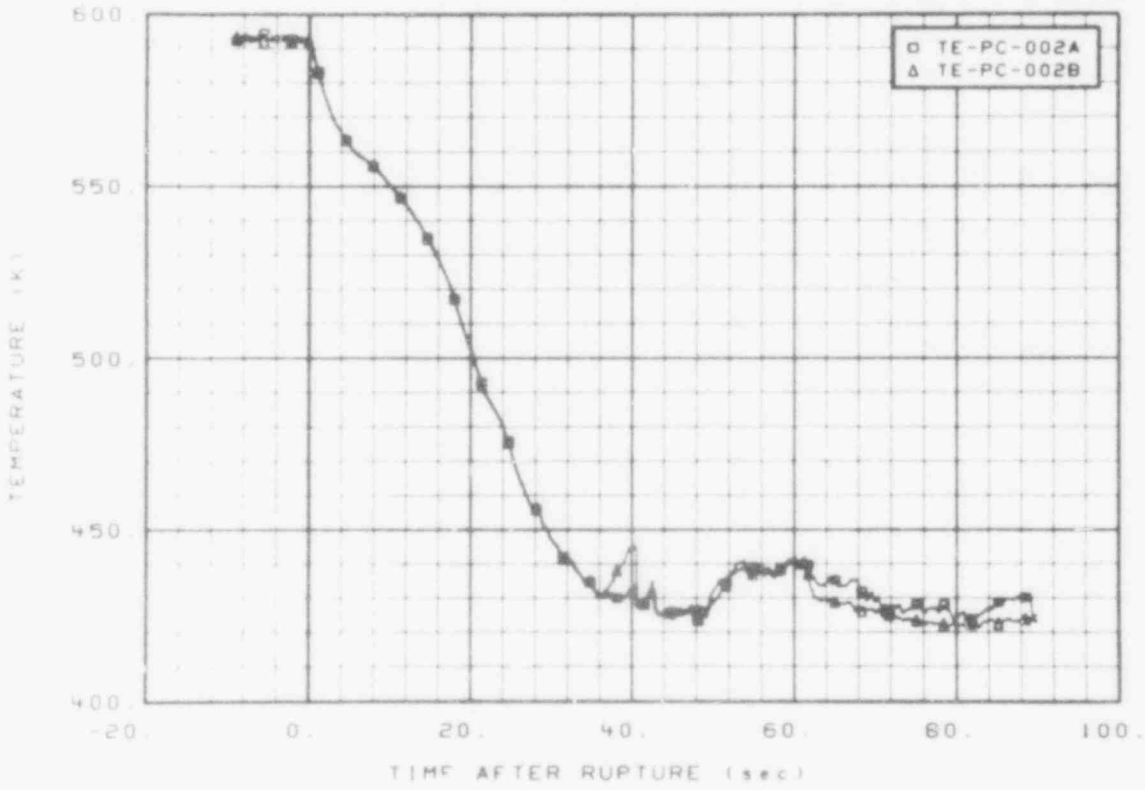

Fig. 31 Temperature in the intact loop hot leg.

480 042

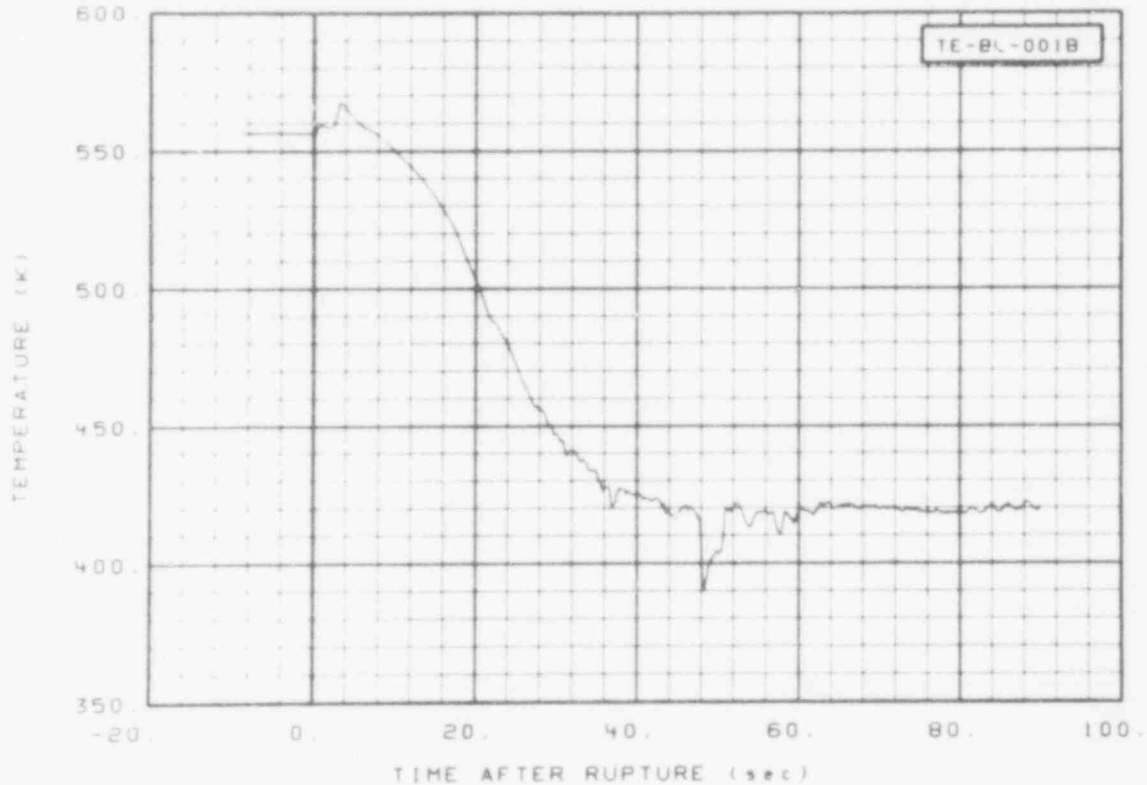

Fig. 32 Temperature in the broken loop cold leg.

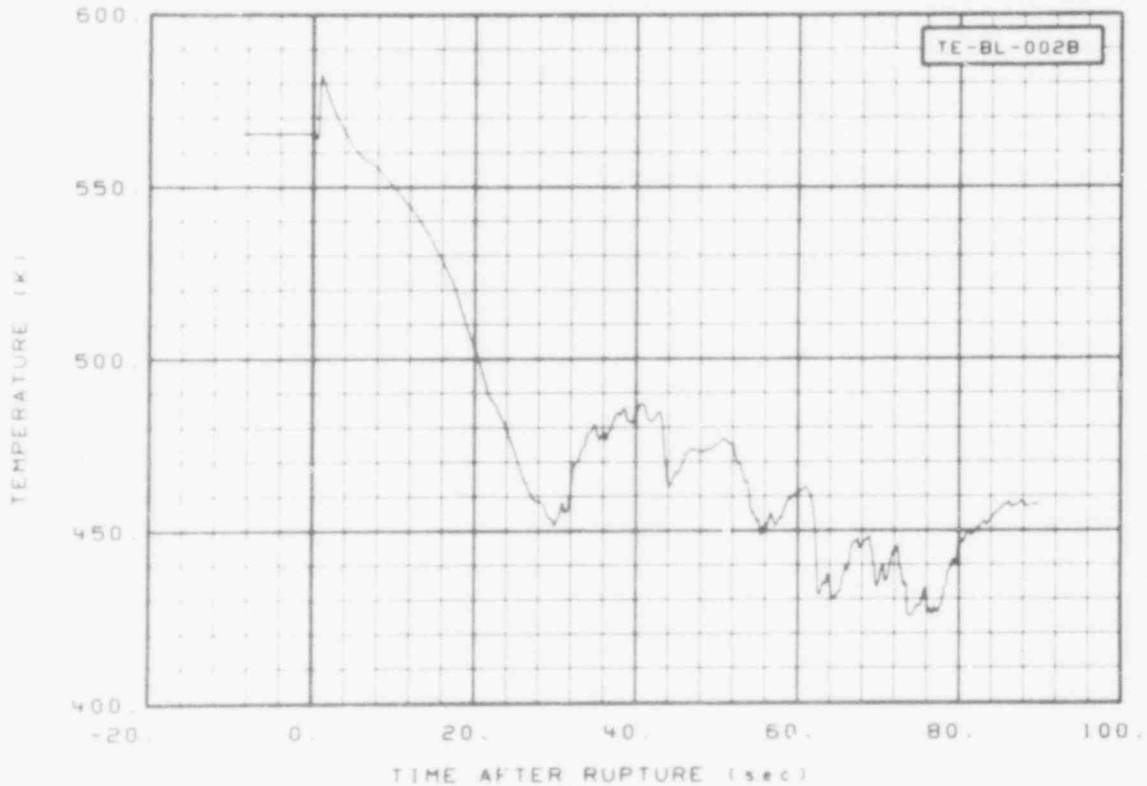

Fig. 33 Temperature in the broken loop hot leg.

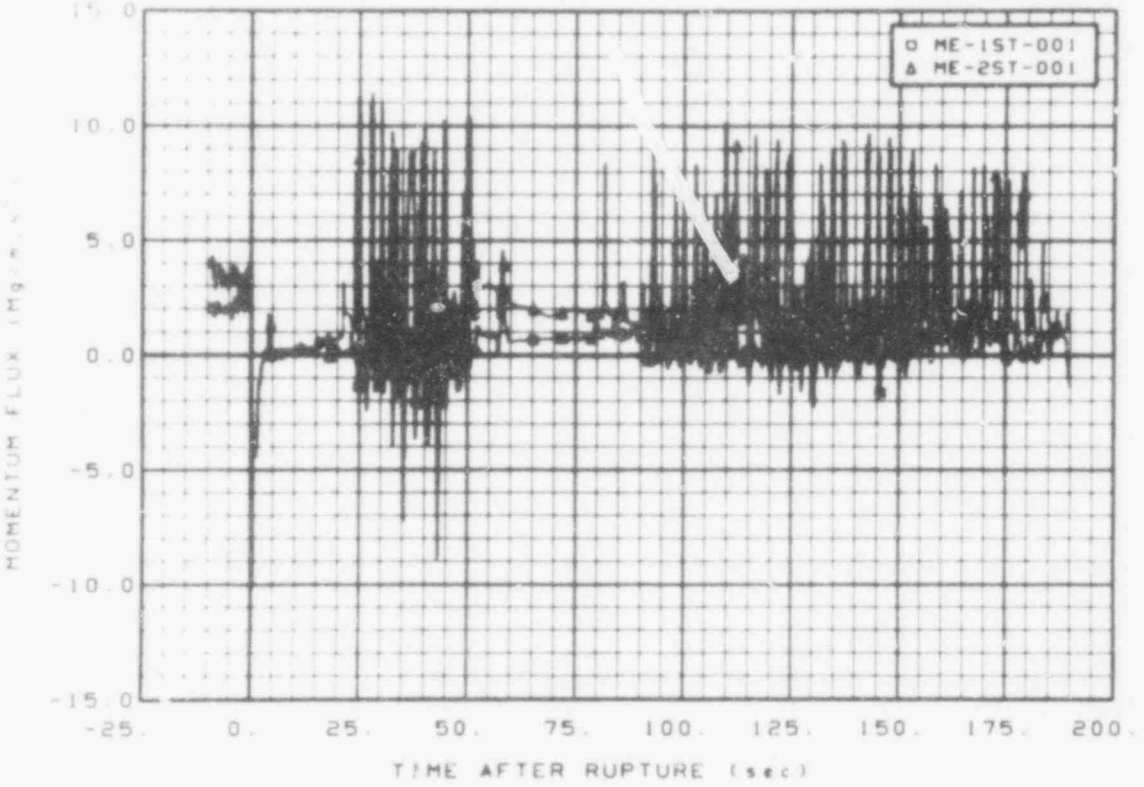

Fig. 34 Momentum flux in the downcomer.

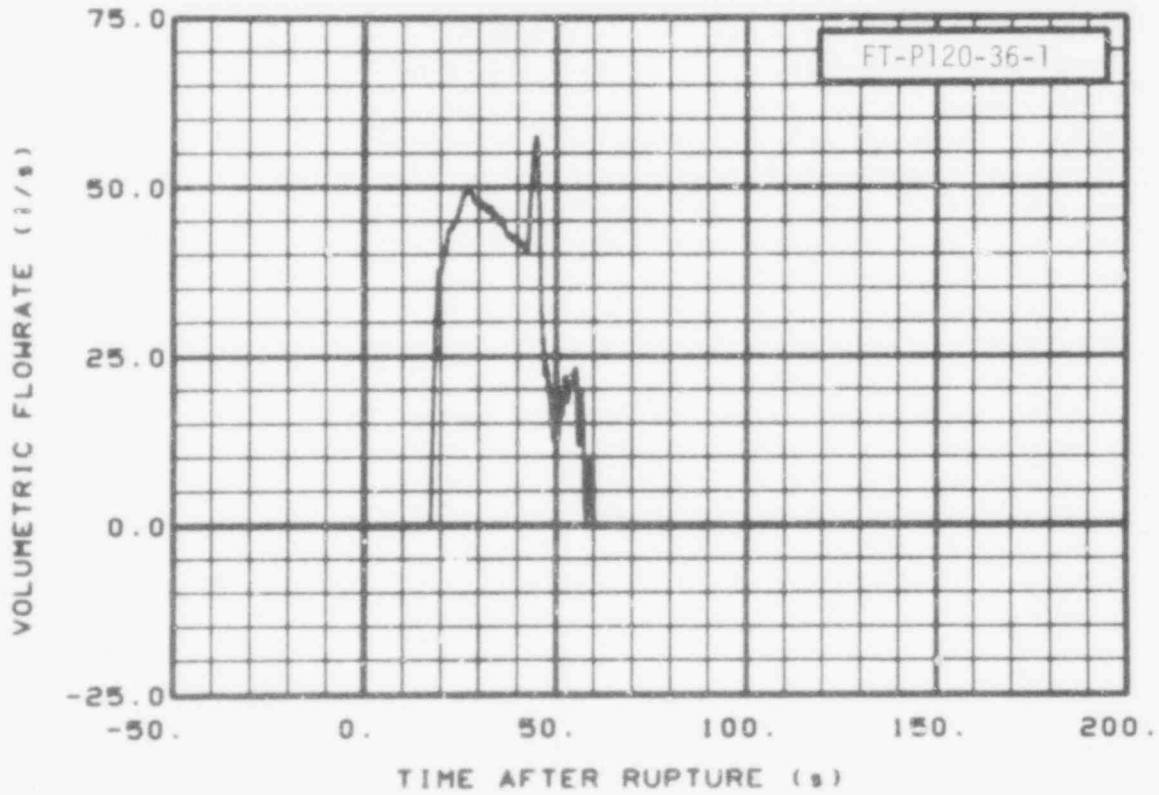

Fig. 35 ECCS accumulator flow rate.

480 044

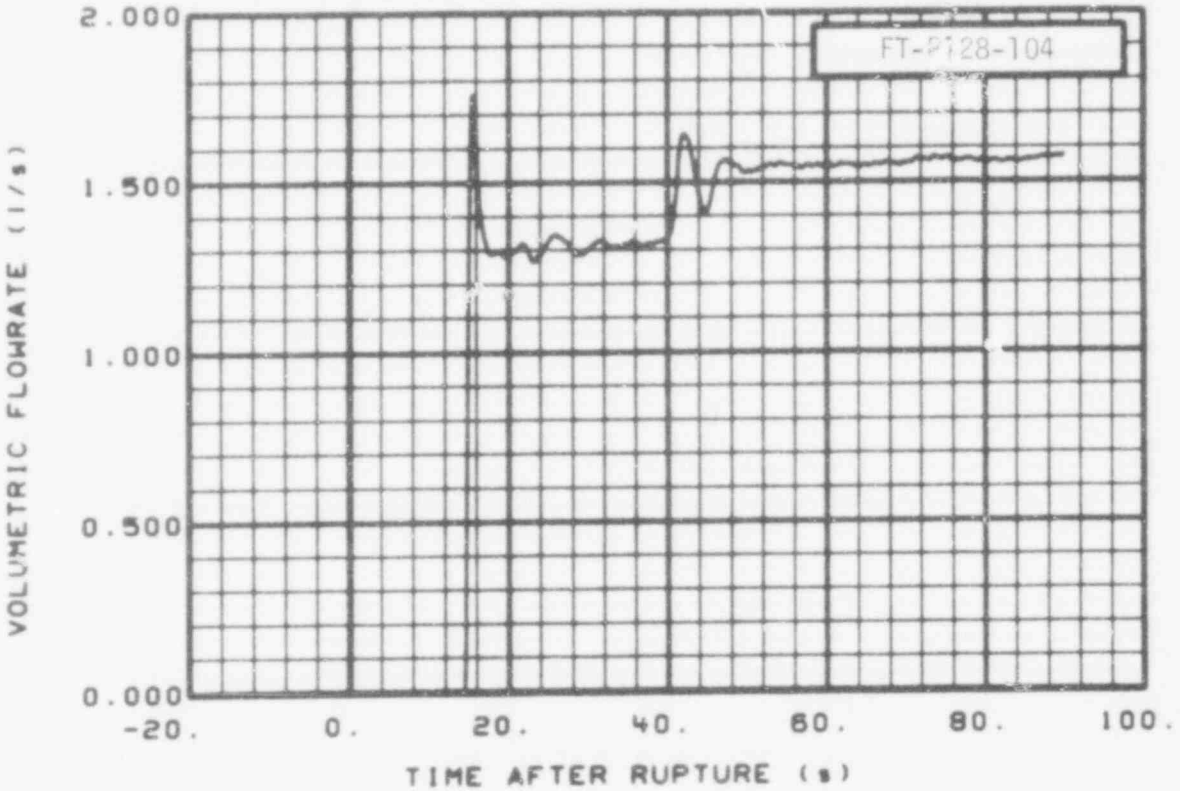

Fig. 36 ECCS HPIS flow rate.

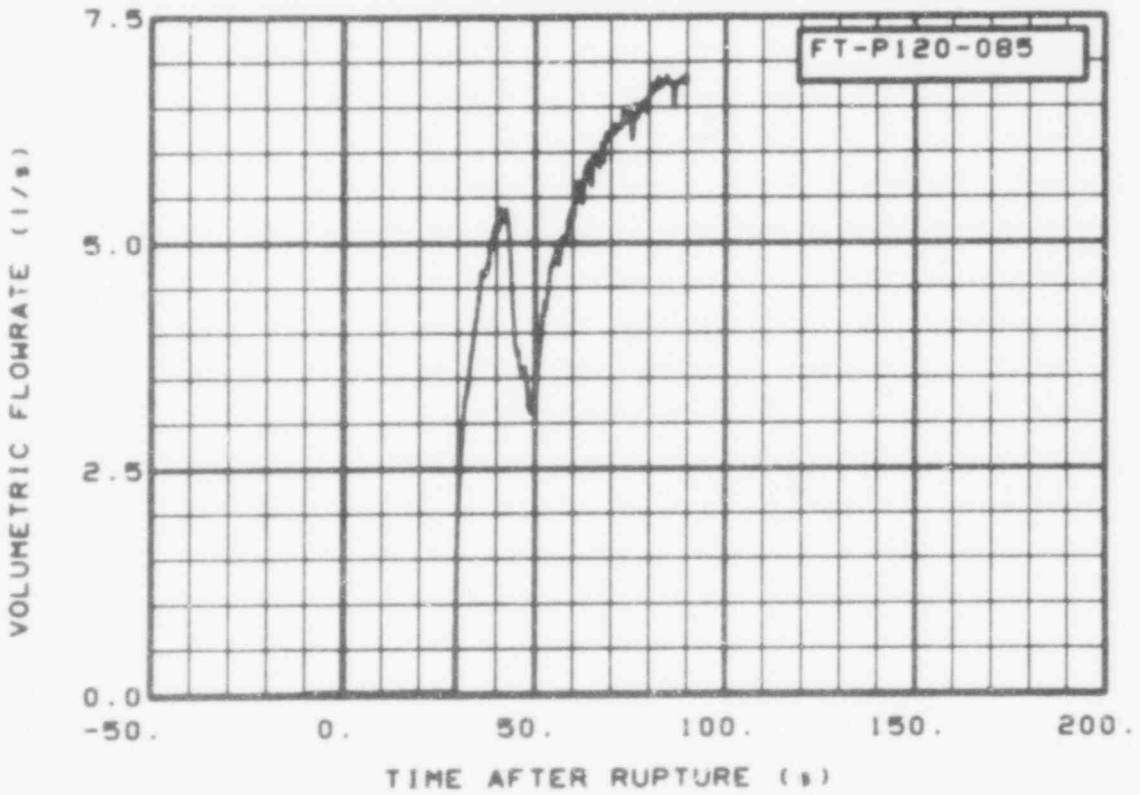

Fig. 37 ECCS LPIS flow rate.

480 045

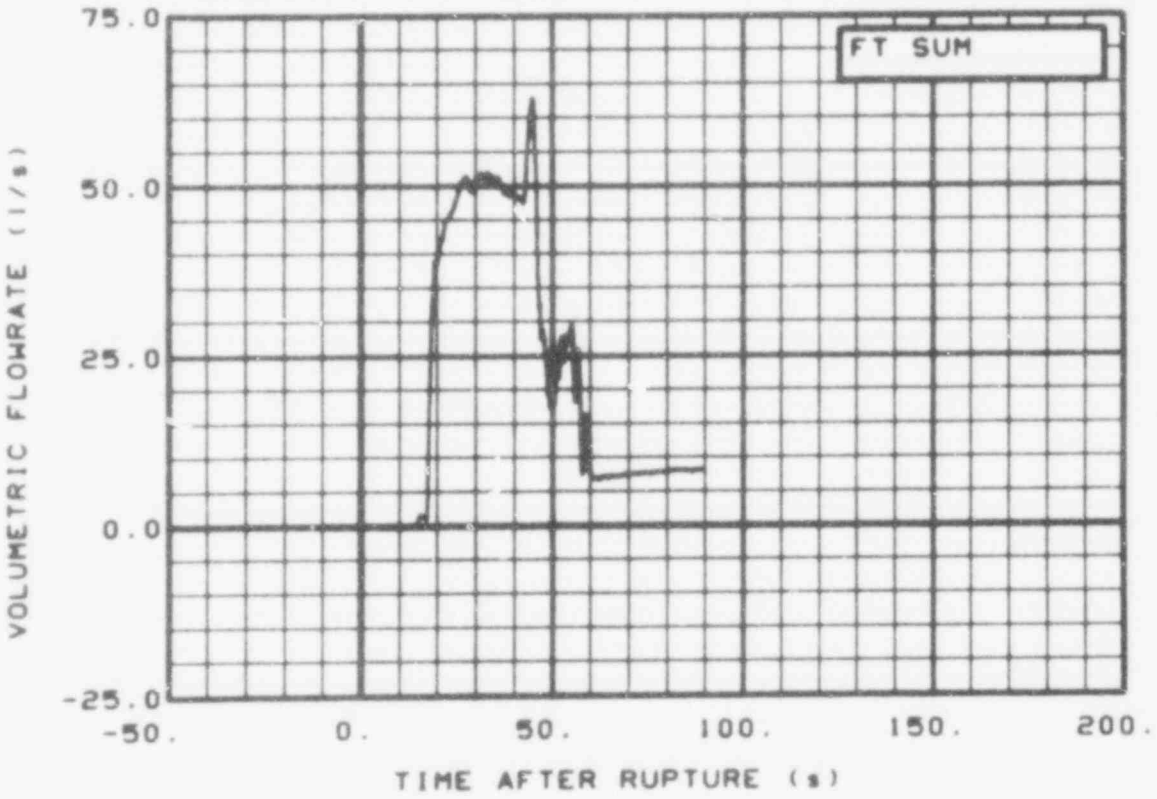

Fig. 38 ECCS total flow rate.

480 046

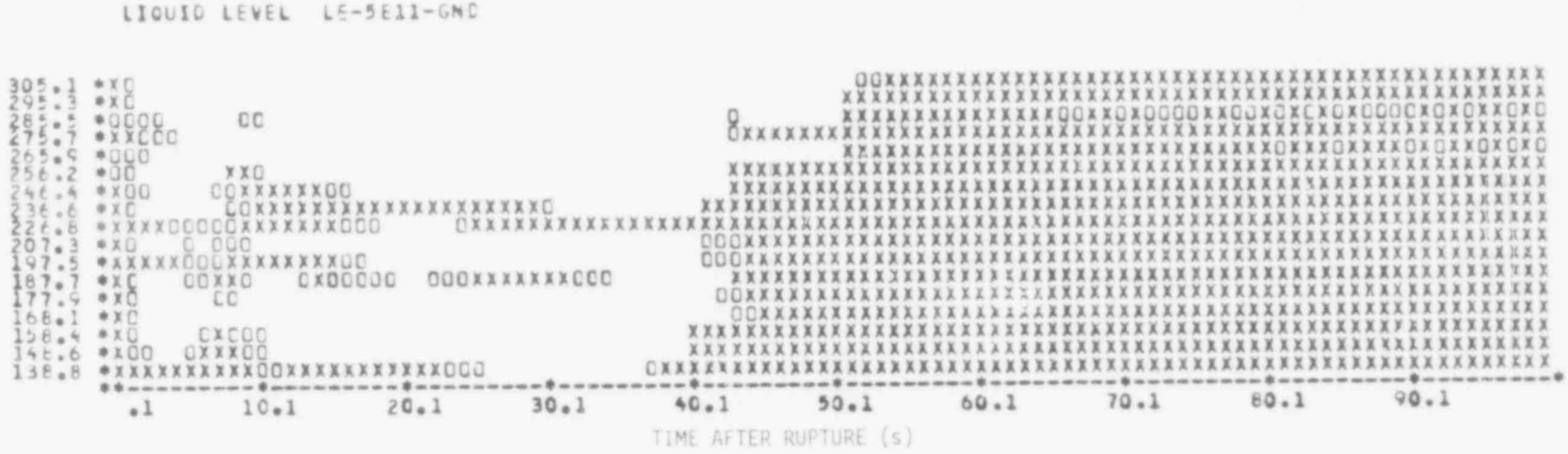

Fig. 39 Liquid level in fuel Module 5.

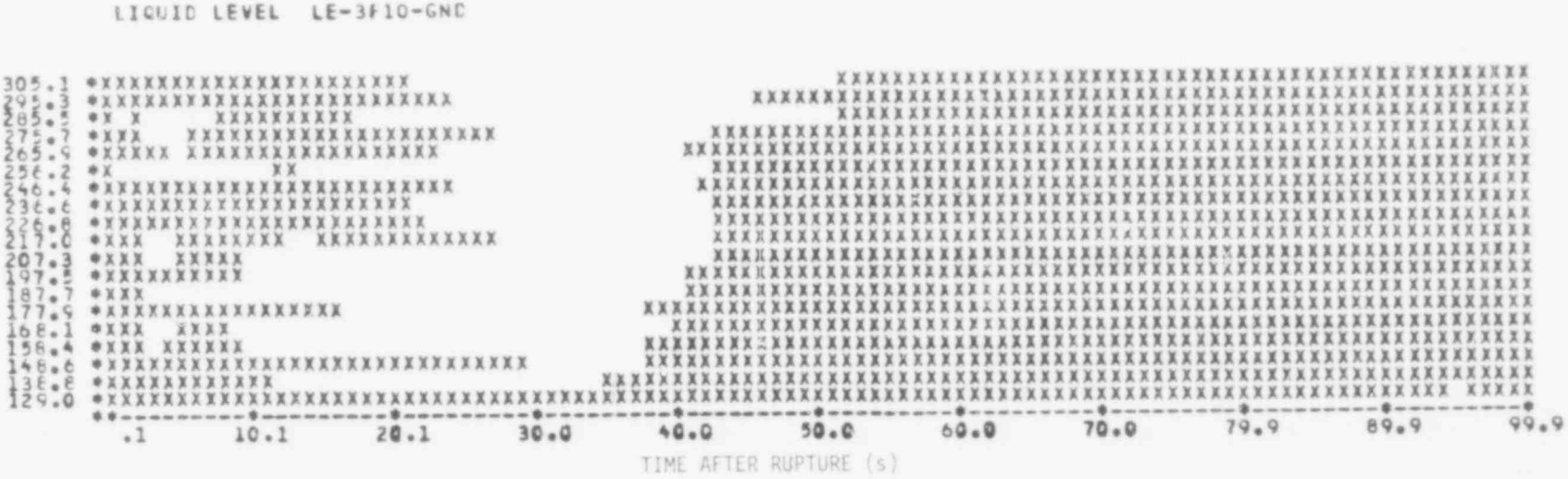

Fig. 40 Liquid level in fuel Module 3.

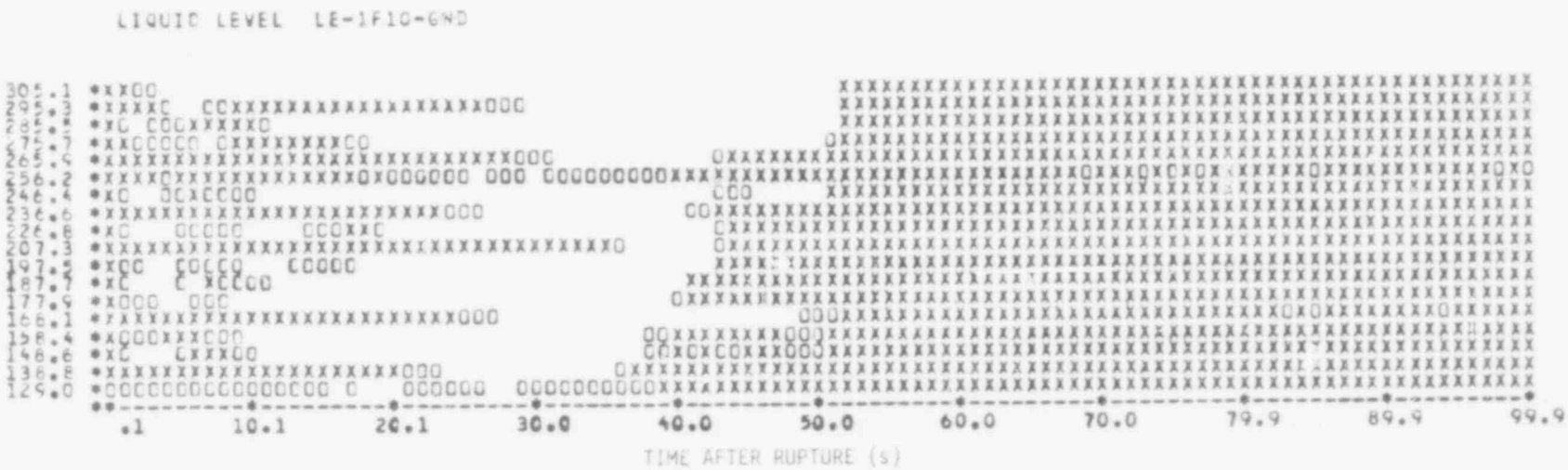

Fig. 41 Liquid level in fuel Module 1.

Fig. 42 Liquid level in downcomer and lower plenum under the broken loop.

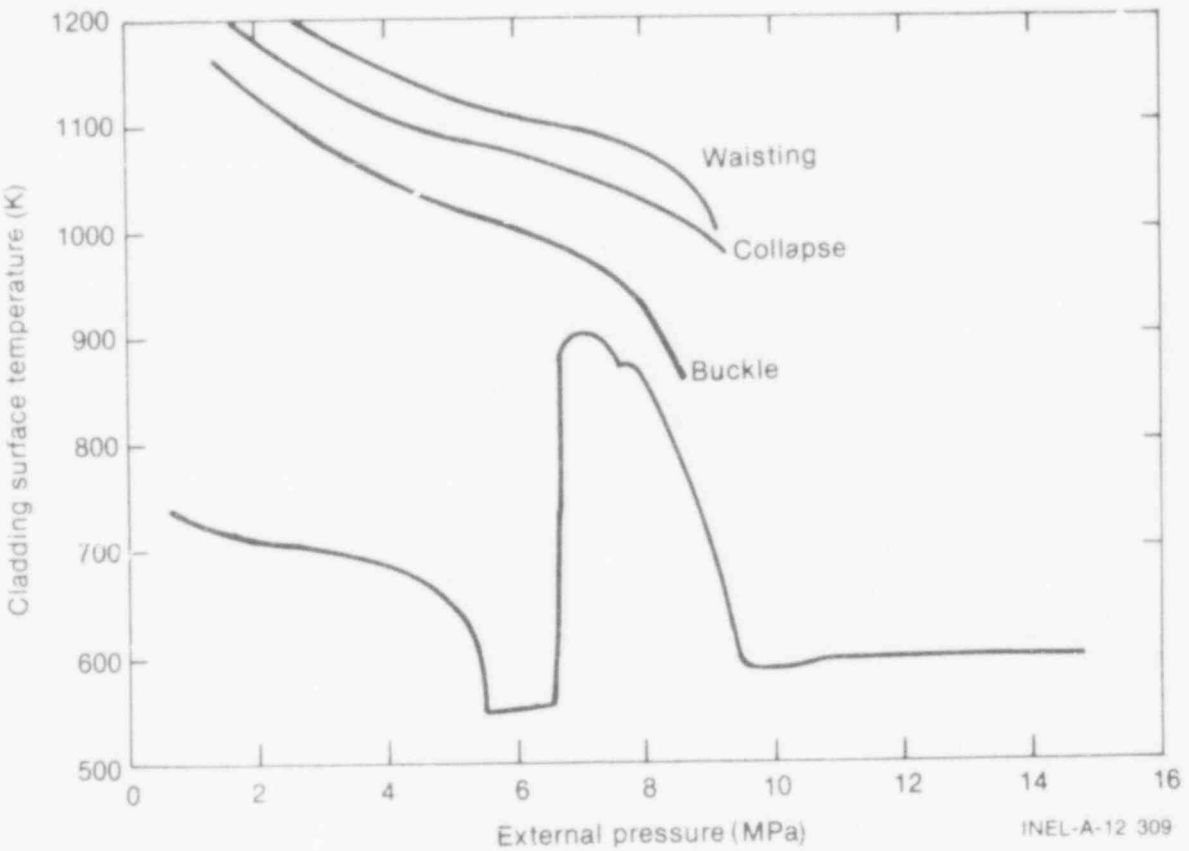

Fig. 43 Modes of cladding deformation at different pressures and temperatures maintained for 15 s.

480 049

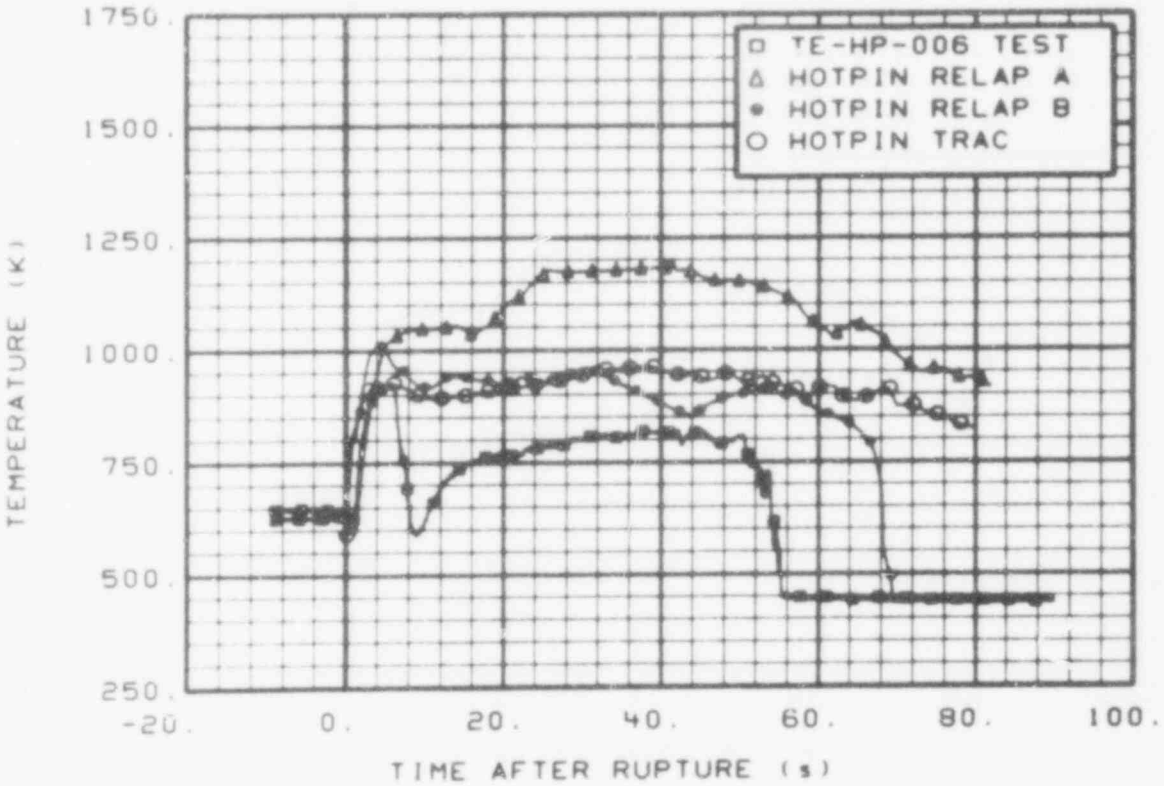

Fig. 44 Comparison of measured and calculated hot pin cladding temperatures.

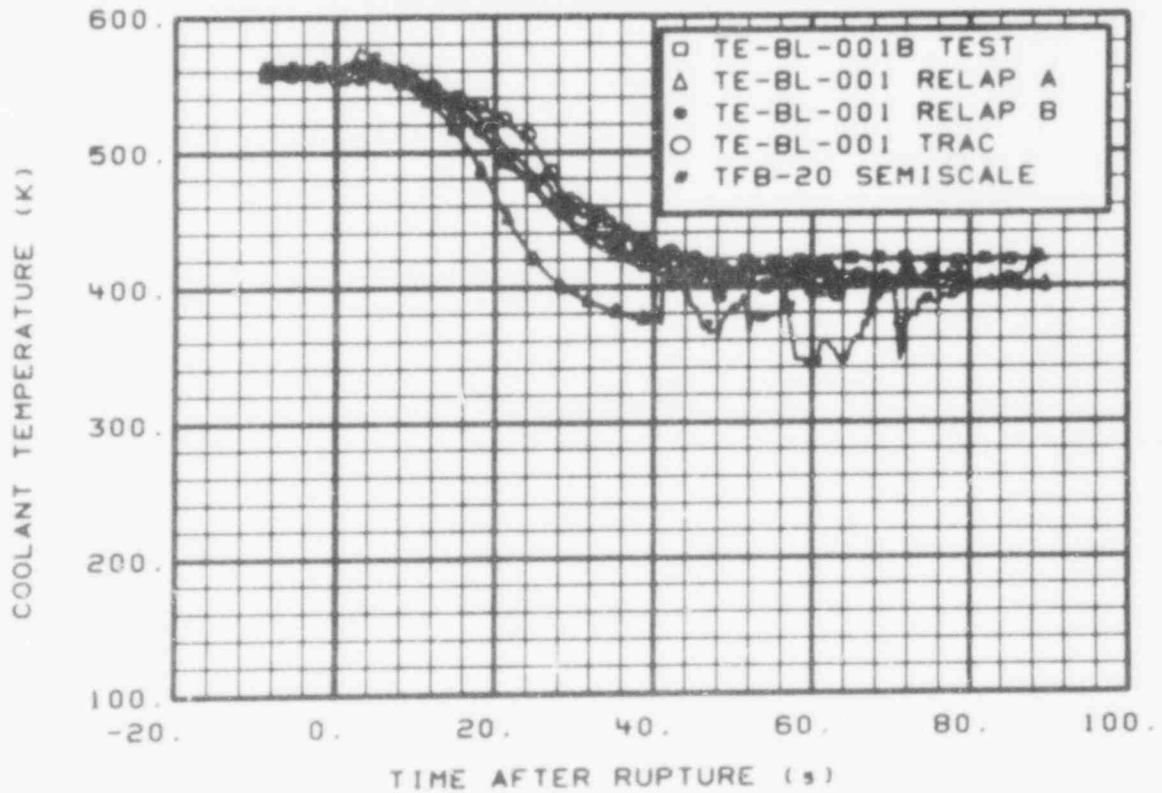

Fig. 45 Comparison of measured and calculated temperature in the broken loop cold leg.

480 050

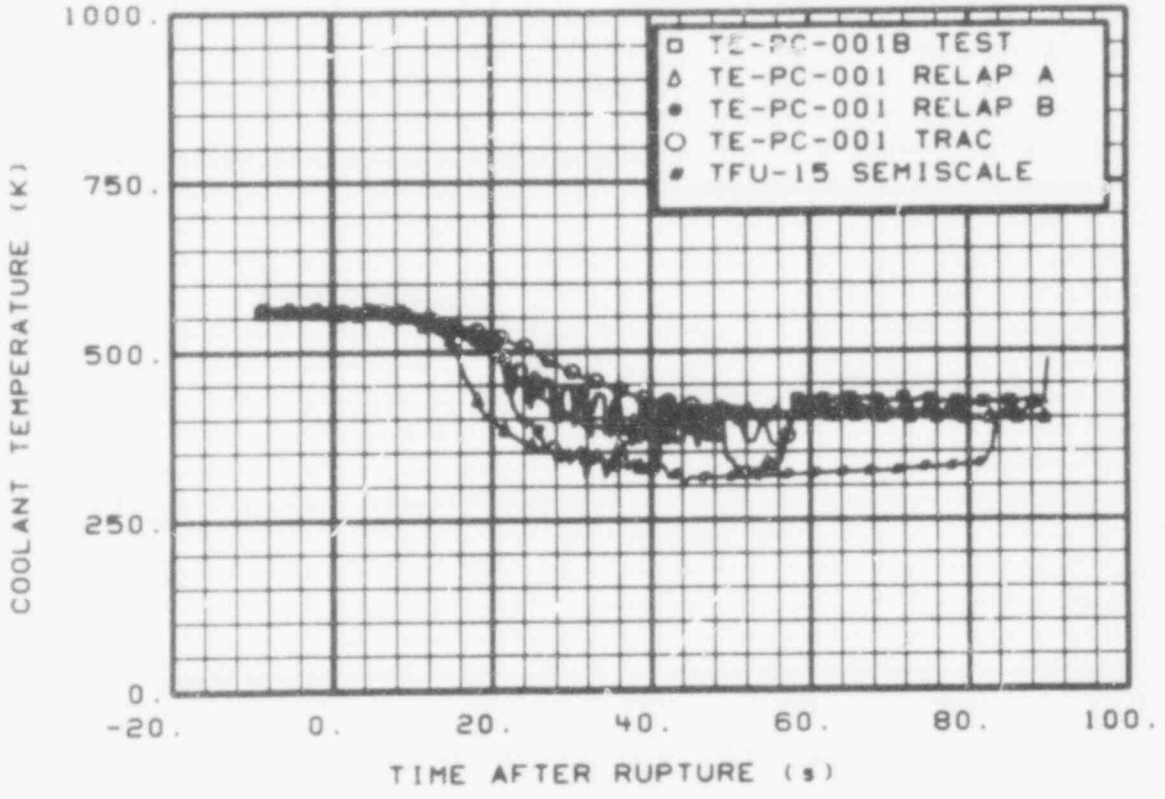

Fig. 46 Comparison of measured and calculated temperature in the intact loop cold leg.

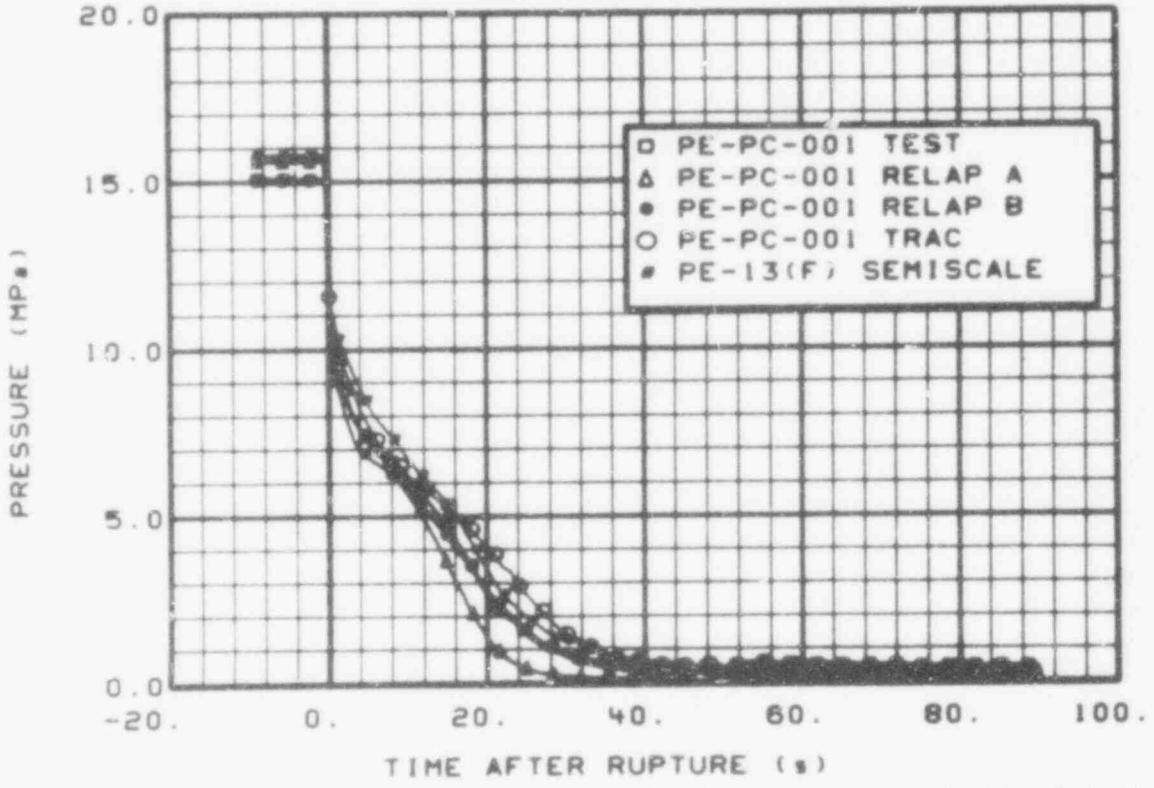

Fig. 47 Comparison of measured and calculated pressure in the intact loop cold leg.

480 051

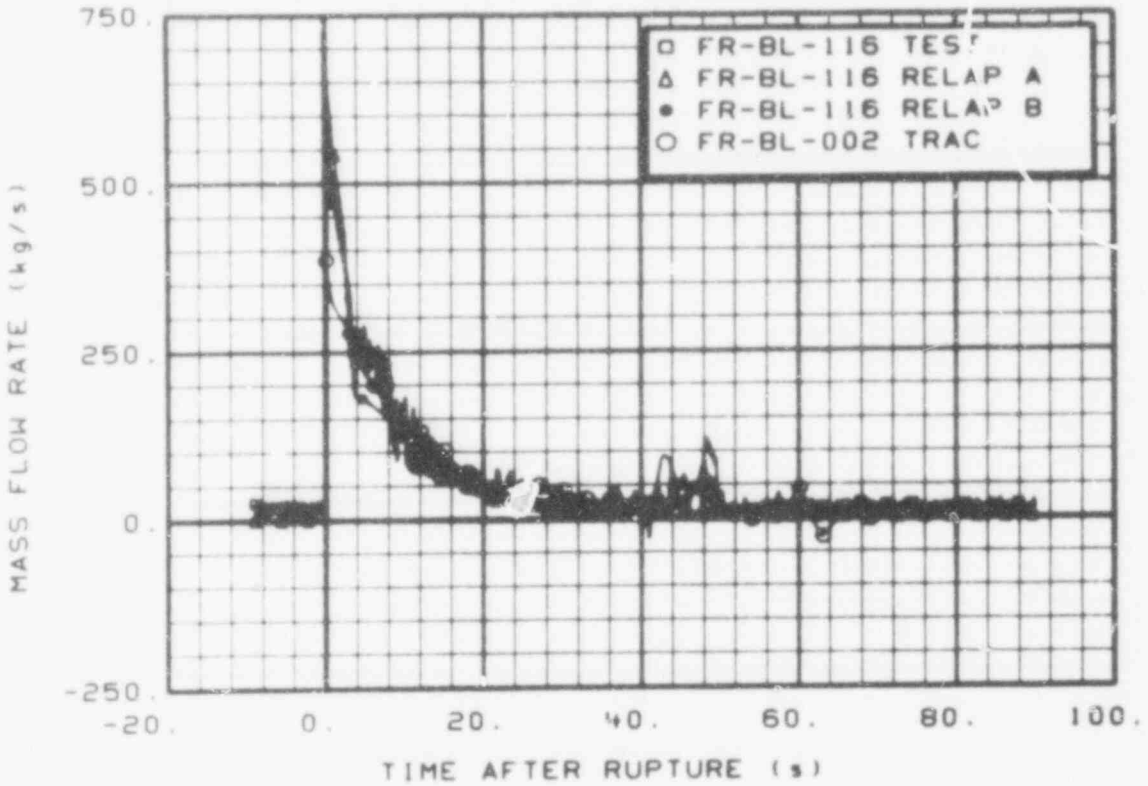

Fig. 48 Comparison of measured and calculated mass flow in the broken loop cold leg.

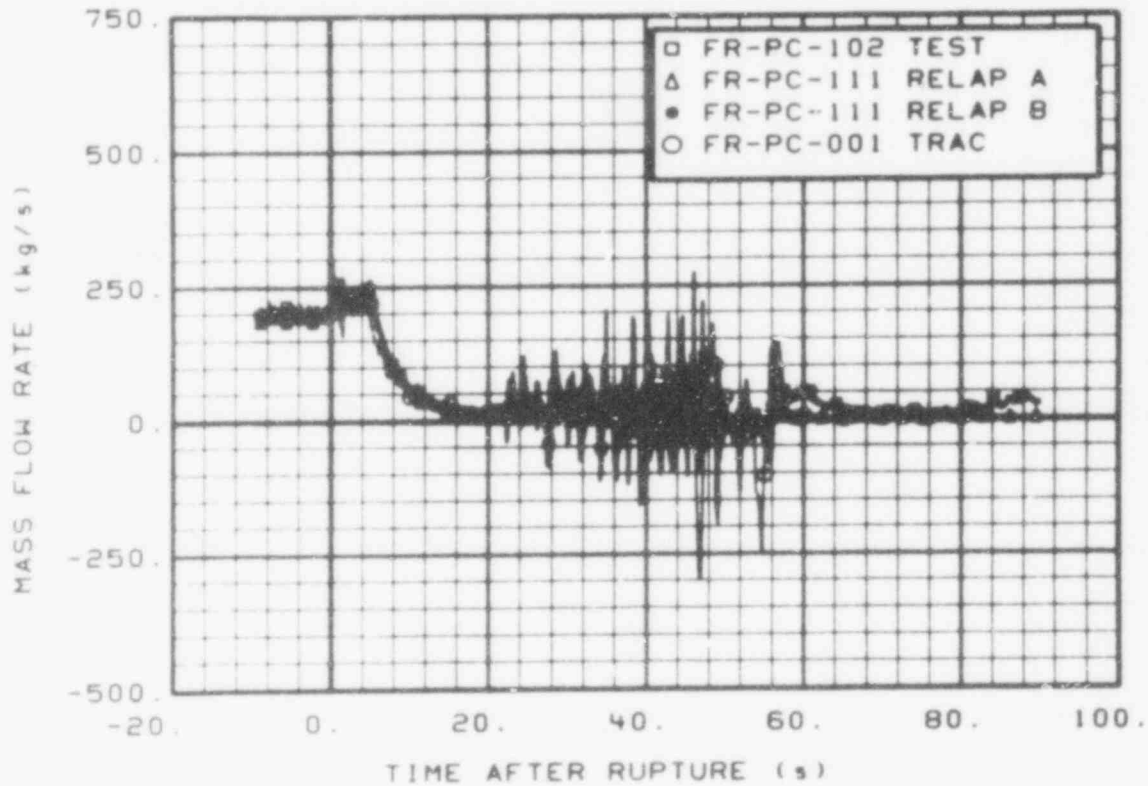

Fig. 49 Comparison of measured and calculated mass flow in the intact loop cold leg.

480 052

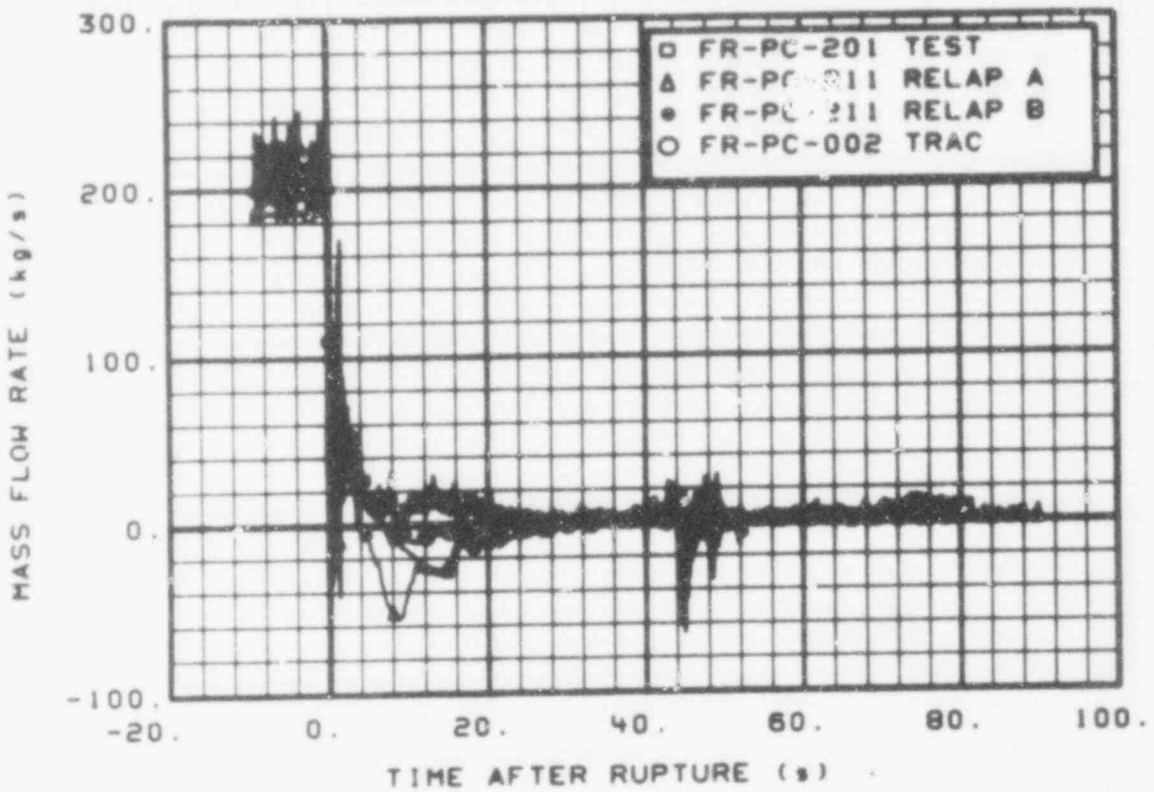

Fig. 50 Comparison of measured and calculated mass flow in the intact loop hot leg.

480 053

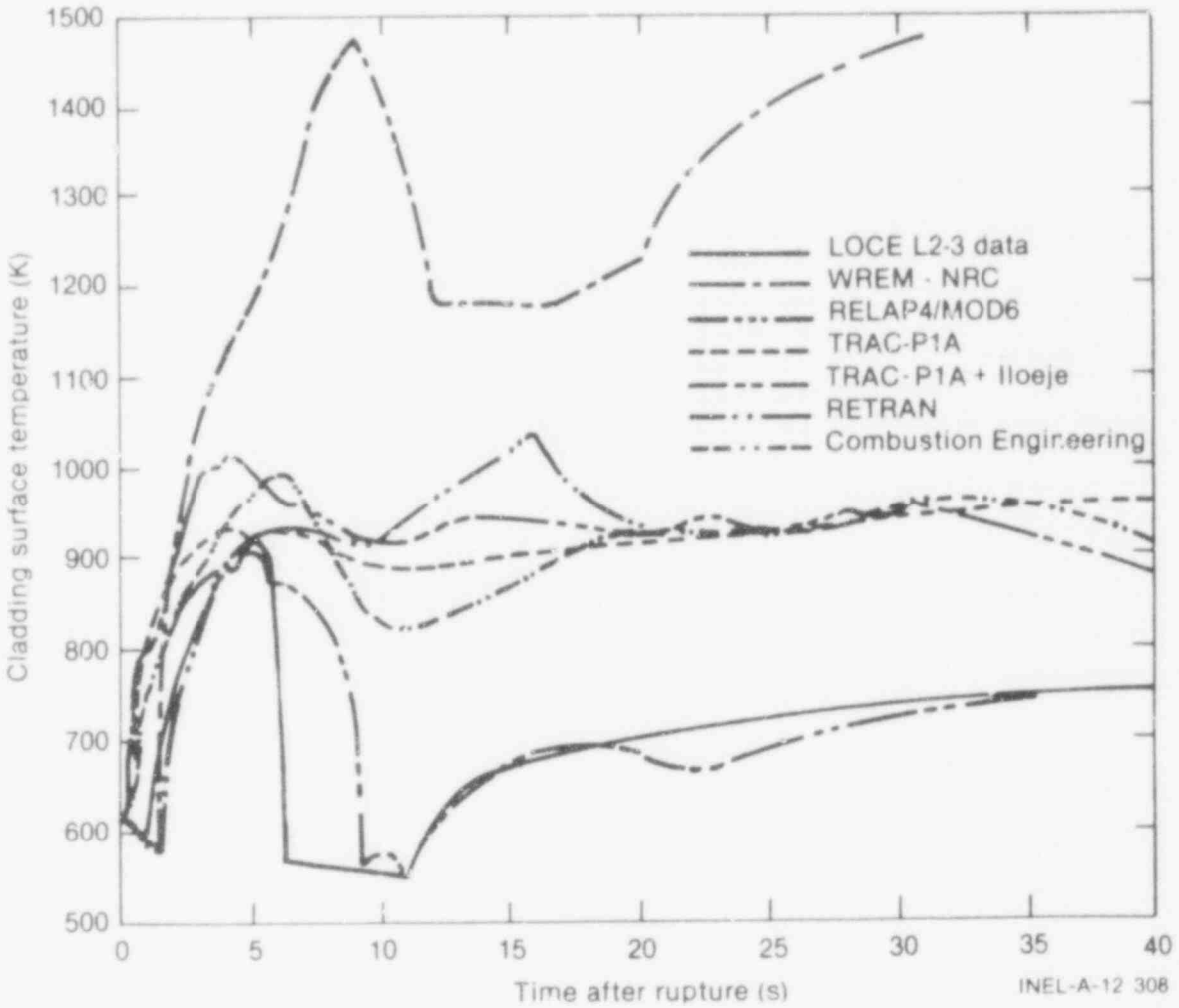

Fig. 51 Comparison of measured peak cladding tempeature with all prediction methods.

480 054

VI. REFERENCES

1. D. L. Reeder, LOFT System and Test Description (5.5-ft Nuclear Core 1 LOTEs), NUREG/CR-0247, TREE-1208 (July 1978).

2. C. W. Solbrig, L. P. Leach, and H. J. Welland, "LOFT Power Ascension Series L2," Appendix B to LOFT EOS, Volume 1, Revision 1 (April 1978).

3. P. A. Harris, T. K. Samuels, and H. J. Welland, "Power Ascension Test Series L2," LOFT Experiment Operating Specification, Volume 2, NE L2 Series, Revision 2 (July 1978).

4. B. L. Collins et al, Experiment Data Report for Semiscale MOD-1 Test S-06-3 (LOFT Counterpart Test), NUREG/CR-0251, TREE-1123 (July 1978).

5. W. H. Grush et al, Best Estimate Experiment Predictions for LOFT Nuclear Experiments L2-2, L2-3, and L2-4, LOFT-TR-101 (November 1978).

6. E. J. Kee and W. H. Grush, Best Estimate Prediction for LOFT Nuclear Experiment L2-3, EP-L2-3 (April 1979).

7. EG&G Idaho, Inc., RELAP4/MOD6 -- A Computer Program for Transient Thermal-Hydraulic Analysis of Nuclear Reactors and Related Systems -- User's Manual, CDAP-TR-003 (January 1978).

8. A. C. Peterson and K. A. Williams, TRAC-P1A Pretest Prediction of LOFT Nuclear Test L2-3, Los Alamos Scientific Laboratory Report LA-UR-79-1134 (May 1979).

9. Los Alamos Scientific Laboratory, TRAC-P1A: An Advanced Best Estimate Computing Program for PWR LOCA Analysis, Vol. I, LA-7777-MS, NUREG/CR-0665 (April 1979).

10. J. C. Wells et al, Pretest RETRAN Analysis for LOFT Test L2-3 (Standard Problem #10), ITI-I-4016 (May 7, 1979).

11. Combustion Engineering, Best Estimate Pre-Test Analysis of LOFT TEST L2-3, LD-79-029 (May 1979).

12. Memorandum, Z. R. Rosztoczy, NRC, to R. Mattson, NRC, "WREM-LOFT Pretest EM Predictions."

13. Letter, K. A. Williams, Los Alamos Scientific Laboratory to Dr. L. Shotkin, NRC, "Pretest Prediction for LOFT L2-3 Using TRAC-P1A+Iloeje" (May 2, 1979).

14. M. S. Jacoby, Experiment Data Report for LOFT Nonnuclear Test L1-5 (Isothermal Test with Core 1 Installed), TREE-NUREG-1215 (June 1978).

480 055

15. M. McCormick-Barger, Experiment Data Report for LOFT Power Ascension Test L2-2, NUREG/CR-0492, TREE-1322 (February 1979).

16. D. J. Varacalle, Jr. and R. W. Garner, PBF/LOFT Lead Rod Program Tests LLR-3, -4, -5 Quick Look Report, TFBP-TR-315 (April 1979).

17. R. C. Gottula, LOFT Transient (Blowdown) Critical Heat Flux Tests, TREE-NUREG-1240 (April 1978).

18. A. M. Eaton et al, LOFT Cladding Surface Thermocouple Calibration Test Results for Zircaloy Clad Rod IH-8029-2, LTR-141-88 (November 1978).

19. C. S. Olsen, Zircaloy Cladding Collapse Under Off-Normal Temperature and Pressure Conditions, TREE-NUREG-1239 (April 1978).

20. L. J. Siefken et al, FRAP-T4 -- A Computer Code for the Transient Analysis of Oxide Fuel Rods, CDAP-TR-78-027 (July 1978).

480 056